Université de Montréal

CORRELATING NERVE FIBER LAYER THICKNESS WITH BLOOD FLOW IN THE NORMAL HUMAN EYE

par

Catherine Ieraci

École d'optométrie

Mémoire présenté à la Faculté des études supérieures
en vue de l'obtention du grade de
Maître ès sciences (M.Sc.)
en optique physiologique

Avril, 1998

Université de Montréal
Faculté des études supérieures

Ce mémoire intitulé:

CORRELATING NERVE FIBER LAYER THICKNESS WITH BLOOD FLOW IN THE NORMAL HUMAN EYE

présenté par:

Catherine Ieraci

a été évalué par un jury composé des personnes suivantes:

Dr Claude Giasson, Ph. D., professeur adjoint	président-rapporteur
Dr John V. Lovasik, Ph. D., professeur titulaire	directeur de recherche
Dr Hélène Kergoat, Ph. D., professeur agrégé	membre du jury

Mémoire accepté le : 98.08.22

SOMMAIRE

La cellule ganglionnaire rétinienne, un neurone visuel de troisième ordre, est responsable du stade final d'intégration de l'information visuelle intra-rétinienne et de la transmission, vers le cortex visuel, des signaux visuels prenant naissance au niveau des photorécepteurs. Elle constitue donc un élément essentiel au processus de la vision. Une déficience au niveau des cellules ganglionnaires peut entraîner une perte irréversible de la fonction visuelle malgré l'intégrité des photorécepteurs et du cortex visuel. La croissance et survie de la cellule ganglionnaire sont assurées par un processus physiologique de base, le transport axonal, dépendant d'un apport énergétique constant. Ainsi, une réduction du flot sanguin à tout niveau de la cellule ou de son axone peut entraîner par ischémie une déficience du transport axonal vital et potentiellement une nécrose de la cellule. Au niveau rétinien, la distribution des axones projetant au nerf optique à travers la couche de fibres nerveuses varie de façon sectorielle. Un plus grand nombre de fibres nerveuses projettent aux pôles supérieur et inférieur du nerf optique. En considérant la projection distincte des fibres visuelles à partir de l'ensemble des régions du fond d'oeil, l'objectif principal de la présente étude était d'établir, pour l'oeil humain normal, la corrélation entre l'épaisseur de la couche de fibres nerveuses autour du nerf optique et le flot sanguin rétinien assurant leur apport métabolique.

La question principale est mise en relation avec la condition clinique connue sous le nom de *glaucome.* Cette neuropathie optique est caractérisée par une perte progressive de cellules ganglionnaires rétiniennes, associée ou non à une pression intra-oculaire élevée et entraînant des pertes localisées du champ visuel et des dysfonctions multiples de la vision. Le glaucome est responsable de 10% des cas de cécité à travers le monde (1) et figure parmi les principales causes de cécité aux États-Unis et au Canada (2).

La neuropathie optique associée au glaucome est caractérisée par une progression typiquement sectorielle. En effet, le site de prédilection de la dégénérescence des fibres nerveuses rétiniennes se situe au niveau des pôles inférieur et supérieur du nerf optique. Cette susceptibilité des fibres nerveuses projetant aux pôles verticaux du nerf optique fait l'objet de multiples questionnements et suggère que l'étude des différences régionales, tant neuro-anatomiques que vasculaires, pourrait servir d'indice à la physiopathologie de la maladie.

Au point de vue anatomique, les pôles supérieur et inférieur du nerf optique sont les lieux de projection d'une grande surface rétinienne, incluant la périphérie supéro- et inféro-nasale, la périphérie temporale et les fibres arciformes. Il y a donc lieu de croire à une activité neuronale très importante dans ces deux régions, entraînant par le fait même une demande métabolique élevée. À cet effet, il a été démontré au niveau du tissu cérébral qu'une augmentation de l'activité métabolique, par exemple associée à la parole, à l'écoute ou au travail musculaire d'un bras, était accompagnée d'une augmentation du flot sanguin (3). La question est donc de savoir si, dans la rétine normale, il existe une distribution préférentielle du flot sanguin vers les régions plus denses en fibres nerveuses en condition de base?

La présente étude a été réalisée sur vingt-quatre (24) jeunes adultes volontaires, ne présentant aucun antécédant d'anomalie oculaire et systémique. Des mesures non-invasives de l'épaisseur de la couche de fibres nerveuses rétiniennes et du flot sanguin ont été obtenues dans quatre sites rétiniens d'intérêt, localisés dans les quatre quadrants principaux de la région péripapillaire (supérieur, inférieur, nasal et temporal) située à environ 1.75 DD du centre du nerf optique.

Les mesures de l'épaisseur de la couche de fibres nerveuses rétiniennes ont été réalisées à l'aide d'un polarimètre à balayage au laser, le *Nerve Fiber*

Analyser I, de Laser Diagnostic Technologies, basé sur le principe de biréfringence de la couche de fibres nerveuses rétiniennes: lorsqu'un faisceau de laser polarisé traverse la structure cylindrique et parallèlement organisée des fibres nerveuses, la lumière réfléchie des couches profondes présente un état de polarisation modifié. Ce changement de phase est appelé "retardation" et est proportionnel à l'épaisseur de la couche biréfringente.

Les mesures locales du flot sanguin ont par ailleurs été obtenues à l'aide du *Laser Doppler Flowmeter, Oculix LDF 5000*, basé sur le principe optique de l'effet Doppler: lorsqu'un faisceau de laser monochromatique est réfléchi par une particule en mouvement (dans le cas présent, les globules rouges du sang), sa fréquence est modifiée par un montant Δf, dépendant de la vélocité de la particule et de l'angle d'incidence du faisceau lumineux. Le paramètre *flot* décrit la distance parcourue par les cellules en mouvement dans le volume échantillonné par unité de temps.

Les résultats ont démontré une différence significative de l'épaisseur de la couche de fibres nerveuses rétiniennes entre les quadrants, les aires rétiniennes échantillonnées dans les quadrants supérieur et inférieur présentant une couche de fibres nerveuses plus épaisse que celles des quadrants nasal et temporal. Les mesures de flot sanguin n'ont par ailleurs démontré aucune variation significative entre les quadrants, pour des sites correspondants aux lieux de mesure de l'épaisseur de la couche de fibres nerveuses. Pour le groupe complet considéré sans distinctions individuelles, aucune corrélation n'a été établie entre le flot sanguin et l'épaisseur de la couche de fibres nerveuses d'aires rétiniennes péripapillaires correspondantes.

Les résultats de la présente étude suggèrent que, en condition de base c'est-à-dire en l'absence d'excitation élevée des cellules ganglionnaires, il n'existe pas de distribution préférentielle de flot sanguin rétinien vers les

couches de fibres nerveuses plus épaisses. Auparavant inconnue, cette relation liant le flot sanguin à l'épaisseur de la couche de fibres nerveuses rétiniennes suggère qu'une uniformité de l'apport sanguin à travers un tissu nerveux de densité variable pourrait donner lieu à une susceptibilité accrue des couches de fibres nerveuses plus épaisses lors d'une diminution globale de la pression de perfusion oculaire. Les bases anatomiques et l'interprétation des résultats obtenus seront révisées dans la présente étude.

Mots clés: *couche de fibres nerveuses rétiniennes, flot sanguin, polarimètre à balayage au laser, fluxmétrie au laser Doppler.*

SUMMARY

Retinal ganglion cells are third order visual neurons responsible for the final stages of intraretinal processing of visual information and transmission of visual signals toward the higher processing sites. Therefore, an alteration in the ganglion cell activity can lead to irreversible losses of visual function, despite the presence of healthy photoreceptors and visual cortex. Axonal transport is the basic physiologic process responsible for the growth and maintenance of the remarkably long axon processes of the retinal ganglion cell. The metabolic process that supports axonal transport is essentially confined to the cell body and is energy-dependant. As a result, conditions such as mechanical compression of the nerve fiber or blood supply insufficiencies can lead to a detrimental blockage of the vital axoplasmic transport of the retinal ganglion cell.

The objective of the present study was to establish the correlation between the nerve fiber layer thickness of peripapillary retinal sites and their associated blood flow. Studies of the retinal anatomy show that the superior and inferior poles of the optic nerve receive a greater number of nerve fibers than the horizontal quadrants, with axons projecting from a large retinal surface, including the peripheral superior and inferior-nasal fibers, the peripheral temporal fibers, as well as the arcuate fibers. The superior and inferior poles of the disc are obviously the site of important neuronal activity, which could result in higher metabolic demands, and consequently a need for a greater blood supply. In the brain, activities such as speach, listening or arm work were reported to cause increases in the brain's blood flow (3). Thus, the objective in the present study was to determine whether at basal conditions there is a preferential increase in retinal blood flow to retinal sites with a thicker nerve fibre layer distribution.

This project aimed at providing better understanding of the underlying causes of ocular diseases involving the retinal ganglion cells and nerve fiber layer, principally focusing on the clinical condition known as glaucoma. Glaucoma is responsible for 10% of all cases of blindness in the world and is one of the leading causes of blindness in the United-States, and in Canada (1, 2). This complex clinical entity includes a number of optic neuropathies, sharing three common features: a progressive loss of retinal ganglion cells, associated in most cases with a susceptibility to elevated intraocular pressure, and resulting in visual field losses and a variety of visual dysfunctions.

Glaucomatous optic neuropathy generally progresses with sectorial differences. Indeed, the superior and inferior poles of the optic nerve head are preferentially damaged in the early stages of the disease. This susceptibility of the vertical poles of the optic nerve head is not fully understood, however it suggests that study of regional neuro-anatomy or vascular perfusion might provide clues to pathogenesis of the disease.

Many studies start with the assumption that nerve fiber damage in glaucoma originates at the optic nerve head, particularly at the level of the lamina cribrosa. However, a review of the anatomy will show that the retinal ganglion cells are surrounded by retinal capillaries which supply them with essential nutrients all along their course, from their origin in the inner nuclear layer up to their passage through the optic nerve head. Theoretically, an interruption of blood supply at any one of these sites can interfere with the cell's normal metabolism and lead to atrophy of the ganglion cell as a whole. This would result in the same clinical picture observed in glaucoma, with subtle losses of axons leading to fine defects in the thin nerve fiber layer and more obvious defects at the edges of the optic nerve head where they finally concentrate. We designed a study to evaluate the levels of blood flow to the retinal nerve fibers around the optic nerve head prior to their passage into the optic nerve.

Twenty-four (24) young healthy volunteers participated in this study. Non-invasive measurements of the nerve fiber layer thickness and of local blood flow were taken in four retinal sites, located in the four principal quadrants of the peripapillary area (superior, inferior, nasal and temporal), about 1.75DD away from the optic disc center.

A scanning laser polarimeter, the *Nerve Fiber Analyser I* from Laser Diagnostic Technologies, was used to assess the nerve fiber layer thickness. This technique is based on the birefringent property of the retinal nerve fiber layer: when a polarized near infra-red laser light is focused onto the retina and partially reflected from the deeper layers, its state of polarization is changed. The amount of phase shift is refered to as *retardation* and is proportional to the thickness of the layer.

The focal measurements of blood flow were obtained using the Laser Doppler Flowmeter, Oculix LDF 5000, based on the optical *Doppler effect:* laser light scattered by a moving particle (red blood cell in this case) is shifted in frequency by an amount Δf, referred to as "doppler shift", dependent on the velocity of the moving particle and on the angle of incidence. The values of *flow* are expressed in arbitrary units and represent the distance covered by all moving cells inside the sample volume per unit time.

Results showed a significant difference in nerve fiber layer thickness between the sampled retinal sites, with the superior and inferior areas showing a thicker nerve fiber layer than the nasal and temporal areas. Flow values did not change significantly across the four quadrants for retinal sites matching those where NFL thickness measurements were made. No correlation was found between the blood flow readings and the nerve fiber layer thickness of corresponding fundus areas.

The results suggest that blood flow is not preferentially distributed to fundus areas of greater nerve fiber layer thickness under basal conditions. Indeed, in the non-stimulated retina, blood flow was uniformly distributed despite significant changes in nerve fiber density. If this observation remains true during a global increment in ganglion cell activity (for example by a diffuse flickering light) or an overall decrease in blood supply, we can assume that the thickest population of fibers may be more at risk for ischemic lesion. This finding is of particular interest in relation to glaucoma. A general review of the literature on the neuro-anatomy and blood supply of the retina and optic nerve head will be followed by a general discussion of the physiology underlying the results.

Key words: *nerve fiber layer thickness, blood flow, scanning laser polarimetry, laser doppler flowmetry.*

TABLE OF CONTENTS

LIST OF TABLES

LISTE OF FIGURES

1. INTRODUCTION

2. LITERATURE REVIEW

3. CORRELATING NERVE FIBER LAYER THICKNESS WITH BLOOD FLOW IN THE NORMAL HUMAN EYE

LIST OF ABBREVIATIONS

µm	Micron
λ	Wavelength
au	Arbitrary unit
AVP	Arterio-venous passage time
BFR	Blood flow ratio
CO_2	Carbon dioxide
CRA	Central retinal artery
CRV	Central retinal vein
DD	Disc diameter
DLS	Differential light sensitivity
EDV	End-diastolic velocity
IOP	Intraocular pressure
LDF	Laser Doppler flowmetry / flowmeter
LGN	Lateral geniculate nucleus
M	Magnocellular
m / s	meter per second
ml	Milliliter
mm	Millimeter
NFA	Nerve Fiber Analyser
nm	Nanometer
NO	Nitric oxide
NPG	Normal-pressure glaucoma
O_2	Oxygen
OA	Ophthalmic artery
ONH	Optic nerve head
P	Parvocellular
PCA	Posterior ciliary artery

PERG	Pattern electroretinogram
POAG	Primary open-angle glaucoma
POBF	Pulsatile ocular blood flow
RBC	Red blood cell
RNFL	Retinal nerve fiber layer
RPC	Radial peripapillary capillary
SEM	Scanning electron microscopy
SLP	Scanning laser polarimetry
VECP	Visually evoked cortical potential
°	Degree
μW	Microwatt
f	Frequency

DEDICATION

In the memory of Francesca Lanzetta-Ieraci (1921-1996).

Through her wisdom and her judicious counsel, she was able to show her children, and later her grandchildren, all the beauty of education. Any one of our academic achievement was also hers. *"All the fortune in the world is little gratification compared to the rewarding feeling of a diploma",* she used to say. She was, and will always be a great source of inspiration.

ACKNOWLEDGMENTS

I wish to thank Dr John Lovasik for his inestimable assistance throughout this project. His constructive comments have contributed to the development of this thesis; they were the basis of intellectual stimulation, and a constant motivation to surpass oneself. Furthermore, I wish to acknowledge his remarkable contribution to the conception of the figures presented in this paper.

I also wish to give my regards to all members of the jury who participated in the evaluation of the present thesis.

Most particularly, I wish to thank Dr Hélène Kergoat for providing me with enlightening advice on several occasions.

I would also like to thank all the subjects who volunteered for this experience.

Special thanks to Mrs Susan Lovasik for her kind hospitality.

Finally, I wish to express my gratitude to my family, especially my husband Charles-André, for their encouragements and patience throughout my studies.

This research project was supported by a grant from the Natural Sciences and Engineering Research Council of Canada (N.S.E.R.C.), to Dr John V. Lovasik.

1. INTRODUCTION

The present study has as its principal objective to determine whether the varying thickness of the retinal nerve fibre layer (NFL) around the optic nerve head (ONH) is differentially perfused by the retinal vasculature. A better understanding of this fundamental correlation between nerve fibre layer thickness and blood flow for the human eye is essential if the etiologies of various neurovascular diseases of the eye are to be elaborated and treated successfully. The principal focus of the present study relates to the clinical condition known as glaucoma. This latter ocular disease is principally manifest as an attrition of axons comprising the retinal NFL because of abnormalities in ocular hydrodynamics that result in either pressure necrosis of these axons or ischemic atrophy of this same population of retinal neurons.

The following sections will describe various aspects of glaucoma, a "silent theft" of vision, that does not discriminate according to a patient's age. This overview will provide the reader with a global understanding of the various biological, sociological and psychological consequences when a patient becomes afflicted with this preventable ocular disease.

Glaucoma is a leading cause of irreversible blindness throughout the world (1). This ocular disease is an optic neuropathy characterized by a progressive loss of ganglion cell axons, preferentially in the vertical poles of the disc, resulting in an undermining of the disc rim tissue and an enlargement of the optic disc cup. These anatomical changes precede visual field loss and are responsible for a wide range of visual function deficits.

Glaucoma accounts for 10% of all cases of blindness in the world (1). Individuals affected by this blinding disease are faced with a great deterioration of their quality of life, and often a loss of personal autonomy. From the

standpoint of a community, glaucoma represents a significant economic cost resulting from loss of manpower and cost of social services.

The most fundamental fact about glaucoma is that it is not a *single disease process*. Glaucoma is now considered a group of disorders with large inter-subject differences in clinical presentations. Figure 1 presents the traditional model of clinical glaucoma whose triad of interactive elements comprises an "abnormal" intraocular pressure, optic nerve damage , and defects in the visual field. Various classifications of glaucoma have been proposed in the literature based on their etiological and mechanical bases (4). Glaucomas are broadly categorized either into "*open angle*" or "*closed angle*" depending on their specific etiology. Furthermore, most forms of glaucoma are *chronic* in nature, although an *acute* form of the disease also exists. The present study will attempt to correlate in the broadest sense the NFL thickness to blood flow and relate this correlation to the various forms of glaucoma found in the clinical environment.

The precise rates for prevalence and incidence of POAG are not fully established. Epidemiological studies in different communities of the United States and different countries of the world show a wide variation in the general estimates for the prevalence of glaucoma. The variation in the reported prevalence of glaucoma may be due to either real variations in the actual prevalences of glaucoma between glaucoma groups or countries, differences in the criteria used to diagnose glaucoma, the methods used to derive the prevalence rates, or the age of the populations studied.

In the United States of America, glaucoma represents the second leading cause of irreversible blindness among white Americans, while it is the first cause among black Americans (2). Quigley et al (5) estimated that by the year 2000, 2.47 million Americans would suffer from primary open-angle glaucoma. In addition, it is estimated that one million individuals have undetected

glaucoma (2). The Baltimore Eye Survey conducted between 1985 and 1988 demonstrated that black Americans were four to five times more likely to develop glaucoma, and up to six times more likely to go blind from it. The prevalence of definite POAG was 1.29% among white and 4.74% among black persons (6).

Recent epidemiological studies have shown a wide variation in the prevalence of POAG around the world. A survey of POAG conducted between 1990 and 1991 in Marne, France showed that the prevalence of POAG cases undergoing treatment was between 0.15 and 0.36% for the whole population (7). In a population of west Ireland, a prevalence of 2% was found for people over the age of 50 (8). The overall prevalence of POAG in the Rotterdam Study (The Netherlands) (9) was 1.1% in the general population of 55 years of age or older, ranging from 0.2% in the age group of 55-59 years to 3.3% in the age group of 85-89 years. Of the untreated POAG patients 38.9% had IOPs of 21 mm Hg or lower. In a population-based survey of people 65-74 years of age living in the municipality of Tierp, central Sweden, open-angle glaucoma was found at a prevalence of 5.70% (10). For populations of 40 years and older, the prevalence of POAG was 0.5% in a province of northern Mongolia (11), 2.68% in Bardo, Tunis (12), and 1.5% in a mixed ethnic population of Western Cape, South Africa (13). The Barbados Eye Study is currently the largest glaucoma study ever conducted in a predominantly black population; the prevalence of open-angle glaucoma was 7.0% in blacks, 3.3% in mixed-race, and 0.8% in whites (14). Open-angle glaucoma incidence was found to increase exponentially with age in the Blue Mountains Eye Study (Australia), with rates of 0.4%, 1.3%, 4.7% and 11.4% amoung persons aged 49-60 years, 60-69 years, 70-79 years and 80 years or older, respectively (15).

Although important disparities exist between the glaucoma prevalence figures reported across studies, one common finding remains: the influence of age and ethnicity on the likelyhood of glaucoma development. Epidemiological

studies can be good indicators of the presence of risk factors but it should be emphasized that they do not always provide information about whether the risk factor occurred before or after the disease. The generally accepted non-ocular risk factors for glaucoma are age, race or ethnicity, family history of glaucoma, gender, vascular abnormalities and systemic diseases such as diabetes mellitus or hypertension.

Several ocular conditions have been identified as important risk factors in the development of glaucomatous optic nerve damage. These conditions include elevated intra-ocular pressure (IOP), myopia, increased cup:disc ratio, asymmetry of disc cupping, disc margin hemorrhage and narrowing or notching of the neuroretinal rim due to localized or diffuse nerve fiber layer defect. (2, 6, 16).

In summary, the personal, medical and socio-economic consequences of glaucoma have been presented. Countless scientific studies have been carried out in order to derive more effective diagnostic and therapeutic approaches for this ocular disease that can cause painless and irreversible loss of vision. While the pathophysiology of glaucoma remains unknown, many of its devastating effects on normal vision are preventable through sufficiently sensitive diagnostic procedures. The importance of early detection in the prevention of the disease is obvious. Detection depends on the ability to recognize the early clinical manifestations of the optic neuropathy and appropriate treatment requires an understanding of the pathophysiological mechanisms involved. The following sections will discuss the normal anatomy and vasculature of the human retina and optic nerve head, as well as the clinical manifestations of glaucoma. This overview of the literature aims at a better understanding and appreciation of the concepts relating to the pathogenesis of glaucomatous optic neuropathy, specifically the "mechanical" and "vascular" theories that may account for the development of glaucomatous damage in the eye.

Fig. 1

SIGNS & SYMPTOMS OF CLINICAL GLAUCOMA

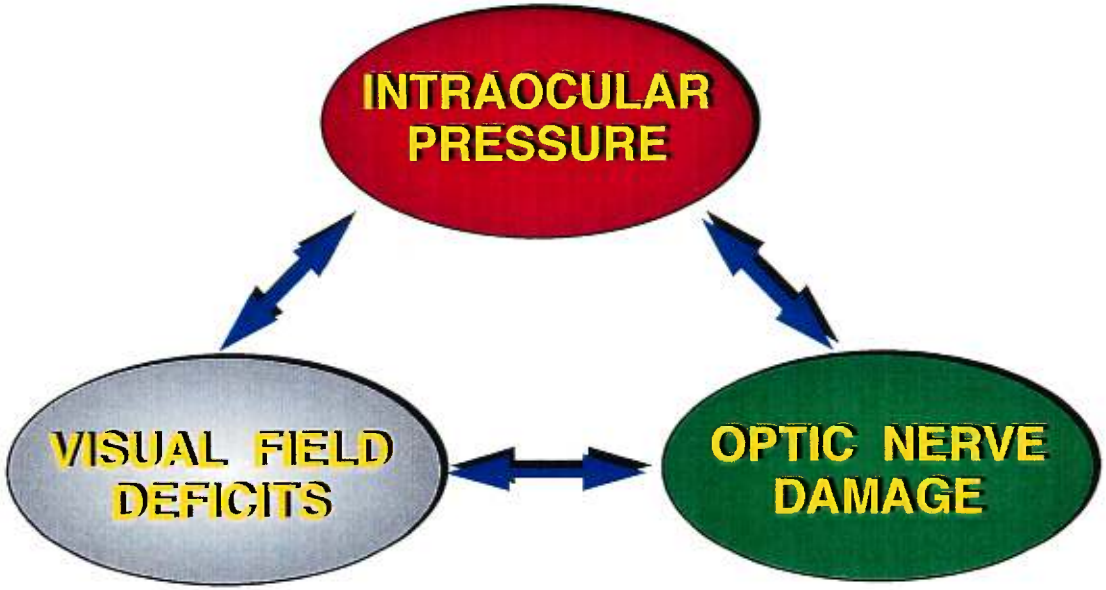

Unfortunately, the pathophysiology and reliable outcome predictors of glaucoma treatment remain UNKNOWN !!

RESEARCH HYPOTHESIS: A dissociation between the different degrees of blood flow required for normal metabolism in different density neural tissue across the fundus would place an eye "at risk" for neuronal dysfunction and / or vision loss as occurs in glaucoma; thus, to minimize physiological risk, fundus regions with a thicker nerve fiber layer are supplied with a greater basal blood flow.

2. LITERATURE REVIEW

2.1 NORMAL ANATOMY OF THE HUMAN RETINA AND OPTIC NERVE HEAD

2.1.1 The retina

The neural retina of the human eye is composed of discrete nuclear and plexiform layers. The regular arrangement of photoreceptors and communicating neurons as well as supporting glial tissue in the primate retina is illustrated in Figure 2. The cell bodies of the photoreceptors, cones and rods, form the outer nuclear layer, while the inner nuclear layer contains the amacrine, horizontal, bipolar and interplexiform cells. These interneurons mediate the transmission of the neural signals between the outer nuclear layer and the innermost nuclear layer containing the retinal ganglion cell, first through synapses in the outer plexiform layer and second, in the inner plexiform layer. Figure 3 schematically illustrates how the axons of each ganglion cell project in an orderly three dimensional pattern into the NFL whose fibers ultimately converge to form the optic nerve. Collectively, the convergence of the ganglion cell axons from all portions of the fundus results in a variation in the thickness of the NFL around the optic nerve head. In a normal eye the NFL along the vertical axis is thicker than the NFL along the horizontal axis.

Within the nerve fiber layer, axons are grouped into individual fiber bundles by the elongated processes of the Müller cell, a specialized astrocyte, and other glial cells. Figure 4 presents a histological section of the NFL showing its ultrastructural components. The parallel arrangement of ganglion cell axons together with the parallel arrangement of the much finer calibre neurofibrils located inside the ganglion cell axons gives the NFL its *birefringent* property. This latter physical attribute allows a non-invasive measurement of the nerve fibre layer thickness in the peripapillary region where glaucoma causes

clinically detectable defects both in the optic nerve head and the associated nerve fibre layer. Figure 4A presents a cross section of a portion of the nerve fibre layer that shows the parallel arrangement of adjacent axons with different cross-sectional thicknesses as well as parallel matrices of the resident neurofibrils in each axon. Figure 4B illustrates schematically the polarimetric principles underlying the measurement of NFL thicknesses.

The glial cells in the retina separate visual neural tissue from the retinal vasculature and maintain a constant physiological microenvironment essential for proper neuronal function. Specifically, the glial tissue participates actively in the exchange of metabolic waste and nutrients between visually active neurons and the retinal capillary plexus delivering oxygen and nutrients essential for normal neuronal activity.

The growth and maintenance of the remarkably long axonal processes of the retinal ganglion cell is made possible by a basic physiologic process, the *axonal transport.* This transport system is characterized by intracellular movement of molecules and organelles from one location to another, occuring within the cytoplasm of the cell. The metabolic organelles that support axonal transport is essentially confined to the cell body. *Orthograde* and *retrograde axonal transport* systems have been identified. Orthograde axonal transport (cell body to axon terminal) is responsible for the growth and maintenance, including synaptic functions, of the retinal ganglion cell. It can occur at a variety of speeds, designated as *slow* (0.5 to 3 mm/day), *intermediate* (5 to 50 mm/day) and *rapid axonal flow* (100 to 500 mm/day) (17). Rapid axonal flow is an active transport system which requires metabolic energy. The retrograde transport (axon terminal to cell body) occurs at a speed of about 50 to 260 mm/day (17). It provides feedback information to the ganglion cell body and functions as a "cleanup" system by removing or recycling materials from the axon or synaptic region back to the cell body (17, 18). Blockage of the normal

axoplasmic flow by compressive forces or vascular disturbances may be detrimental to the retinal ganglion cell.

Glaucoma is generally thought to be a disease of the inner neural retina specifically involving the retinal ganglion cells, their axons and consequently the size and shape of the ONH and its excavation. Studies have also shown that POAG does not involve photoreceptor loss (19, 20). As a result, the following sections will focus chiefly on the structure and function of the NFL and the optic nerve.

2.1.1.1 The nerve fiber layer

The retinal ganglion cells are the third order neurons through which visual information is transmitted from the eye to the brain. All ganglion cell dendrites receive their input from synapses with amacrine, bipolar and interplexiform cells in the inner plexiform layer, providing the final stage of intraretinal information processing. The visual signals, encoded as sequences of action potentials, are then transmitted along the axons within the retinal NFL through the optic nerve, reaching the optic chiasma and continuing towards the thalamus where the optic nerve fibers synapse in the various layers of the lateral geniculate nucleus (LGN).

2.1.1.2 Classification of the retinal ganglion cells

Two major classes of retinal ganglion cells have been described, based on their morphology, functional characteristics, and their site of entry in the LGN.

The p-type ganglion cells known as the *P-cells* project to the dorsal, parvocellular layers of the LGN. They have smaller somata, smaller receptive fields, thinner axons and predominate in the foveal region. They comprise about 90% of the ganglion cells that project to the LGN (21). They are characterized by a slower conduction velocity (about 13 m/s) (21), high spatial

but relatively low temporal resolution, and are involved in central visual acuity, color sensitivity and spatial contrast sensitivity (22). The small ganglion cells receive input predominantly from the cones; those with input from the cones with shorter wavelengths responses (blue-end of the spectrum) are larger and their axons conduct faster than those with cone input sensitive to longer wavelengths (red-end of the spectrum) (21, 22).

The m-type ganglion cell known as *M-cells* project to the ventral, magnocellular layers of the LGN. They comprise about 10% of the ganglion cell population (21, 22) and are more sparsely packed in the retina, but predominantly located in the retinal periphery. The M-cells have larger receptive fields, large-diameter axons with higher conduction velocity (about 21 m/s) (21). They show little color selectivity, phasic responses to changes in light intensity, and high temporal but relatively low spatial resolution (21, 22). The magnocellular visual pathway is primarily involved in interpretation of spatial organization based on motion and depth perception (22).

Clinical and psychophysical studies have indicated that the larger axons and ganglion cells (presumably M-cells) may be preferentially damaged in the early stages of glaucoma (21, 22, 23). Glaucoma is associated with visual function disturbances such as elevation of motion threshold (22), reduced color sensitivity in the blue-yellow region (22, 24), reduced contrast sensitivity, primarily to coarse gratings and low-contrast stimuli (22), reduced *flicker fusion frequency* (frequency at which the flickering of a light is first detected) (24), increased latency of visually evoked cortical potentials (VECP) and abnormal pattern electroretinogram (PERG) stimulated by high temporal and low spatial frequencies (22).

2.1.1.3 Morphological organization of the retinal nerve fibers

The retinal NFL is composed primarily of ganglion cell axons and to some extent, of astrocytes, retinal vessels and Müller cell processes. The ganglion

cell layer contains approximately 970 000 (25) to 1 200 000 ganglion cells (26, 27), with great variations between individuals. It is estimated that about 5000 retinal nerve fibers are lost through non-pathological senescence yearly throughout life (25). The ganglion cell layer is thickest in the macular region, with at least two layers of cells in the macular area. At this level, the foveal cones have a 1:1:1 relationship with a bipolar cell and ganglion cell; this relationship explains the highly specific response of the fovea (28). In consequence, in the parafoveal region, the ganglion cell layer reaches its maximum thickness of up to six cells, while the foveola itself has no ganglion cells. In the fundus periphery, the ganglion cells are single-layered and less densely placed.

The origin and displacement pattern of the ganglion cell axon across the posterior fundus is illustrated schematically in Figure 3. The ganglion cell axons describe a well defined pattern as they course from their origin in the retinal ganglion cell layer and enter the ONH. Ganglion cell axons from the nasal, superior and inferior retina describe a relatively straight course. However, axons originating from the temporal retina follow an arcuate pathway above and below the macula and enter the ONH at its superior and inferior temporal poles, respectively. These latter fibers are generally known as the *arcuate nerve bundles.* These fibers do not cross the horizontal mid-line temporal to the fovea, and thereby create a temporal or median *raphé* (24). The axons originating from ganglion cells nasal to the fovea run directly to the temporal edge of the ONH and form the *papillomacular bundle.* Mikelberg et al (25) have found a higher axonal density and a smaller mean axon diameter in the temporal inferior segment of the nerve, which is consistent with the fact that the major portion of the papillomacular bundle enters this area. Furthermore, a larger mean axon diameter, and consequently a lower axonal density, was found in the nasal segment of the optic nerve, corresponding with the fact that mostly large-diameter axons enter this quadrant of the nerve (25). This histological description of the location of large and small axons within the optic

nerve indicates that the larger diameter fibers do not exclusively populate the vertical meridians where most of the glaucomatous damage is found. Thus it may not be the size of the ganglion axon diameter that determines its vulnerability in glaucoma but the blood flow in the peripapillary sites subserving fibers that project from the vertical and horizontal quadrants of the optic nerve head. As a result, the present study will compare blood flow in the principal meridians to determine if there is a vascular basis for the preferential loss of nerve fibers in the vertical meridian, which normally has a greater number of nerve fibers compared to those in the horizontal quadrants.

Furthermore, the ganglion cell axons extend from their cell body inwards toward the vitreous, passing between the axons of cells located more peripherally and running parallel to the retina. As a result, axons from the peripheral retina run closer to the choroid and enter the outer edge of the neuroretinal rim of the ONH. Axons from ganglion cells located closer to the posterior pole are more superficial in the NFL and enter the ONH toward the inner edge of the neuroretinal rim (23, 24, 29). This three-dimensional topographic projection of ganglion cell axons into specific portions of the ONH is illustrated schematically in Figure 5. As a result of this 3-D NFL architecture, a lesion in the central portion of the ONH could result in visual field defects located close to the physiological blind spot, whereas damage to the peripheral portion of the ONH would result in visual field loss far from the blind spot and towards the visual field periphery.

The above-mentioned characteristic projection pattern of the nerve fiber bundles in three dimensional space accounts for the large changes in the retinal NFL thickness across the fundus, especially in the peripapillary zone. The RNFL thickness increases from the fundus periphery to the ONH, with distinct regional differences. The accumulation of fibers is generally higher in the inferior temporal region, because the fovea is situated slightly inferior to the optic disc center, and increasingly lower at the superior disc pole, the nasal

region and finally the temporal region. In their histological study on postmortem human eyes, Varma et al (30) found a mean RNFL thickness at the disc margin of 405, 376, 372 and 316 microns for the superior, inferior, nasal and temporal quadrants, respectively. The nerve fiber layer thickness decreased with increasing distance from the disc, and was inversely related to age in the superior and inferior poles of the disc (30).

2.1.1.4 The nerve fiber layer in glaucoma

At a clinical level, the diagnosis of glaucoma is traditionally based on positive findings in a diagnostic triad as shown in Figure 1. Loss of nerve fibers in glaucoma can occur in either a diffuse and/or a localized fashion with subsequent alterations of the ONH. The etiology of NFL loss in glaucoma is attributed to either "vascular" or "mechanical" factors. Figure 6 differentiates these opposing causal mechanisms. Studies have suggested that higher IOP leads to more diffuse damage than do lower IOP levels (31). Patients with normal or low-tension glaucoma tend to have deeper, steeper, and more localized structural defects than do glaucoma patients with elevated IOP (31). Focal damage to the ONH from glaucoma is thought to be related more to vascular insufficiency than to elevated IOP (32). Specifically, areas that are chronically hypoperfused even in the presence of normal IOP undergo ischemic atrophy that can be manifest as nerve fibre layer "drop-out" or notching of the optic nerve head margin, or narrowing of the neuro-retinal rim at the affected site.

Early visual field loss in glaucoma commonly occurs within the arcuate NFL area, which correlates with the predilection of the superior and inferior temporal poles of the optic nerve head for early glaucomatous damage (24). The affected fibers originate from ganglion cells located about 15-20° from the fovea, close to the temporal raphé. Glaucomatous cupping generally occurs in the inferior temporal pole of the ONH before that of the superior pole. This anatomical distribution of fibres highlights the need to examine the optic nerve

head and surrounding areas for regional differences in both nerve fibre layer distribution and blood flow parameters. It is believed that as much as 30 to 50% of the nerve fibers may be atrophied by glaucoma before any visual field defect can be detected by standard clinical visual field tests (31, 33).

Early glaucomatous field defects can often present as A) generalized reduction in visual thresholds or B) localized minor disturbances, defined as variable threshold responses to repeated testing of the same area, which have been found to precede a definitive field defect in that same area (24). These variable threshold responses have been linked to possible disturbances of vascular autoregulatory mechanisms in discrete areas of the inner retina (34).

More characteristic visual field defects related to glaucomatous disturbances in the retinal nerve fiber bundles include arcuate nerve fiber bundle defects, nasal steps, and less commonly, vertical steps and temporal sector field defects (24). In advanced glaucoma, progressive field loss eventually leads to complete double arcuate scotomas, extending to the peripheral limits in all areas, except temporally. The preserved *central* and *temporal islands of vision* progressively diminish in size, with the more resistant temporal island of vision persisting after central vision is lost. Eventual destruction of the remaining temporal island leaves the patient with no light perception (24).

Several studies have been conducted to determine the effectivness of various ONH parameters to predict the presence of established and impending field losses. Such parameters include cup-to-disc ratio, neuroretinal rim area, disc cup area, etc. No single parameter or combination of parameters in glaucomatous optic atrophy has been found to be totally satisfactory in predicting visual field loss. However, defects in the retinal NFL are reported to correlate most closely to future field loss (24). Manni et al (35) reported a significant decrease in retinal ganglion cell density and an associated decrease

in NFL thickness after 10 days of experimental intraocular hypertension in rabbits, which confirmed the very early involvement of the retinal nerve fiber layer in glaucoma. In the same context, several studies (36, 37, 38, 39, 40, 41) have demonstrated that retinal nerve fiber layer parameters are strongly related to visual field defects in glaucoma. It was shown that NFL parameters yield better correlations to the visual field than abnormalities of the ONH such as excessive cupping or a narrowing of the neuroretinal rim area (38, 39). In their longitudinal study on individuals with ocular hypertension, Quigley et al (42) showed that early nerve fiber layer atrophy was a good indicator of future visual field loss. Furthermore, nerve fiber layer assessment was reported to be an excellent screening tool for detecting glaucoma in the general population (43, 44).

Therefore, a better understanding of the functional and anatomical aspects of the retinal ganglion cell and NFL can provide essential information as to how they may be involved in pathological processes such as glaucoma. The present study concentrated on the relationship between the retinal NFL thickness and its underlying vascular supply.

In this study, the nerve fiber layer thickness was quantified in healthy young adults by scanning laser polarimetry (SLP), based on the birefringent property of the NFL. This technique presents the advantages of allowing fast, objective, *in vivo* measurements of the nerve fiber layer thickness, without the need for pupillary dilation. In normal subjects, SLP is reported to have a good reproducibility of NFL measurements, with a coefficient of variation of 3.6 to 5.2% for repeated measures (45, 46). Also, this technique showed a 96% sensitivity and a 93% specificity for detecting glaucoma (45).

2.1.2 The optic nerve head

Within the nerve fiber layer, retinal ganglion cell axons are segregated into individual nerve fiber bundles which form the optic nerve. To allow an easier visualization of the various layers of the ONH, Figure 7 presents an overview of the neural and vascular interrelation of the anterior portion of the optic nerve. For descriptive purposes, the ONH can be divided into four regions, from anterior to posterior in relation to the NFL and the lamina cribrosa (18, 23, 24, 47, 48, 49):

1. *Surface nerve fiber layer*. This NFL is continuous with the adjacent NFL of the retina and is composed predominantly of unmyelinated axons of retinal ganglion cells. About 5% of its volume is occupied by blood vessels and glial tissue (23). The optic disc, or papilla, measures approximately 1.5 mm in horizontal diameter and 1.7 mm in vertical diameter (49). The surface of the ONH, adjacent to the vitreous, is covered by a thin inner limiting membrane, which merges at the edges with the thicker inner limiting membrane covering the surface of the retina.

2. *Prelaminar region*. This portion of the ONH is located between the surface NFL and the lamina cribrosa. It is comprised essentially of ganglion cell axons along with their supporting glial tissue and blood vessels. At this level, there is a significant increase in the quantity of astroglial tissue. Astrocytes surround the bundles of axons like tubes and often end as footplates on the blood vessels. This type of glial cell provide structural support to the retina and optic nerve and also contribute to the nourishment of the neuron as an intermediary of metabolism. Furthermore, they form a barrier between the nerve fibers and the vessels, contributing in part to the blood-brain barrier (49). The bundles of ganglion cell axons are confined to the outer edges of the prelaminar region, forming the *neuroretinal rim* seen clinically.

3. *Lamina cribrosa region*. This region represents a continuation of the anterior third of the sclera across the posterior scleral foramen. The lamina cribrosa is comprised of approximately ten sheets of connective tissue, which are fenestrated to allow for the passage of the nerve fiber bundles and central retinal vessels. This arrangement is depicted in the ultrastructural section through the laminar portion of the anterior optic nerve in Figure 8. At the same time, the function of the intralaminar part of the optic nerve head is to preserve IOP against a gradient between the intraocular and extraocular spaces. Each lamella forming the lamina cribrosa is composed of elastin and collagen, which provide this region of the eye with tensile strength and resistance to distorsion. Approximately 200 to 600 irregular pores cover the surface of the lamina cribrosa (23). Pores in the superior and inferior poles of each lamella are larger and less supported by surrounding connective tissue than in the nasal and temporal regions. The nasal part contains the smallest pores and the thickest connective tissue and glial columns. This may explain the greater susceptibility of the superior and inferior poles to distorsion from an increase in the IOP. The effect of elevated IOP on changes in the structure of the lamina and the ganglion cell axons transitting the laminar pores has been the basis for speculation of the pathophysiology of glaucoma

4. *Retrolaminar region*. Posterior to the lamina cribrosa, the optic nerve leaves the eye and assumes its intraorbital position. Here the axons of the ganglion cells become myelinated, and thus cause an increase in the calibre of the nerve posterior to the lamina cribrosa. At this point, the optic nerve becomes ensheethed from outside inwards by three intracranial meningial layers: the outer *dura matter*, the intermediate *arachnoid,* and the inner *pia matter.*

2.1.2.1 The optic nerve in glaucoma

Glaucoma causes various progressive changes in the optic nerve head during the early and advanced stages. Since the ganglion cell axons are the principal cells in the ONH, a progressive loss of axonal fibers causes an enlargement of the optic disc cupping and a thinning of the neuroretinal rim. For unknown reasons, fibers residing in the inferior and superior sectors of the ONH are affected earlier by glaucoma than fibers occupying the temporal or nasal sectors of the ONH. Figure 9 shows a cross-section of the lamina cribrosa in confirmed glaucoma, illustrating the selective atrophy of the superior and inferior nerve fibers, leaving evacuated laminar pores. The higher susceptibility of the superior and inferior poles of the ONH to glaucomatous damage accounts for the characteristic vertical elongation of the ONH cupping.

It is believed that the structure of the lamina cribrosa may play a role in the vulnerability of the vertical poles because the larger pores with less supportive connective tissue surrounding the nerve fiber bundles are found in the superior and inferior sectors. Compression and rearrangement of successive sheets of the scleral lamina cribrosa have been reported (30). The laminar pores may progressively enlarge or distort, leading to an ectasia or backbowing of the lamina cribrosa. With progression of the disease, changes in the composition of the laminar tissue and extracellular matrix may result in a loss of compliance and development of stiffness of the scleral lamina (32). This stiffness may "choke" off the axons passing through the rigid laminar plates and cause permanent visual field loss.

Fig. 2

Retinal layers and neural elements

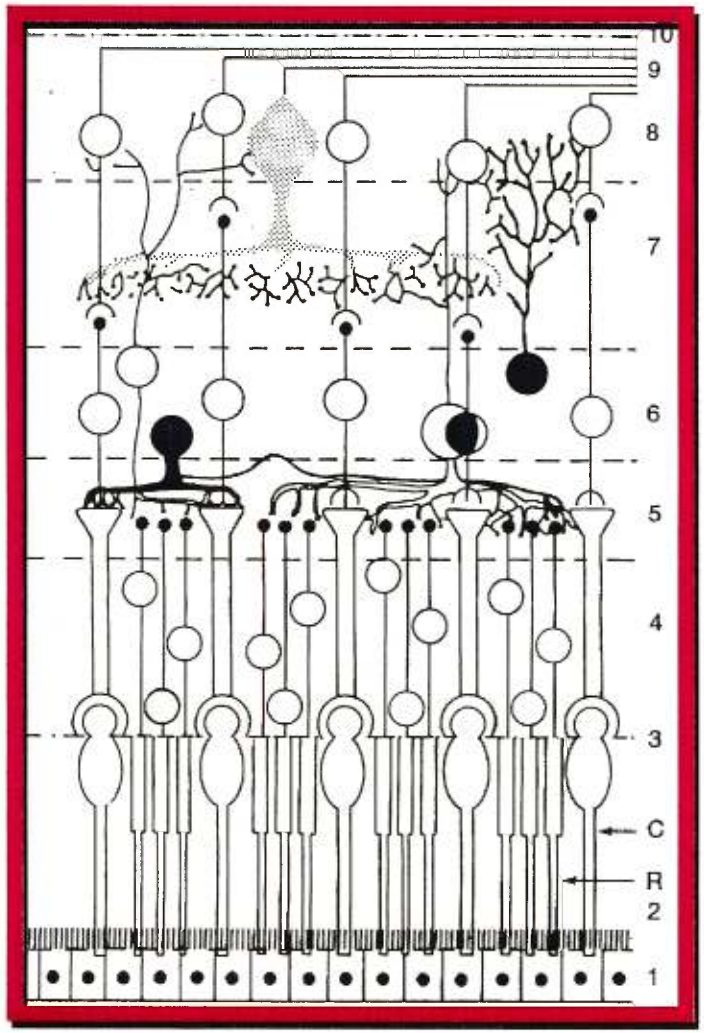

10. Internal Limiting membrane
9. Nerve Fiber Layer

8. Ganglion Cell

7.Inner Plexiform;
Amacrines,Bipolars

6. Inner Nuclear

5. Outer Plexiform;
Rods / Cones, Horizontals

4. Outer Nuclear

3. External Limiting Membrane

2. Photoreceptor: Rods/Cones

1. Pigment Epithelium

Fig. 3

Morphological organization of the RNFL and the corresponding clinical measurement by Scanning Laser Polarimetry

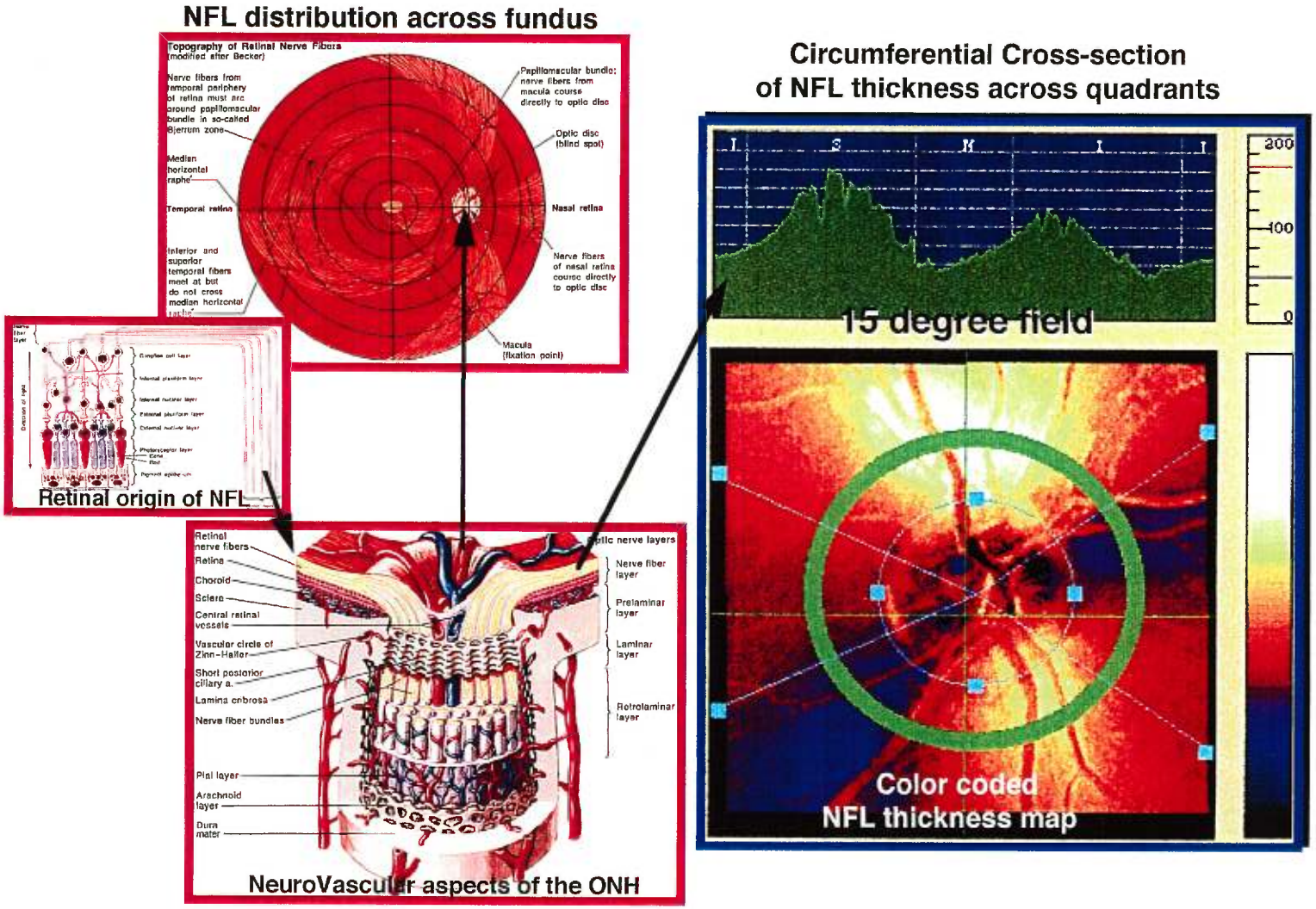

Fig. 4

SCANNING LASER POLARIMETRY
- neuro-optical basis for NFL thickness measurements -

Longitudinal histological section of NFL

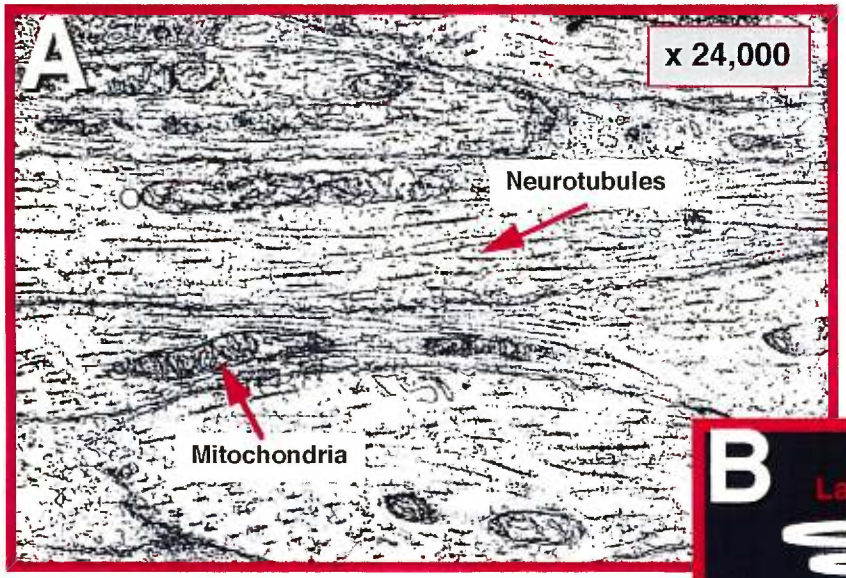

Adapted from: Hogan, Histology of the human eye.

A. The NFL is well vascularized. The ganglion cell axons comprising the NFL vary in cross sectional diameter (0.6 to 2.0 μm), are grouped into bundles, and are surrounded by glial and Muller cell processes.

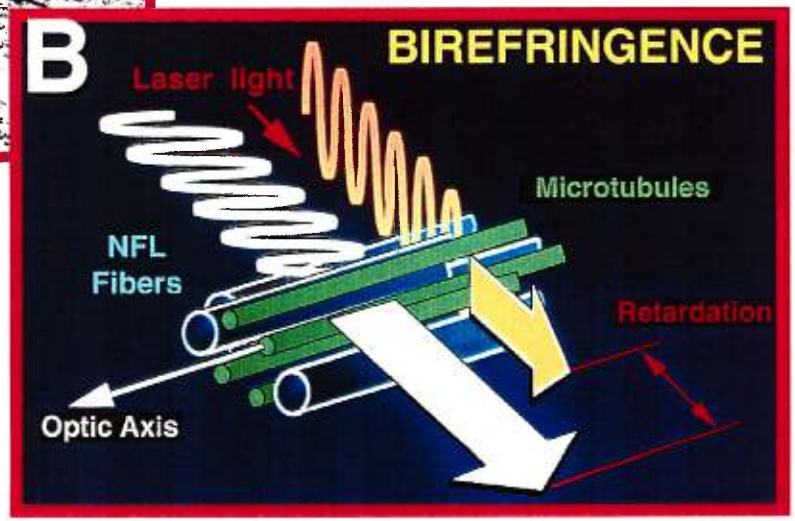

B. The parallel arrangement of the ganglion cell axons and their neurotubules give rise to the birefringence property of the NFL layer in the human retina

Fig. 5

THREE DIMENSIONAL TOPOGRAPHIC PROJECTION OF RETINAL GANGLION CELL AXONS

The specific distribution of nerve fibers within the optic nerve head and their topographical projection to the cone and rod photoreceptors underlies the visual dysfunction characteristic of ocular disease.

Laser doppler flowmetry is a vital tool for elaborating the underlying pathophysiology of neuro-vascular disorders that cause permanent vision loss. In the present study, the fundamental correlation between blood flow and nerve fiber mass was quantitatively examined in normal healthy eyes.

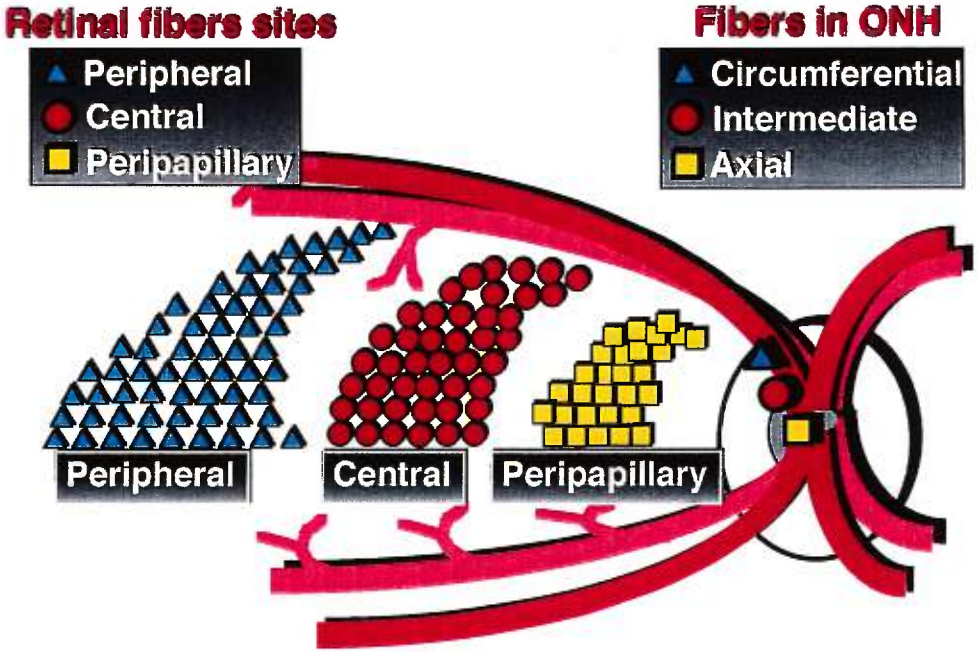

Fig. 6

PATHOPHYSIOLOGY OF GLAUCOMA IN RELATION TO THE PHYSIOLOGICAL VITALITY OF THE NERVE FIBER LAYER

MECHANICAL

Compression from the central ONH outwards causes predictable visual field losses because of the very specific topographic projection of nerve fibers in depth.

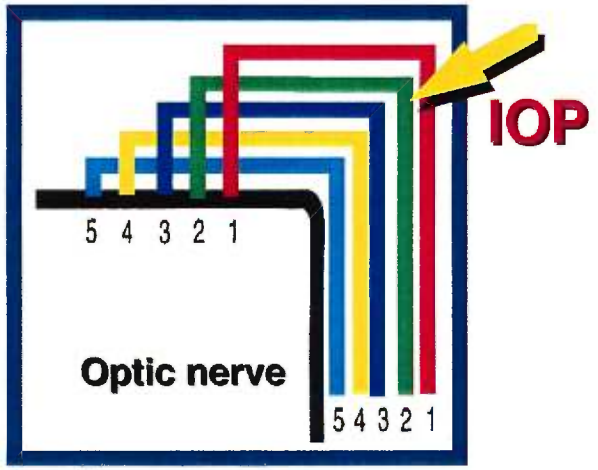

VASCULAR

The normal arterio-venous drainage in the ONH area creates potential for a "watershed" and ischemic neuronal atrophy.

Fig. 7

Neurovascular features of the human optic nerve head

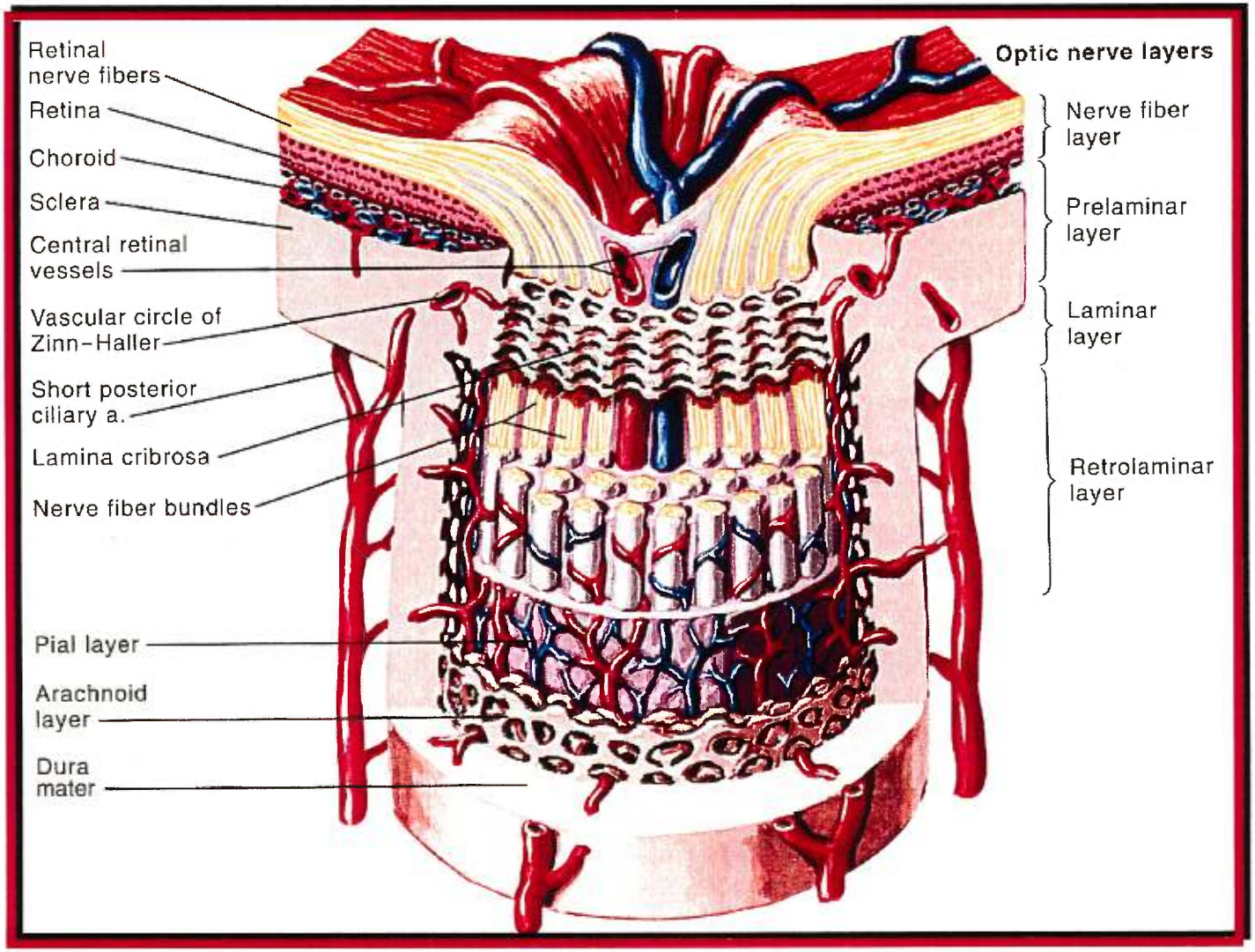

Fig. 8

Ultrastructural appearance of the lamina cribrosa

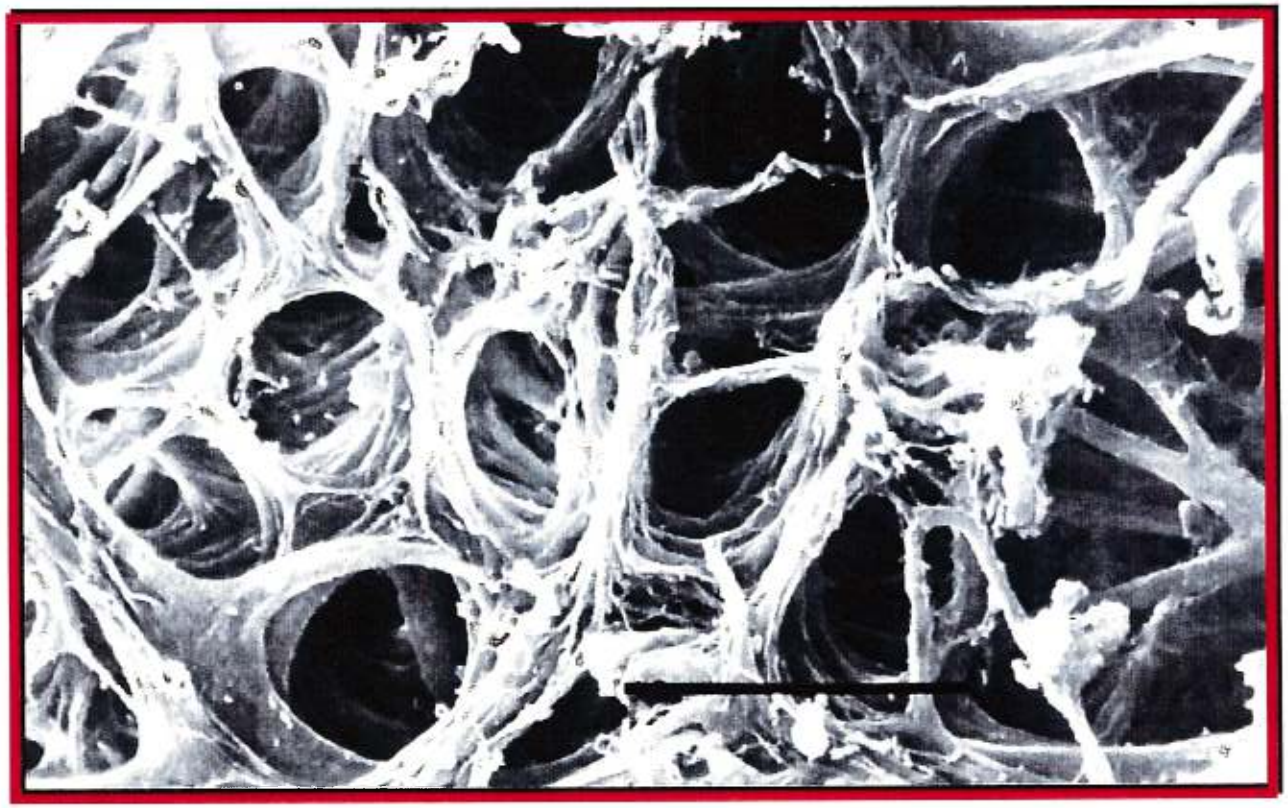

The lamina is composed of collagen beams forming a complex interwoven structure with pores of various size. The pores may be divided by connective tissue struts. Calibration line = 100 μ. Mag X 460. (Adapted from The Glaucomas: Ritch, Shields, Krupin, 1996).

Fig. 9

SELECTIVE NERVE FIBER DAMAGE IN GLAUCOMA

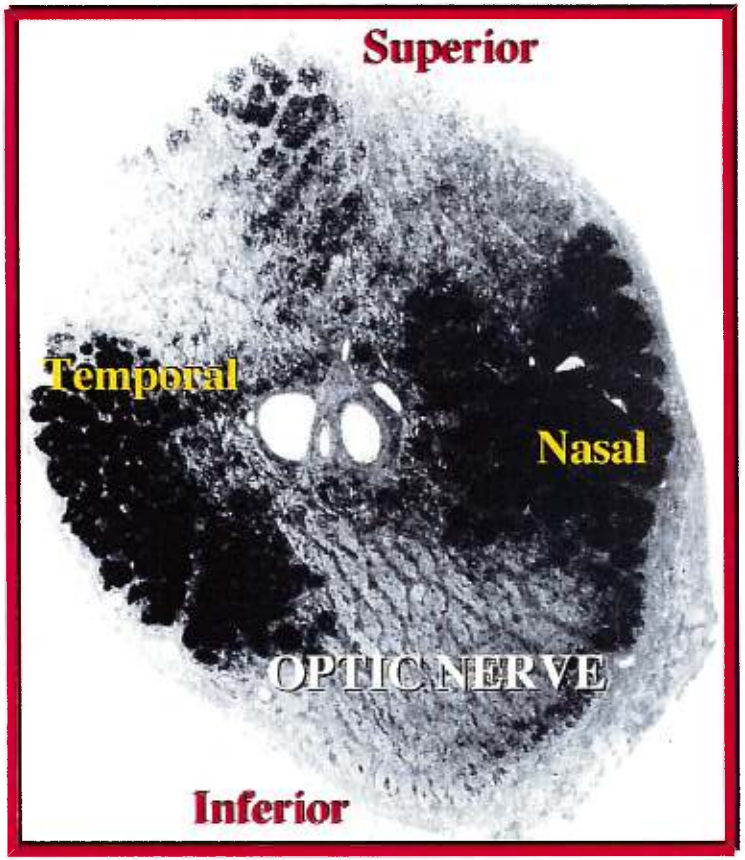

HISTOPATHOLOGY:

- Preferential nerve fiber damage
- Superior/inferior fibers affected first
- Lack of supportive tissue in vertical meridian may lead to sectorial nerve fiber atrophy

2.2 VASCULAR SUPPLY TO THE EYE

A general review of the vascular supply of the retina and ONH is essential for understanding the mechanisms involved in the growth and maintenance of retinal ganglion cells, as well as the micro-environmental disturbances that can lead to cellular atrophy.

In humans, all blood vessels to a single eye are derived from the ophthalmic artery (OA), which is a branch of the internal carotid artery. The ophthalmic artery branches into the central retinal artery (CRA), two or three posterior ciliary arteries (PCAs), and several anterior ciliary arteries. (50)

2.2.1 Vascular supply of the retina

The human retina has a dual vascular supply, with the retinal vasculature perfusing the inner 2/3 of the retina, while the choroid nourishes the outer 1/3 (50). The central retinal artery (CRA) with its subdivision of arteries and capillary plexus perfuses all the cells of the neural retina with the exception of the photoreceptors which are nourished by the choroidal vasculature. The CRA pierces the optic nerve approximately 10 mm behind the eyeball (50) and assumes a central position at the optic disc, where it branches into four major vessels. Each of these main branches supply one quadrant of the retina. The retinal circulation is end-arterial in nature; the central retinal artery has no communication with adjacent afferent vessels (51, 52). Thus, if the central retinal artery or one of its branches is occluded, arterial blood cannot reach the corresponding perfused sector of the retina, causing rapid death and atrophy of the surrounding neural and glial tissues of the inner retinal layers, while sparing the deeper retinal layers supplied by the choroid. Another possible implication of this end-artery system is that a potential "watershed zone" can be created at the limits of the territories supplied by two or more end-arteries; the neural tissue comprising this area of comparatively lower perfusion pressure may be more at risk of ischemia during global decreases in ocular perfusion pressure.

Fluorescein angiographic studies have revealed the presence of such "watershed zones" for the PCAs, which are also end-arteries (48). However, this technique has limited capacities for the description of retinal perfusion levels since the *continuous* endothelium of retinal capillaries shows little to no leakage of fluorescein (50). Therefore, retinal watershed zones have not been demonstrated, but are theoretically plausible. In such a case, watershed zones falling in the vertical meridian of the ONH could place "at risk" for ischemia the denser populations of nerve fibers occupying this area.

Figure 10 illustrates schematically the dual vascular supply to the retina described above. In the present study, the perfusion state of the retinal vasculature which perfuses the inner 2/3 of the retina is the focus for blood flow measurements.

Within the retina, there are regional variations in the density and pattern of capillary distribution. The larger blood vessels lie in the innermost portion of the retina, mainly in the nerve fiber and ganglion cell layers. The outer retinal layers (including the photoreceptors) and the fovea are avascular (50, 51). Figure 11 presents an erosion casting of the vessels in the foveo-macular area to illustrate that the fovea is devoid of retinal vessels and is nourished exclusively by the underlying choriocapillaris. The smaller vessels (precapillary arterioles, postcapillary venules and capillaries) are found between the nerve fiber and inner plexiform layers; the inner nuclear layer receives 2.4% of the capillary volume, the inner plexiform layer, 0.5%, and the ganglion cell and nerve fiber layers, 1.3% (51).

In contrast to most microvessels, the arterioles and venules of the retina do not run parallel courses in close proximity to each other. Figure 10 illustrates how these retinal vessels are connected through elaborate networks of capillaries, suspended from two arterioles situated in the superficial layers (53). From a single terminal arteriole there arises a plexus of 10 to 20 interconnecting capillaries each approximately 5μm in diameter (51, 53). Figure 12 shows the

intricate layout of retinal arterioles and capillaries based on an erosion cast obtained from a monkey retina. Laser Doppler blood flow measurements in the present study reflect the blood flow in such a fine retinal capillary network. The retinal capillary network has multiple arteriolar feed-points, thus blockage of a single terminal arteriole will not lead to total cessation of flow in the immediately surrounding capillary bed (51).

The retinal capillary bed is a complex meshwork of small-caliber channels which tend to be arranged in layers. In most regions of the retina, the flat capillary networks are two-layered, with the superficial capillaries residing in the nerve fiber and ganglion cell layers; the deeper capillary layer is found in the inner nuclear layer. The average meshwork diameter varies between 50μm and 65μm for the outer and inner networks, respectively (51, 53). This basic two-layered capillary pattern differs across the various regions of the retina. At the posterior pole, in the peripapillary region, the capillary networks are dense and may become three or four-layered, whereas in the periphery, the deep net disappears, leaving a single layer of wide-mesh capillaries. The extreme periphery is avascular. For the macular region, a single layer of capillaries is found in the perifoveal area, while a capillary-free zone of 400 to 500μm is found around the fovea itself (51) (refer to Figure 11). This differential distribution of retinal vessels across the fundus may represent an effort to maintain arterial blood supply proportional to the metabolic demands and density of the nerve fiber tissue, which become rarer towards the fundus periphery, with the exception of the vital fovea. To compensate for the lack of retinal vessels at the macula, a thicker underlying choriocapillaris is found at this level, and retinal capillary meshworks become multilayered in nerve fiber layers immediately adjacent to the limits of the macular area. This inhomogeneity of retinal capillaries across the fundus supports the fundamental premise of the present study that retinal blood flow could show regional differences in accordance with variations in the NFL thickness.

Aside from the basic capillary arrangement discussed above, there is a distinct stratum of capillaries occupying the superficial portion of the NFL in the peripapillary retina, the *radial peripapillary capillaries* (RPCs). This superficial layer of capillaries extends from the optic disc, with its main extensions in the upper and lower temporal directions, mainly following the course of the arcuate fibers. The RPCs are found to a lesser extent in the nasal quadrants adjacent to the disc and are absent from the central macular region temporal to the disc. The radial capillaries are characterized by a long pathlength, few arteriolar feedpoints and few anastomoses. Their function is to nourish the superficially located nerve fibers surrounding them. They are fed along their course by the same arteriole that supplies the deeper capillary networks. It is thought that an increase in the IOP may cause blood to deflect from the higher resistant radial capillaries into the deeper capillaries (51). The projection pattern of the RPCs raises the possibility that they are implicated in the development of Bjerrum's scotomas in glaucoma (52).

A characteristic periarterial capillary-free zone of about 120μm is found around the retinal arteries (52, 54). Sometimes described as oxygen-rich areas, these free spaces around the large vessels may represent a compromise between optimal visual function and the nutritive needs of the delicate neuronal network (54). In the present study, blood flow measurements by LDF were carried out in retinal areas devoid of large visible retinal vessels. However, due to great intersubject differences in the distribution of the retinal vessels, some measurements were likely obtained from regions immediately adjacent to arterioles, which could have influenced the absolute value of blood flow in the test site. Less prominant capillary-free zones around the retinal veins have also been reported (51, 54).

A cursory comparison of the physical attributes of the dual vascular supply of the retina reveals that vessels comprising the retinal capillaries are smaller in caliber (about 5 to 7μm) than the ones forming the choriocapillaris (10μm and

greater) (54). An overlay of the retinal arterio-capillary structure and the underlying choriocapillaris is presented in Figure 13 for comparison of vessel geometry. The combination of small caliber retinal capillaries and the relatively sparse distribution of the retinal vessels explains the low blood flow volume in the retina (0.5 to 1.7 ml/min per gram tissue) compared to the choroid (18.0 ml/min per gram tissue) (54). The choroid in fact is "overperfused" with respect to its nutritive needs in the outer retina. Considering the higher metabolic activity of the retinal tissue, this vascular architecture results in a larger arterio-venous pO2 difference and consequently a lower capacity to tolerate periods of reduced perfusion. This physiological vulnerability may explain the need for a vascular autoregulatory system in the retinal blood supply. A more detailed comparison of retinal and choroidal blood flow will be presented in a subsequent section.

Retinal capillaries are of the *continuous* type, like the capillaries found in the cerebral tissue (50, 51). Continuous capillaries are the most impermeable type because of tight connections between adjacent cells of the endothelium. This anatomical feature accounts for the blood-retinal barrier, and among other things, for the lack of fluorescein leakage from the retinal capillaries during fluorescein angiography. Carrier mediated transport systems are responsible for the exchanges of important metabolic substrates. The blood-retinal barrier can be altered by a variety of stimuli, including drugs, ocular diseases, surgical trauma and systemic diseases such as diabetes and hypertension (50). All of these can lead to a transfer of infectious organisms into the retina whenever the integrity of the vessel wall is compromised.

Retinal veins are also present in the inner retina where they alternate with retinal arteries. At the posterior pole, the retinal veins drain into the central retinal vein (CRV) while towards the periphery venous drainage occurs via the vortex veins. At the ONH level the sole efferent vessel for the retinal venules is the central retinal vein (CRV) (52).

2.2.2 Vascular supply of the optic nerve

Figure 7 (section 2.1) presents an artist's conception of the neuro-vascular elements of the ONH, given for reference to the following description of the ONH vasculature. The blood supply to the ONH comes from one to five posterior ciliary arteries (PCAs) and the central retinal artery that arises from the ophthalmic artery. The posterior ciliary arteries, usually distributed in the medial or lateral side of the optic nerve, form two *long PCAs* and many *short PCAs.*

Hayreh (48) is one of the most cited authors for his extensive and detailed work on the blood supply to the ONH. He has studied the vasculature of the ONH since 1955 in anatomical, histological, experimental and clinical studies. Most of the following descriptions of the ONH features are based on Hayreh's work. The blood supply to the ONH will be described according to its four distinct anatomical regions, as discussed in the previous chapter. A line drawing showing these anatomically overlapping regions of the ONH is presented in Figure 14.

1. *Surface nerve fiber layer of the ONH.* Like the retina, this surface layer of the optic disc is mainly supplied by the retinal arterioles, which are continuous with the peripapillary retinal and long radial peripapillary capillaries. Posteriorly, they anastomose with vessels of the prelaminar region. In some individuals, the temporal sector of this layer may be supplied by the posterior ciliary circulation of the prelaminar region; occasionally, these vessels may enlarge to form *cilio-retinal* arteries. The capillaries of this surface layer of the nerve are mostly of venous nature, draining into the central retinal vein or its tributaries.

2. *Prelaminar region of the ONH.* This region is mainly supplied by centripetal branches from the large peripapillary choroidal arteries, which are of ciliary-origin. These branches arise from the short PCAs and have a segmental

distribution. The temporal part of this region is the most vascular. The central retinal artery and the peripapillary choriocapillaris do not contribute branches to the prelaminar region. Capillaries from this region drain into the central retinal vein or through the choroid into vortex veins.

3. *Lamina cribrosa region of the ONH.* This region is a highly vascular section of the ONH. It is supplied by ciliary vessels, which come directly from the short posterior ciliary arteries, as well as some from the recurrent pial branches from the peripapillary choroid. In some cases, the ciliary arteries provide an incomplete vascular system around the lamina cribrosa, called the *circle of Zinn-Haller.* The central retinal artery plays no role in perfusing the lamina cribrosa region. The venous drainage of the lamina cribrosa is primarily via the central retinal vein.

4. *Retrolaminar region of the ONH.* This region is mostly supplied by the pial arteries whose main branches run parallel to the optic nerve and send out smaller radially inward vessels into the optic nerve. The peripheral pial plexus of the retrolaminar region may occasionally be supplied by centripetal branches from the central retinal artery and other orbital arteries. Frequently, but not always, the central retinal artery may also provide axial centrifugal branches. Venous drainage is once again into the central retinal vein.

There are both transverse (centripetal) and longitudinal blood vessel systems in all portions of the optic nerve. The principal blood supply to the anterior optic nerve comes from the SPCAs. Short PCAs contribute to some extent to all portions of the optic nerve, whereas the branches of the central retinal artery supply only the superficial nerve fiber layer and the axial portion of the retrolaminar region (23). Although derived from both the retinal and ciliary circulations, the capillaries of the ONH resemble more closely the features of the continuous retinal capillaries. In the present study, blood flow measurements were carried out in retinal peripapillary sites and correlated with

corresponding NFL thicknesses. Retinal sites were preferentially chosen over sites on the ONH for LDF measurements, principally to eliminate interpretational difficulties inherent to measurements on the much smaller optic nerve head which is also supplied by a continuous dual arterial system.

A continuity between small vessels from the retrolaminar region to the retinal surface has been observed (24). Hayreh (48) points out that the presence of a continuous capillary network does not exclude a sectorial distribution of blood supply in the ONH. Effectively, the ciliary blood supply to the lamina cribrosa and prelaminar regions displays a segmental distribution, perhaps reflecting differing metabolic needs across the optic nerve sections. The main PCA supplies the nasal or temporal half in some cases, and the superior and inferior half in others. The smaller short PCAs may supply smaller segments of the optic nerve which may be quadrantic or smaller (55). Thus, the most anterior portion of the optic nerve that includes the prelaminar and laminar zones has a segmental blood supply. If such a segmental distribution of capillary blood flow in the optic nerve occurs and has a functional significance, then a similar distribution of blood flow by segment in the peripapillary zones is a possibility and may reflect differential physiological requirements by the perfused neural tissue. Such could be the case for the retinal nerve fibers which are found across the entire fundus, but occur in greater number in the vertical quadrants in the normal eye. As a result, the present study will investigate whether the degree of retinal blood flow is proportional to the nerve fiber layer thickness in the four major quadrants.

Hayreh (48) has found a marked inter-individual variation in the blood supply to the ONH in man. This variation is the result of many factors, including variations in the distribution pattern of the blood vessels, variations in the pattern of posterior ciliary artery circulation, and the location of the so-called "watershed zone(s)" that occur between the various posterior ciliary arteries and represent areas of potential hypoperfusion. This inter-individual variation in the pattern of vessel distribution could result in marked inter-individual

differences in local retinal blood flow values when measurements are made with a sensitive technique such as laser Doppler flowmetry.

Each posterior ciliary artery is an end-artery system, perfusing a specific volume of tissue with no anastomoses between vessels. When a tissue is supplied by two or more end-arteries, the area between the territories of distribution of any two end-arteries is called a *watershed zone.* In the event of a fall in perfusion pressure in the vascular bed of one or more end-arteries, the watershed zone, being an area of comparatively poor vascularity, is most vulnerable to ischemia. The location of the PCA watershed zone in relation to the optic disc depends upon the distribution pattern of the various PCAs and determines the vulnerability of the corresponding part of the optic disc to reduced perfusion pressure (48). For an individual with a medial and lateral posterior ciliary artery, the watershed region may be found anywhere between the nasal edge of the optic disc and the fovea. Such individual variations may influence the relative susceptibility of the optic nerve to potential ischemic damage resulting from an increase in the IOP. As described previously, the retinal vasculature is also composed of end-arteries; therefore, watershed zones may also occur at the level of the inner retinal layers and account for ischemic changes in peripapillary regions.

Fig. 10

PERFUSION DEPTH OF DUAL RETINAL VASCULATURE

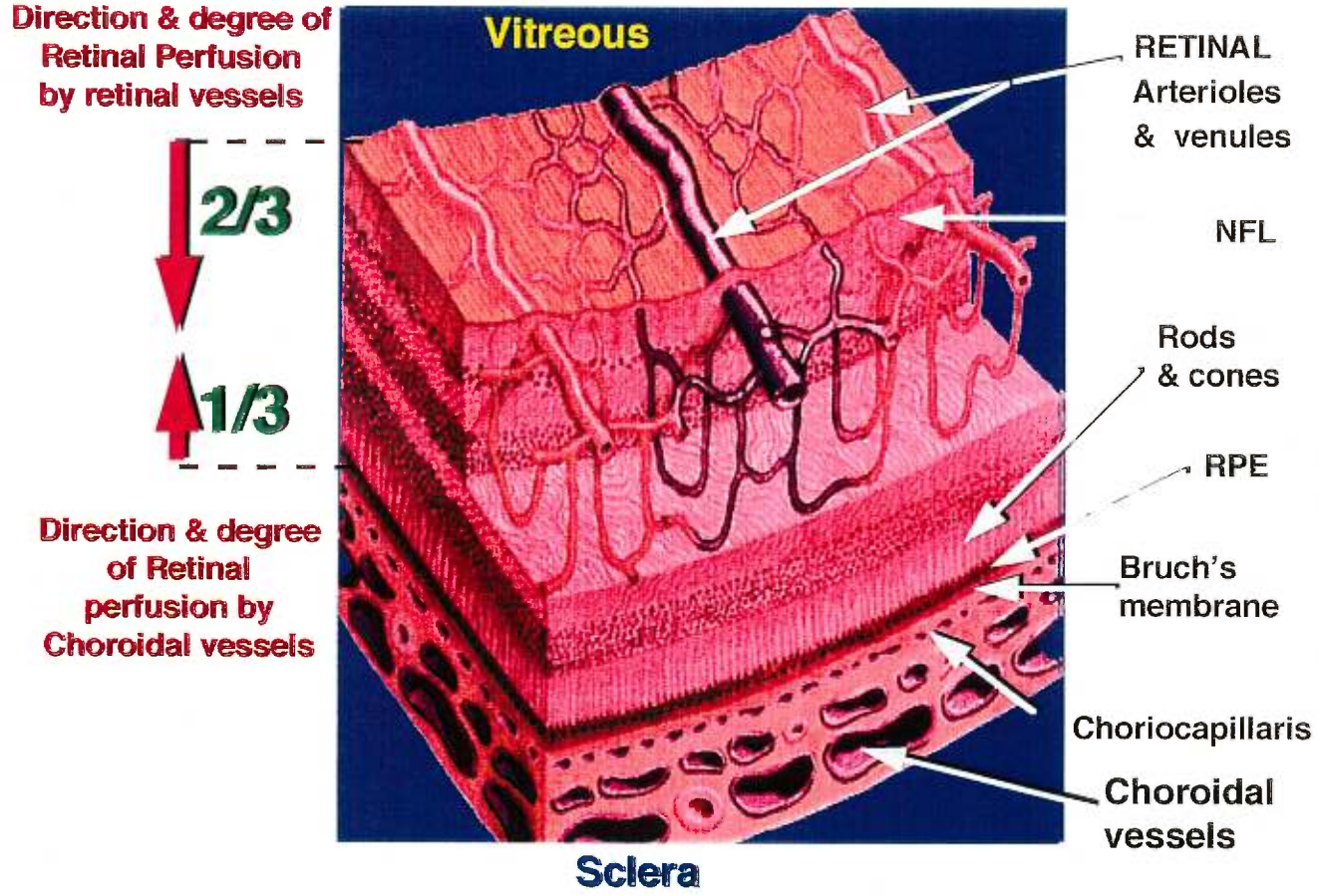

Fig. 11

SEM of resin cast showing capillary-free zone in the macular area (cynomolgus monkey)

Fig.12

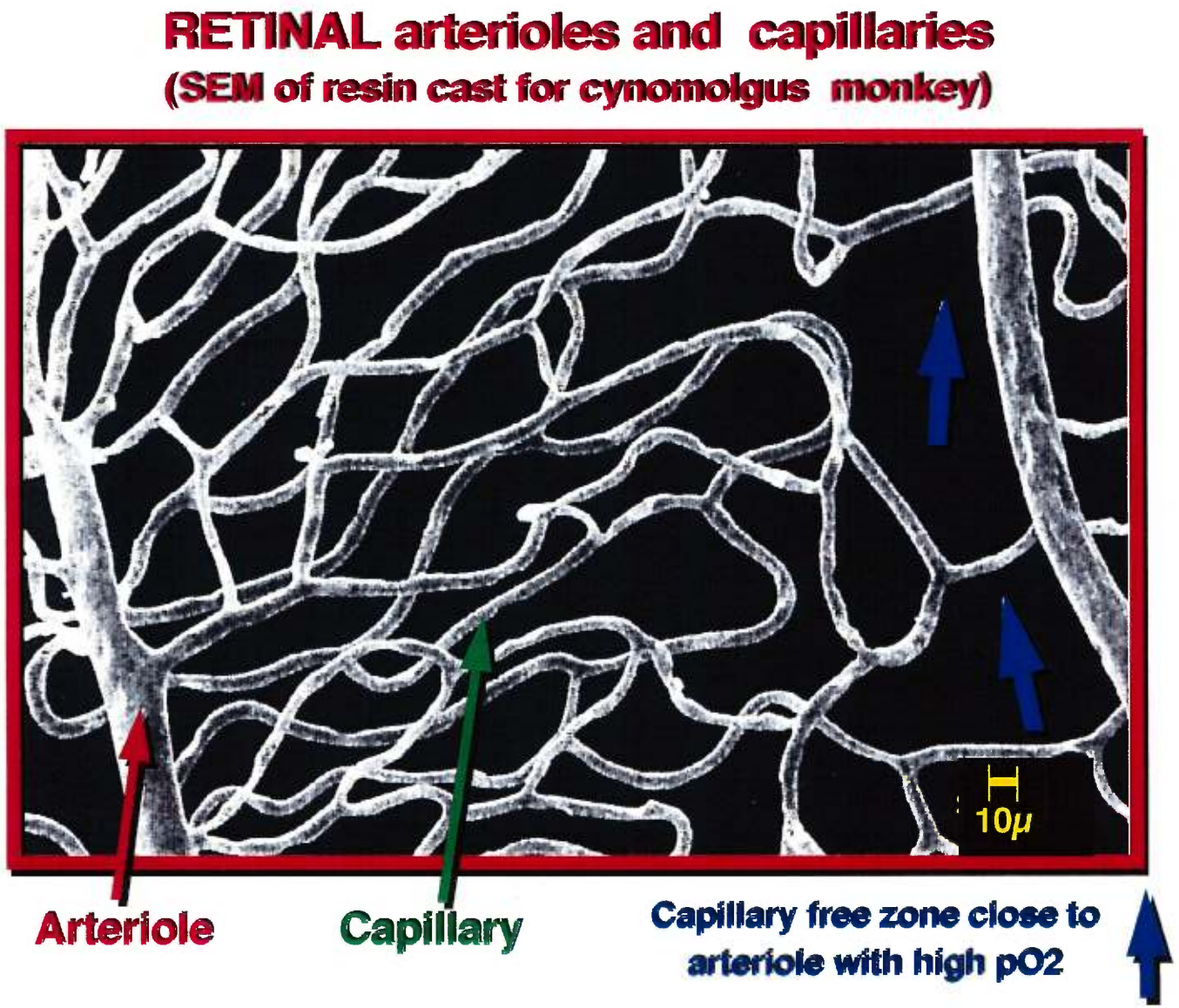
RETINAL arterioles and capillaries
(SEM of resin cast for cynomolgus monkey)
10μ
Arteriole
Capillary
Capillary free zone close to
arteriole with high pO2

Fig. 13

Retinal vs Choroidal vasculature; blood flow sampling possibilities during Laser Doppler Flowmetry

10 μm and greater diameter Choroidal lobules provide a blood flow of ~18 ml / min per gram tissue.

5-7 μm diameter Retinal capillaries provide a blood flow of ~ 0.5 - 1.7 ml / min per gram tissue.

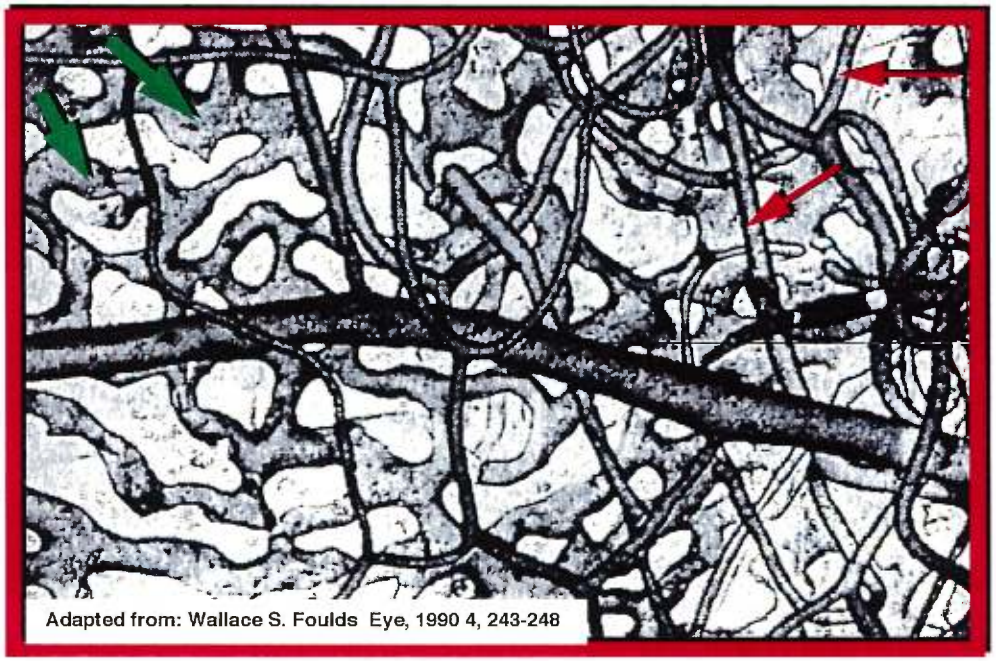

SEM of a resin cast of a retinal and choroidal site highlighting the size difference between the retinal capillaries and the underlying choriocapillaris. LDF measurements of blood flow at different retinal sites most likely measures blood flow exclusively in the retinal capillary plexus because of 670nm laser tissue penetrance; a longer wavelength laser diode is required for sampling blood flow in the choroid which lies beyond the retinal pigment epithelium.

Fig. 14

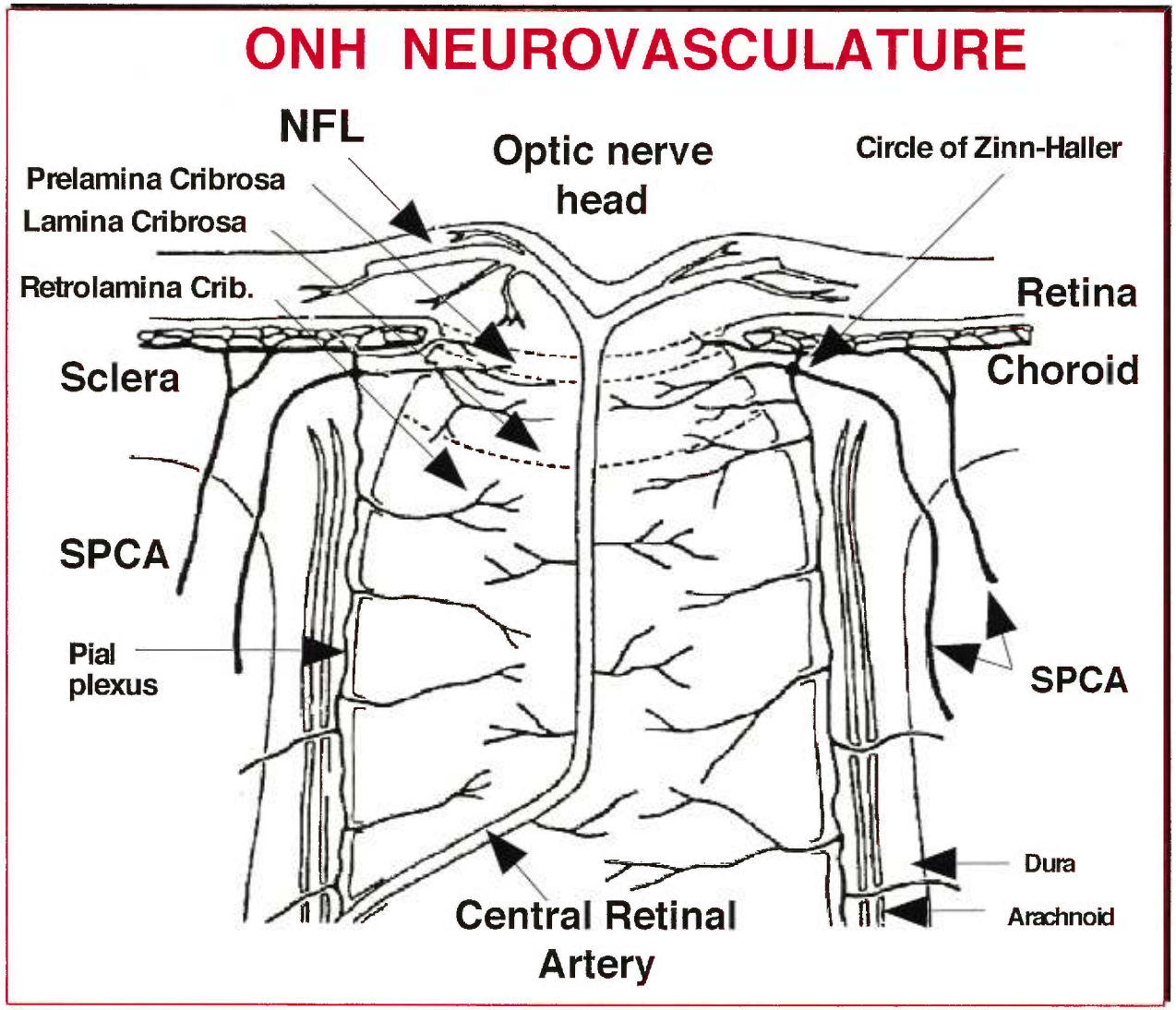
ONH NEUROVASCULATURE
NFL
Optic nerve head
Circle of Zinn-Haller
Prelamina Cribrosa
Lamina Cribrosa
Retrolamina Crib.
Retina
Choroid
Sclera
SPCA
Pial plexus
SPCA
Dura
Arachnoid
Central Retinal Artery

2.3 THE PATHOGENESIS OF THE OPTIC NERVE HEAD IN GLAUCOMA

Glaucoma is a complex multifactorial optic neuropathy. Although voluminous literature has been devoted to the study of this disease, its etiology and pathophysiology is still not fully understood, mainly because of the lack of uniformity in the clinical findings related to the disease. It was thought for a long time that elevated IOP was the sole factor leading to axonal atrophy in glaucoma. Consequently, even to this day, treatment of the disease has concentrated on lowering the IOP to some arbitrary level. However, cases of patients developing an optic atrophy clinically identical to that of glaucoma in the absence of raised IOP have now been reported routinely. This form of "low tension" glaucoma cannot have an elevated IOP as its sole cause. Also, in many instances patients treated for high IOP with effective pressure lowering drugs continue to show a progressive optic neuropathy and an extension of visual field loss. Such cases have prompted clinicians and scientists to consider other factors than IOP *per se* as leading to glaucomatous changes in neural structure and ultimately visual dysfunction.

The pathogenesis of glaucomatous optic atrophy has remained a matter of controversy since 1858 when two conflicting concepts were introduced. Müller (56) advanced the "*mechanical*" theory of glaucoma which maintains that direct pressure on the nerve fiber results in glaucomatous changes in the optic nerve.

The "*vascular*" theory of glaucoma introduced by von Jaeger (57), suggested that some vascular abnormality was the major underlying cause of optic atrophy in glaucoma. Some 'vasogenic' theories propose that the IOP *per se* may be a determining factor in the impairment of blood circulation in the ONH (24, 58). A clear understanding of the cause of optic atrophy in glaucoma is essential for its early detection and effective treatment. A schematic comparison of the possible mechanisms underlying the "vascular" versus "mechanical" theories of glaucoma is presented in Figure 6 (section 2.1).

2.3.1 The mechanical theory

Epidemiological studies have reported an average IOP of about 15 mm Hg in the normal population, with 95% of non-glaucomatous adults having IOP values between 10 and 22 mm Hg (59). Thus, IOPs of 22 mm Hg and above are generally considered "abnormal" or more likely to be associated with a glaucomatous process. Although not predicted by the absolute value of the intraocular pressure, the risk of developing glaucomatous damage increases exponentially with increasing IOP (18). Thus IOP is considered a major risk factor for glaucoma and continues to be the principal factor targeted by today`s therapeutical strategies.

There is evidence that elevation of the intraocular pressure fundamentally alters the function of the structural and neural elements of the retina and the optic nerve. Damage to ganglion cell axons appears to occur at the level of the scleral lamina cribrosa by a blockage of normal cytoplasmic axonal transport. As described earlier, axonal transport is an energy-dependent process that is essential for the survival of the axon. In animal experiments, both orthograde and retrograde axonal flows were found to be blocked at the level of the lamina cribrosa after an acute elevation of IOP (33). In an earlier study, Quigley (60) discribed several mechanisms by which an increase in the IOP could preferentially compress nerve fibers along the vertical axes and cause a characteristic vertical elongation of the physiological blind spot. Figure 15 presents three such mechanisms involving the lamina cribrosa.

Elevated intraocular pressure can create an inside-outside push that compresses the laminar sheets and bows them outward. According to the mechanical theory, a compression of the scleral laminar sheets and distorsion (or misalignment) of the laminar pores could lead to a crimping or pinching of the ganglion cell axons as they pass through this area thereby causing a blockage of axonal transport (32). Microtubules within the axon play an essential role in both orthograde and retrograde axonal transport. Therefore,

compression of an axon resulting in a crushing, distortion, or bending of the microtubules could lead to the blockage of axonal transport and ultimately death of the nerve cell. Interestingly, in the nerve fiber bundles, axons located closer to the edges are more susceptible to axoplasmic obstruction than those located in the central part of the axonal bundles.

The lamina cribrosa, which can be visualized in Figure 8 (section 2.1), is typically presumed to be the principal site of injury to the nerve fibers. This notion of the lamina cribrosa being the principal site of neuronal damage in glaucoma may be partially explained by its unique anatomical features. The lamina cribrosa is the site of maximal fiber convergence along the course of the nerve fiber bundles from the eye to the brain. The addition of interaxonal glial tissue between the disc and the line of myelinisation further contributes to the tissue congestion in this region of the optic nerve. These anatomical features may contribute to the susceptibility of axons to pressure-induced axon injury at the level of the lamina cribrosa. Furthermore, the lamina cribrosa is the site of a large pressure gradient between the intra and extraocular axon segments; it is very likely the boundary between eye and brain pressure and is a region where compression would most likely distort axonal bundles with indentation by surrounding glial beams.

However, the lamina cribrosa may not be the only site of damage to the nerve fibers in glaucoma. Since axonal transport is an energy-dependent process, an adequate supply of oxygen to the ganglion cell is also essential to maintain the vital transport systems. Thus, a reduction in blood supply to the nerve or any portion of the axon to a level that results in ischemia, could also block axonal transport and lead to death of the nerve cell. In this context, the role of blood flow in glaucoma will be discussed.

2.3.2 The vascular theory

There are many clinical observations of glaucoma-like changes (3) which cannot be explained by a pressure mechanism alone; the following presents a few examples of why pressure alone cannot adequately explain the development of glaucomatous changes in neuronal structure and function.

1) Glaucoma-like optic atrophy is often seen in individuals consistently showing IOPs lower than 22 mm Hg (so-called low or normal tension glaucoma);

2) Visual field loss may progress in hypertensive glaucoma patients despite lowering of the IOP;

3) Some individuals with IOPs consistantly higher than 22 mm Hg never develop visual field defects;

4) The incidence of glaucoma is higher in females than in men, although men and women have approximately the same IOP;

5) The average IOPs of blacks and whites are about the same; yet blacks are 4 times more likely to develop glaucomatous damage;

6) In Japan, although the incidence of glaucoma increases with age at about the same rate as it does in western countries, the IOP diminishes with advancing age (contrary to the west) (3, 59).

It is then likely that glaucomatous optic neuropathy may derive not only from elevated intraocular pressure, but also from a variety of other risk factors which are only now being identified and understood. Consequently, the term *low-* or *normal-pressure glaucoma* (NPG) was introduced to define glaucomatous optic neuropathy without clinically noticeable elevation of the IOP. The vascular theory supports the idea that vascular abnormalities, whether the primary result of elevated IOP or, an unrelated vascular lesion, are the underlying cause of glaucomatous optic atrophy through ischemic processes (18, 24). It is implied

that an "uncontrolled" reduction in blood supply to the retinal ganglion cell may reduce the energy source necessary to maintain the axoplasmic transport which is essential to the survival of the cell.

Many scientists and clinicians believe that the various types of glaucoma may be explained by different factors, with one or more being predominant over the others in a singular form of glaucoma. As mentioned in a previous section, optic nerve damage from glaucoma can occur in either a diffuse of focal pattern. Several studies (3, 32) have demonstrated that patients with predominantly localized defects are usually older and do not have high IOPs. Thus, focal damage in glaucoma is thought to be related more to vascular insufficiency than elevated IOP. Since local nerve fiber damages in glaucoma occur principally in the vertical poles of the ONH, it is essential that the vascular supply to these susceptible areas be studied to understand basic hemodynamics in these areas. Therefore, in the present study, the normal distribution of retinal blood was evaluated through non-invasive measurements of blood flow in peripapillary sites of varying NFL thickness. The main objective was to determine whether, in the normal human retina, regions of thicker NFL at the vertical poles of the ONH would benefit from higher blood flow levels in proportion to the number of nerve fibers to be nourished in this area.

2.3.2.1 Evidences for vascular disturbances in glaucoma

There is increasing evidence supporting a vascular origin for glaucoma. Nonetheless, some disparities exist between the various findings in support of a vascular basis for glaucoma. Both a reduction in the number and size of peripapillary choroidal vessels (32) and a reduction in the capillary plexus of the optic nerve have been demonstrated in glaucoma (58). This loss of small vessels in the optic nerve head was thought to accompany atrophy of axons. However, studies by Quigley et al (24, 61) failed to reveal a major selective loss of optic nerve head capillaries in early glaucoma. This suggests that the capillary dropout is not the cause of glaucoma changes in the ONH, but

secondary to neural atrophy. Most capillaries in the retinal and prelaminar regions dropout only in the late stages of glaucoma. Interestingly, the capillaries in the lamina cribrosa are preserved even in absolute glaucoma when vision loss is severe (33). Other studies have shown capillaries present in the scleral lamina in glaucoma patients at all stages of the disease, with the percentage of capillaries remaining remarkably constant (32). Capillaries are lost at a rate that maintains the usual ratio of capillaries to axon to glial cells. Earlier reports had described a selective atrophy of the radial peripapillary capillaries supplying the arcuate areas of the nerve fiber layer; however, these observations were later disproved (32). These findings suggest that disturbances in the quality or quantity of blood available to the retinal neurons, rather than a loss of vascular tissue *per se*, may account for nerve fiber loss in glaucoma.

The major arteries perfusing the globe have also been implicated in glaucoma-like neuronal damage. Occlusion of either the short posterior ciliary arteries or the central retinal artery can obstruct axonal transport and lead to a "dropout" in the NFL (32). In addition, fluorescein angiography has demonstrated a general retardation of blood flow in the retina, optic disc and possibly the choroid when the IOP is elevated (24, 33). Also, most studies examining changes in blood flow in glaucoma have concluded a higher incidence of filling defects when compared to non-glaucomatous eyes. Perhaps the most pertinent finding in glaucoma is a persistent hypoperfusion of the ONH, which correlates with visual field loss in the corresponding visual field projection. The filling defects found in glaucoma are characterized by decreased blood flow, a smaller vascular bed, narrower vessels, and increased permeability of the vessels (24, 33). Splinter disc hemorrhages have also been observed in many cases of glaucoma, often associated with or preeceding the development of the visual field defects. These hemorrages are usually located in the superficial layer of the optic nerve head and occur more often in cases of

low-tension glaucoma rather than in glaucoma with elevated IOP (33). Their possible role in the pathogenesis of glaucoma is not fully understood.

More recent studies on ocular hemodynamics have also shown increasing evidence of the possible contribution of circulatory disturbances in the pathogenesis of glaucoma. For instance, studies have demonstrated the presence of high concentrations of glutamate in the vitreous body of animal and human eyes with glaucoma (61, 62, 63). It is known that ischemic mechanisms involving the optic nerve and ganglion cells can cause an elevation in glutamate concentration to levels potentially toxic to retinal ganglion cell neurons. Furthermore, several studies have reported a "slowing" of the blood flow in the ocular vessels of glaucomatous eyes as a result of artificially increased IOP. Laser-Doppler velocimetry studies at the level of the optic nerve head microcirculation revealed that the velocity of the red blood cells (RBCs) was reduced and the aggregability of the RBCs was increased in POAG and normal-pressure glaucoma (NPG) patients compared to healthy patients (64, 65). Also, studies using color Doppler imaging techniques demonstrated in POAG and NPG patients a decrease in the end-diastolic velocity (EDV) of the ophthalmic artery (OA) and ciliary arteries (CA), as well as an increased resistance to blood flow in the central retinal artery (CRA), in the OA, and in the CA (66, 67, 68, 69). A reduction of blood flow velocity in the ophthalmic and central retinal arteries was also demonstrated by the finding of a delayed carotid-retina circulation time in normal tension glaucoma (70). Therefore, it is possible that a reduction in blood flow velocity and increased resistance to flow in the major ocular arteries could result in a corresponding decrease in blood flow in the terminal retinal capillary beds which they supply.

Other studies have demonstrated the detrimental effect of high IOP on ocular circulation. For instance, pulsatile ocular blood flow (POBF) was significantly lower in NTG patients compared to normal subjects and showed a substantial decrease with increasing intraocular pressure (71, 72). In some cases, lowering the IOP was reported to improve the quality of ocular

circulation. Indeed, fluorescein angiographic sudies revealed that the arterio-venous passage time (AVP) was significantly reduced in patients with chronic open-angle glaucoma after lowering the IOP by filtering surgery (73). Finally, in a population-based prevalence study of glaucoma, it was found that lower perfusion pressure (average arterial blood pressure minus IOP) was strongly associated with an increased prevalence of POAG (74).

All of the abovementioned findings are in support of the concept that the ocular hemodynamics may be primarily deficient in glaucoma, or significantly impaired as a result of IOP levels exceeding the tolerance thresholds of the eye.

In order to better understand the role of vascular factors in the pathogenesis of glaucoma and the nature of the parametric measurements forming the basis of the present study, three important terms will be defined. These terms include *blood flow*, *perfusion pressure* and *vascular autoregulation*.

2.3.2.2 The basics on ocular hemodynamics

The basis for the vascular theory of glaucoma is that a rise in IOP causes a reduction in blood flow in the intraocular vessels. In the retina and optic nerve head, autoregulatory mechanisms rapidly restore blood flow in response to moderate rises in intraocular pressure or a decrease in blood pressure, thus preventing any ischemic tissue damage (32). One hypothesis related to glaucoma is that eyes with increased susceptibility to glaucoma damage have impaired vascular autoregulation in the optic disc (18).

A) Blood flow

Blood flow is defined as the total volume of blood passing a point in a vessel per unit time (51). Blood flow depends on the following factors: mean blood pressure, intraocular pressure and peripheral vascular resistance. The term "microcirculation" is used to describe blood flow through capillaries and the immediately adjacent arterioles and venules. These vessels are implicated

in metabolic exchanges of respiratory gases, nutrients, and waste products between blood and tissues. They form a major part of the systemic vascular resistance, especially at the level of the precapillary arterioles (51).

Retinal arterial and venous blood flow is *laminar*, with arterial flow having a very small *pulsatile* component. The pulsatility of blood flow in the retinal microcirculation was detectable in continuous recordings of blood flow obtained in this study by means of laser Doppler flowmetry.

In capillaries, flow of cells and plasma is unequal; cells flow faster in the axial stream, while the plasma near the wall moves more slowly. This phenomenon may be compared to a simple hydrodynamic system like a long straight pipe with a constant flow through it: the flow in this pipe can be regarded as a series of concentric laminae moving fastest at the axis and with a fall in velocity away from it. Each lamina is slipping over an adjacent one. This type of flow is termed "laminar" and is said to obey to *Poiseuille's law,* were the pressure head (Δp) in a cylinder is directly proportional to the length (L), the flow (F), the viscosity of the fluid (μ), and inversely proportional to the fourth power of the cylinder radius (R): (51)

$$\Delta p = (8 L \mu F) / (\pi R^4)$$

This equation indicates that a very small reduction in the diameter of a blood vessel can lead to a rather large drop in blood flow in the perfused tissue.

As the rate of flow increases, the regular lines of laminar flow are lost and the flow becomes *turbulent* so that Poiseuille's law no longer applies. The point of transition from laminar to turbulent flow depends upon the value of the Reynolds' number (R*e*), which is directly proportional to the diameter of the vessel (D), the mean velocity of flow (V), the density of the fluid (*p*), and inversely proportional to the viscosity of the fluid (μ): (51)

$$Re = V D p / \mu$$

Pure laminar flow is expected in the retinal vessels under almost all conditions since the calculated critical value of Reynolds number for breakdown of laminar to turbulent flow is about 2000 for blood (51). This critical value of Reynolds number is considerably elevated compared to the approximate value of 0.52 calculated for a main retinal arteriole under normal conditions. Furthermore, under atypical conditions, such as at arterio-venous crossings where the vein can be severely narrowed, the calculated Reynolds number increases to an approximate value of 4, which is still much to small to expect turbulence (51).

Under normal circumstances, erythrocytes (red blood cells, RBCs) pass single file through capillaries of 5 to 8μm in diameter, such as those found in the retinal capillary networks. When blood flow through a vessel is slowed, the red blood cells tend to lose their alignment and take up a random orientation, resulting in RBC aggregation or sludging. This results in an apparent increase in viscosity and a greater resistance to flow. This phenomenon is termed *coherence resistance*. It explains how, in cases such as glaucoma, a reduction in RBCs velocity in the principal arteries can lead to an increased resistance to flow secondary to an increase in the aggregation of RBCs. It may also explain the loss of the linear relationship between pressure and flow in vascular beds when the pressure is reduced to low values; in such conditions, flow slows more than would be predicted from the reduction in pressure (51).

As previously mentioned, the retinal arterial flow has a very small *pulsatile* component. With each cardiac ventricular contraction a pressure wave is established. This pressure wave propagates in the walls of the aorta and eventually reaches the arterioles. The pulse wave decreases in amplitude as it travels from the aorta to the periphery, finally being damped in the arterioles of 100μm diameter. Nonetheless, pulsatility of blood flow is still detectable in the

microvascular beds, as shown during LDF recordings. Because of the inertia of blood, a phase difference occurs between the pressure gradient and flow. As the pressure gradient increases the flow lags behind it and when the pressure gradient declines or reverses the momentum of the blood tends to keep it moving in the original direction for a short time. The arterial pressure pulse differs from a pure sine wave. By means of a *Fourier analysis* , the periodic complex wave form of the pressure pulse can be analysed into a fundamental frequency and different proportions of harmonics (51, 52).

B) Vascular perfusion pressure

Blood circulation in any organ depends on the perfusion pressure and vascular resistance to blood flow. The *perfusion pressure* is the difference between the mean arterial and the venous pressures (arteriovenous pressure difference) (18, 33). Since the venous pressure is approximately equal to the IOP, the perfusion pressure can be expressed as the difference between the mean arterial pressure and the intraocular pressure. Consequently, an elevation of the IOP or a decrease in arterial pressure can lead to a decrease in the perfusion pressure and impairment of the blood flow. The term vascular *autoregulation* is used to define the process which operates locally in a vascular bed to maintain blood flow constant in the face of external stresses such as changes in blood pressure, in the IOP, and in the ocular perfusion pressure (OPP) (32, 33, 51). There is strong experimental evidence for autoregulation in the central nervous system, as well as for the retina and vessels in the optic nerve (18, 33, 48, 51).

C) Vascular autoregulation

Autoregulation in microvascular beds serves to maintain constant blood flow despite changes of perfusion pressure, which can occur as a consequence of changes in arterial blood pressure or the IOP. Evidence for autoregulation has been found in the retina and optic nerve; earlier studies on autoregulation in the choroid failed to produce evidence of such a control mechanism for blood

flow (18, 33, 48, 51). However more recent studies in the rabbit by Kiel (75), and in humans by Lovasik (76) provided some preliminary evidence for vascular autoregulation in the choroid.

Autoregulation is considered a feature of the terminal arterioles, although its exact mechanisms are not fully understood. With the rise or fall of blood pressure beyond critical levels, the arterioles constrict or dilate respectively, to regulate the blood flow. Figure 16 illustrates that the capillary system plays a major role in controlling retinal vessel tone via capillary constriction / dilation stimulated by one of several factors presented below. The mechanism behind autoregulation is twofold, with one myogenic and one metabolic component, that normally operate together (50). The *myogenic mechanism* acts in response to variations in the transmural pressure difference (difference between the intravascular and the extravascular pressures) or variations in the degree of arterial stretching. For example, an increase in intraocular pressure, leading to a decrease in transmural pressure difference, will cause a reduction in arteriolar tone and consequently a lower vascular resistance to compensate for the fall in perfusion pressure. The *metabolic mechanism* is activated as a response to local conditions such as carbon dioxide concentration, pH, or oxygen level. When the concentration of CO_2 accumulates because of inadequate blood flow, the vessels dilate and blood flow increases.

Autonomic innervation of the extraocular vessels as well as of the choroidal vessels has been reported in various studies (3, 50). However, no neural innervation of the vessels of the retina and optic nerve head has been found to date, although alpha- and beta-adrenergic and cholinergic receptors are present (3). Sympathetic nerves, derived from the superior cervical sympathetic ganglion, innervate the central retinal artery up to the lamina cribrosa, but not beyond, whereas all uveal vascular beds are innervated (50). Therefore, the vascular tone of the retinal arterioles depends on the contractile state of smooth muscle cells and pericytes, which is regulated by neurotransmitters, circulating hormones, myogenic and metabolic factors, as well as by endothelium-derived

factors, rather than by autonomic nervous control. Endothelium-derived factors include nitric oxide, prostacycline, angiotensin, and endothelin-1 (77, 78). Nitric oxide (NO) and prostacycline are vasodilators and inhibitors of platelet function (78, 79). Angiotensin receptors are responsible for the vasoconstrictor effect of angiotensin-II on the vascular smooth muscle cells (80). Endothelin-1 also induces potent vasoconstrictor effects (80).

Vascular autoregulation cannot compensate for all levels of change in the ocular perfusion pressure. Autoregulation in the retinal vasculature becomes ineffective when the perfusion pressure rises or falls beyond certain limits. It was shown that the retinal blood flow is autoregulated up to a mean systemic blood pressure increase of about 41% above baseline values or during an increase in the IOP leading to a mean decrease in the retinal perfusion pressure of less than 50% (81). A fluorescein angiographic study also showed that an acute rise in IOP (above or equal to 30 mm Hg) can cause an insufficiency of retinal autoregulation, even in healthy subjects (82). Furthermore, an acute rise in IOP in albino rats was reported to cause ischemia in the retinal NFL and optic nerve, with consequent nerve cell death after only 45 minutes of ischemia (83). Thus, ischemic damage to the retinal ganglion cell can result from insufficient autoregulatory responses to elevated IOP. It is likely that inter-individual differences exist in the range of IOPs which can be tolerated in the retina and optic nerve head by effective vascular autoregulation responses. Adequacy or inadequacy of vascular autoregulation may be a determining factor in deciding whether a patient with elevated IOP develops glaucomatous optic nerve damage.

The homeostatic importance of autoregulation is not only to maintain a constant blood flow and nutrient supply but also to maintain a relatively constant capillary pressure that is important for tissue fluid balance (84). Several physiological states can lead to activation of autoregulatory mechanisms and blood flow changes in the retina and optic nerve head. These factors include

arterial oxygen tension (O_2), carbon dioxide concentration (CO_2) and neuronal activity.

When blood pressure and flow to tissues are lowered below normal levels, local tissue oxygen delivery and the products of cell metabolism appear to dominate the regulation of local arterial smooth muscle tone in most vascular beds (84). The control of retinal oxygen levels by variations in the tone of retinal arterioles has also been attributed to autoregulation. High oxygen levels in the tissues lead to vasoconstriction and consequently, a decrease of retinal blood flow velocity (85). Reduction in the diameter of a vessel of only 10 or 25% will account for a decrease in flow through this vessel of approximately 30 or 70% respectively (86). Breathing 100% oxygen has been reported to reduce blood flow in the optic nerve head by about 25% (85). Hyperoxia reduces, and hypoxia increases leukocyte velocity in the macular capillaries as seen in blue field entoptoscopy (50).

On the other hand, hypercapnia has been reported to lead to a moderate dilation of visible retinal vessels, an increase in the macular capillary blood velocity, and an increase in optic nerve head blood flow (50,85, 87, 88, 89). Although carbon dioxide has little effect on vessel caliber (88), it can have a profound effect in preventing the vasoconstriction caused by oxygen and also prolonging the time taken for ischemic visual blackout (51).

The principal focus of the present study was to relate blood flow levels to neuronal metabolic demands in the retina based on the density of the nerve fibers. Vascular perfusion and the degree of tissue metabolism are tightly coupled. Any reduction in arterial inflow causes a buildup of vasodilator metabolites in the tissue (84). Autoregulation means the capacity of an organ to regulate its blood supply in accordance with its underlying functional and metabolic needs. For example, in the brain, functional tasks such as speech, listening or arm work, cause an increase in cerebral blood flow, coupled to increases in local metabolism (3). At the level of the eye, the state of light

adaptation of the retina influences retinal metabolism and blood flow. For instance, dark adaptation is known to induce a higher oxygen consumption by photoreceptors in the rabbit (50). Also, in monkey eyes, glucose uptake in the photoreceptor layer was higher in darkness, while constant light reduced the metabolism of the photoreceptors (50, 90). However, the activity of the ganglion cells was about the same in the light exposed and dark exposed eyes (90). On the other hand, flickering light has been reported to increase metabolic activity in the optic nerve of monkey eyes (90). An increased glucose uptake in the inner parts of the retina indicated that flashing light caused activation of the ganglion cells. In the cat, changes in optic nerve head blood flow was reported to increase in response to diffuse luminance flicker (91). Of particular interest was the observation that flicker produced a differential response in the increased blood flow in the ONH in man; specifically, the increase in blood flow was greatest in the superior and inferior temporal quadrants (92). This finding lends support to the present research hypothesis that blood flow may be preferentially increased in discrete fundus areas.

Reductions in ocular perfusion pressure can lead to neuronal ischemia if autoregulatory mechanisms are unable to maintain blood flow close to normal basal levels. The presence of an ischemic condition can be demonstrated by the level of glucose consumption in the affected tissue. Ischemia will cause anoxic cells to switch from aerobic to anaerobic glycolysis. The latter requires much more glucose than aerobic glycolysis. In monkey eyes subjected to a 50% decrease in blood flow, there was an increase glucose uptake in the retina as well as in the prelaminar region of the optic nerve, indicating that partial ischemia caused the expected metabolic shift (90).

Oxygen consumption is nonuniformly distributed across the retina. It is higher in the photoreceptor inner segments than elsewhere, resulting in gradients of pO_2 across the retina (81). Furthermore, studies on the cat's retina have shown that there are inhomogeneities of blood flow distribution across the retina when going toward the periphery: the inflow rate per unit area was

reported to decline when passing toward the periphery of the retina, which is consistent with the decreasing density of the retinal capillary bed (93). However, the same study did not show in the healthy retinal circulation any preferential redistribution of blood during acute rises of IOP, that could represent an attempt to preserve the most vulnerable tissue during transient ischemia. In monkey eyes, marked regional differences in blood flow through the retina and choroid have been found; blood flow around the fovea and around the optic nerve head was much higher than blood flow in the peripheral parts (50). This vascular architecture would appear to be a protective one wherein in fundus sites populated by neurons for acute central vision and the single conduit for all afferent neurons to the visual cortex must be protected by a redundant vasculature. There is reason to believe that a similar trend might exist in the human eye, considering histological findings of an increased number of superimposed capillary meshworks around the fovea and the optic nerve head in the human eye (refer to section 2.2.1, *Vascular supply of the retina*).

2.3.3 Retinal versus choroidal blood flow

A review of the fundamental differences between the choroidal and retinal vasculatures will be given below with a view to providing a clearer understanding of how ocular blood flow is normally distributed in the eye. In addition it is hoped that a comparison of the dual retinal vasculature may explain the differential vulnerability of the retinal vs choroidal vasculature to hydraulic forces such as the IOP that typically has minimal detrimental effects on the choroid.

Animal studies of blood flow distribution estimate that the choroid receives anywhere from 65% to 85% of the total ocular blood flow, whereas only 5% or less of the total ocular blood flow perfuses the retina (52). In the human eye, the blood flow volume per amount of tissue is significantly higher in the choroidal capillaries than in the retinal capillaries. Approximately 90% of the total

ophthalmic flow is received by the ciliary arteries and roughly 10% serves to supply the retinal arteries (54, 80). In monkeys, blood flow through the choroid is extremely high compared with blood flow in other tissues such as the brain's grey and white matter, the cardiac muscle and the kidney cortex. The combined retinal and choroidal blood flow is about 10 times that of the gray matter of the brain (50). A corresponding difference in metabolic requirements does not exist. Consequently, more blood flows through the choroid than is required by the metabolic needs of the outer retinal layers; this "functional overperfusion" is demonstrated by the low arteriovenous pO_2 difference in the choroid (about 3%), which means that oxygen extraction from each ml of uveal blood is very low (50, 54). In contrast, the oxygen content of retinal venous blood in humans is about 38% lower than that in arterial blood (50, 54). This larger arteriovenous pO_2 difference is due to a combination of a relatively low total blood flow volume and a high metabolic activity of the retinal tissue (54). The retinal circulation is said to be one of the most precarious vascular beds as it has a high arteriovenous oxygen difference and the perfusion pressure is opposed by the intraocular pressure (51). This results in a low capacity to tolerate periods of decreased perfusion.

At the choroidal level, the high rate of blood flow is of great importance for the supply of nutrients to the outer retina and to serve as a vital "heat sink" for light energy that is focused on the fovea. Despite low oxygen extraction from choroidal blood, the choroid plays an important role in the distribution of nutrients and oxygen to the retina. In primates, the fovea is nourished mainly by the choroid. Also in lower mammals, a major part of the nutrients consumed by the retina is derived from the choroidal blood vessels. In these animals, anywhere between 60 to 80% of the oxygen and 75% of the glucose consumed by the retina is delivered by the choroid (50).

Furthermore, not only the high rate of blood flow through the uvea gives a high oxygen tension in the uvea, which enhances the diffusion of oxygen into

the retina, but it also helps to protect the eye from thermal damage by heat convection. This characteristic seems to prevent damaging increments in tissue temperature when light is focused on the fovea (50).

As already mentioned, there is growing evidence for autoregulation in the choroid. However, moderate increments in intraocular pressure can be followed by a reduction in choroidal blood flow. Choroidal blood flow is closely linked to the OPP. Nonetheless, this reduction in blood flow does not seem to reduce the supply of nutrients to the retina, since the extraction of oxygen and glucose from each ml of blood is increased, therefore maintaining the same level of net extraction despite large variations in blood flow (50). Intuitively, reaching the limits of this "overperfused" vascular bed during normal or even the highest neuronal activity seems very unlikely. In such conditions, there might never be any need for choroidal autoregulatory mechanisms to react quickly and completely to transient changes in the ocular perfusion pressure. On the other hand, efficient vascular autoregulation responses are essential in the inner retina if the metabolic needs of its neural elements are to be met despite changes in the ocular perfusion pressure.

Fig. 15

MECHANICAL MECHANISMS BY WHICH LAMINAR SHEETS (L) MAY COMPRESS THE NERVE FIBER BUNDLES (NF) AFTER IOP ELEVATION

A. Increased internal-external pressure gradient causes posterior laminar sheets to bow and compress NF.

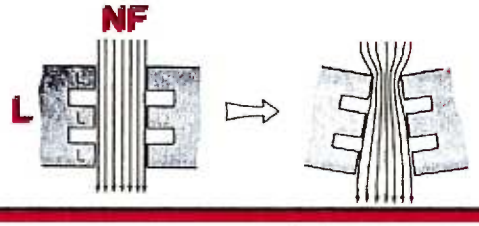

B. The increased tension on the scleral wall is greater in one direction and hence causes distortion and compression of NF along one axis.

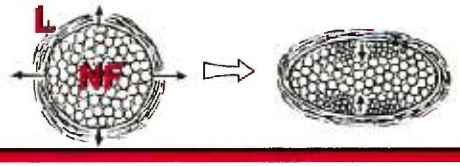

C. Unequal radial movement of successive laminar sheets cause a misregister of successive sheets and compression of NF.

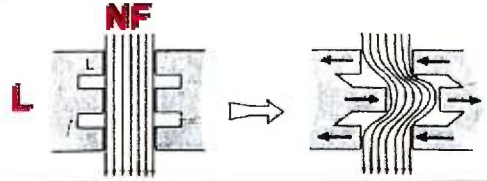

Harry A Quigley et al. " The mechanisms of optic nerve damage in experimental acute intraocular pressure elevation" IOVS 1980

Fig. 16

Factors regulating RETINAL vessel tone

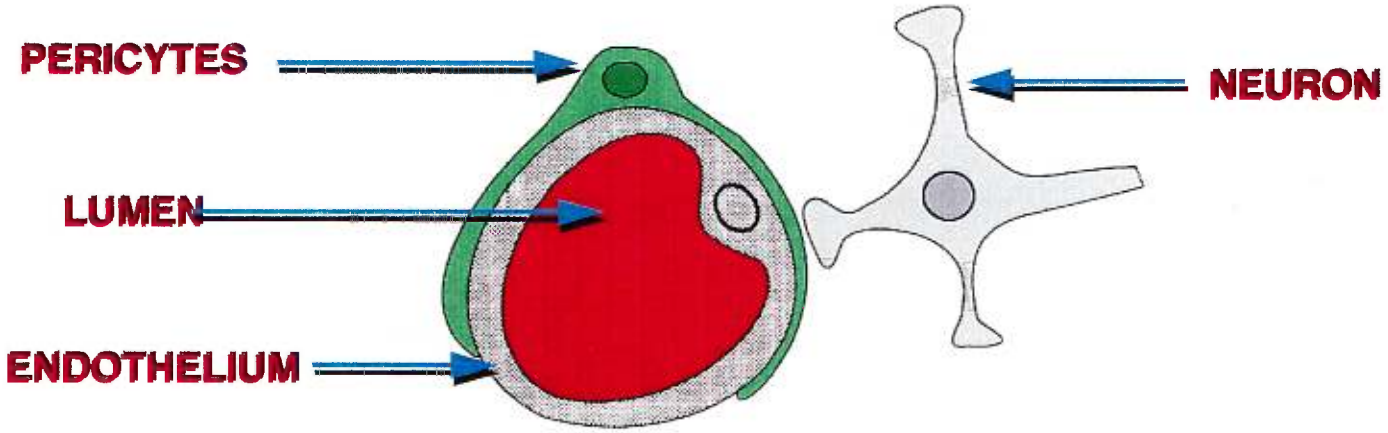

The vascular tone and hence the degree of vascular perfusion can be changed by several factors:

1) **PERICYTES** surrounding the capillaries

2) **LUMEN** of vessel brings in systemic or local mediators (hormones, prostaglandins)

3) **ENDOTHELIUM** contracts /dilates by smooth muscles in arterioles

4) **NEURONS** activate capillaries by vasoactive factors

2.4 OBJECTIVES OF THE PRESENT STUDY

The preferential loss of nerve fibers at the vertical poles of the optic nerve head in glaucoma suggests that a study of regional vascular function or neuroanatomy might provide new important clues to pathogenesis of glaucoma. Various hypotheses have been proposed, some related to the possibility of differential mechanical forces acting on the nerve fiber bundles at the level of the lamina cribrosa (refer to section 2.3.1, *The mechanical theory*), while others relate to the distribution of blood supply at the optic nerve head. At the level of the lamina cribrosa, the upper and lower poles of the nerve fiber bundles show a lower density of connective tissue beams and a larger intercapillary distance. It is thought that if vascular function is compromised with positional shifts of the laminar beams, the vertical poles might be affected because of their larger capillary spacing (18). Hayreh (48), on the other hand, has proposed that the vertical poles of the optic nerve head may frequently fall within socalled "*watershed zones*" between sectors supplied by separate branches of the short posterior ciliary arteries, which might explain their particular vulnerability to ischemia especially since the nerve fibers are found in larger number at the vertical poles. However, experimental measurements in monkeys failed to reveal any regional differences in blood flow across the nerve head in normal or glaucomatous monkey eyes (18). The present study concentrated on evaluating possible regional differences in blood flow at the level of the retinal nerve fiber layer.

In the current literature, considerable attention has been directed at the circulation of the optic nerve head, probably because it corresponds to the site where the loss of ganglion cells in glaucoma is the most evident. However, the optic nerve head presents many difficulties for the measurement and interpretation of blood flow parameters, mainly because of the obstructing presence of the vascular tree formed by the central retinal vein and artery, and also because of the presence of vascular networks in different segments of the anterior portion of the optic nerve arising from different arterial systems. Most

importantly, a review of the anatomy clearly shows that retinal ganglion cells, which are predominantly affected in glaucoma, are surrounded by vascular elements of the retinal circulation all along their course, from the original location of their cell body in the inner nuclear layer, up to the passage of their axon through the optic nerve head. Therefore, an insufficiency of blood supply at any point of the axon's course could have detrimental effects on the metabolism of the entire retinal ganglion cell, and thus lead to gradual attrition of nerve fibers in the nerve fiber layer which become more discernable as they concentrate at the edges of the optic nerve head. Hence, it is possible that abnormalities of the retinal circulation may have some role in the etiology of glaucomatous optic atrophy.

The review of the retinal neurovascular elements presented in the preceeding sections emphasized the pattern of nerve fiber distribution across the retina and around the optic nerve head. The superior and inferior peripapillary quadrants have the thickest nerve fiber layer because a much larger number of ganglion cell axons project toward these areas. A large portion of the retina, including the metabolically active temporal macular area, is represented along the vertical poles of the disc. Consequently, during visual excitation these fundus sites are likely to be metabolically more active than fundus regions with a thinner NFL that comprises ganglion cell axons that converge from smaller sectors of the fundus. As a result, sectors with a thicker NFL are likely to have greater metabolic demands that must be met by a greater delivery of blood.

Furthermore, a review of the topographic distribution of the capillary meshwork across the fundus reveals that there are clear regional differences in the number of capillary meshworks supplying the inner retina: the paramacular, and arcuate region have extralayers of retinal capillaries. Giving that there are natural inhomogeneities in the distribution of ganglion cell axons comprising the NFL and the retinal capillary plexus across the fundus, the present study examined the possibility that the distribution of these two vital components of

the retina were quantitatively related. Specifically, the correlation between the thickness of the NFL and the retinal vasculature perfusing the NFL was examined to determine whether the basal metabolic demand in relation to the thickness of the NFL along the vertical and horizontal meridians was correlated with blood volume, velocity, or flow in the same area.

2.5 REFERENCES

1. Thomas, J.V. General considerations. In: Thomas, J.V., ed. *Glaucoma surgery.* St-Louis: Mosby Year Book, 1992; 1: 1-2.

2. Klopfer, J., Paikowsky, S.J. Epidemiology and clinical impact of the glaucomas. In: Lewis, T.L., Fingeret, M., ed. *Primary care of the glaucomas.* Norwalk: Appleton & Lange,1993; 2: 7-16.

3. Flammer, J. To what extent are vascular factors involved in the pathogenesis of glaucoma? In: Kaisers, H.J., Flammer, J., Hendrickson, Ph., ed. *Ocular blood flow. New insights into the pathogenesis of ocular diseases.* Switzerland: Karger, 1996: 12-39.

4. Lewis, T.L. Definition and classification of glaucomas. In: Lewis, T.L., Fingeret, M., ed. *Primary care of the glaucomas.* Norwalk: Appleton & Lange,1993; 1: 3-5.

5. Quigley, H.A., Vitale, S. Models of open-angle glaucoma prevalence and incidence in the United States. *Invest Ophthalmol Vis Sc.* 1997; 38 (1): 83-91.

6. Wilson, M.R. Glaucoma: epidemiology and risk factors. In: Higginbotham, E.J., Lee, D.A., ed. *Management of difficult glaucoma: A clinician's guide.* Boston: Blackwell Scientific Publications, 1994; 1: 3-7.

7. Bour, T., Blanchard, F., Segal, A. Données épidémiologiques sur le GPAO et son traitement dans la Marne. *J Français Ophtalmol.* 1993; 16 (6-7): 367-79.

8. Coffey, M., Reidy, A., Wormald, R., Xian, W.X., Wright, L., Courtney, P. Prevalence of glaucoma in the west of Ireland. *Br J Ophthalmol.* 1993; 77 (1): 17-21.

9. Dielemans, I., Vingerling, J.R., Wolfe, R.C., Hofman, A., Grobbee, D.E., de Jong P.T. The prevalence of primary open-angle glaucoma in a population-based study in the Netherlands. The Rotterdam study. *Ophthalmology.* 1994; 101 (11): 1851-5.

10. Ekstrom, C. Prevalence of open-angle glaucoma in central Sweden. The Tierp Glaucoma Survey. *Acta Ophthalmologica Scandinavica.* 1996; 74 (2): 107-12.

11. Foster, P.J., Baasanhu, J., Alsbirk, P.H., Munkgbayar, D., Uranchimeg, D.,Johnson, G.J. Glaucoma in Mongolia. A population-based survey in

Hovsgol province, northern Mongolia. *Arch Ophthalmol.* 1996; 114 (10): 1235-41.

12. Ouertani, A., Zhioua, R., Trabelsi, A., Jrad, J. Prévalence du glaucome chronique à angle ouvert dans une commune de Tunis. *J Français Ophtalmol.* 1995; 18 (3): 178-82.

13. Salmon, J.F., Mermoud, A., Ivey, A., Swanevelder, S.A., Hoffman, M. The prevalence of primary angle closure glaucoma and open-angle glaucoma in Mamre, western Cape, South Africa. *Arch Ophthalmol.* 1993; 111 (9): 1263-9.

14. Leske, M.C., Connell, A.M., Schachat, A.P., Hyman, L. The Barbados Eye Study. Prevalence of open- angle glaucoma. *Arch Ophthalmol.* 1994; 112 (6): 821-9.

15. Wang, J.J., Mitchell, P., Smith, W. Is there an association between migraine headache and open-angle glaucoma? Findings from the Blue Mountains Eye Study. *Ophthalmology.* 1997; 104 (10): 1714-9

16. Thomas, J.V. Primary open-angle glaucoma. In: Moses, R.A., Hart, W.M., ed. *Adler's physiology of the eye: Clinical application.* 9th ed. Saint-Louis: Mosby Year Book, 1992; 117: 1342-62.

17. Minckler, D.S. Neuronal damage in glaucoma. In: Varma, R., Spaeth, G.L., Parker, K.W.,ed. *The optic nerve in glaucoma*, Philadelphia: J. B. Lippincott Company, 1993; 4: 51-8.

18. Anderson, D.R., Quigley, H.A. The optic nerve. In: Moses, R.A., Hart, W.M., ed. *Adler's physiology of the eye: Clinical application.* 9th ed. Saint-Louis: Mosby Year Book, 1992; 20: 616-37.

19. Kendell, K.R., Quigley, H.A., Kerrigan, L.A. Primary open-angle glaucoma is not associated with photoreceptor loss. *Invest Ophthalmol Vis Sc.* 1995; 36 (1): 200-5.

20. Wygnanski, T., Desatnik, H., Quigley, H.A., Glovinsky, Y. Comparison of ganglion cell loss and cone loss in experimental glaucoma. *Am J Ophthalmol.* 1995; 120 (2): 184-9.

21. Shapley, R. Retinal ganglion cell function. In: Varma, R., Spaeth, G.L., Parker, K.W.,ed. *The optic nerve in glaucoma*, Philadelphia: J. B. Lippincott Company, 1993; 2: 27-34.

22. Drance, S.M. Psychophysics and electrophysiology in glaucoma: an overview. In: Kaufman, P.L., Mittag, T.W., ed. *Glaucoma.* Vol 7. London: Mosby, 1994; I: 7.1-7.5.

23. Lewis, T.L., Wing, J.T. Anatomy and physiology of the optic nerve. In: Lewis, T.L., Fingeret, M., ed. *Primary care of the glaucomas.* Norwalk: Appleton & Lange,1993; 4: 47-62.

24. Shields, M.B. *A study guide for glaucoma.* Baltimore: Williams & Wilkins, 1982.

25. Mikelberg, F.S., Drance, S.M., Schulzer, M., Yidegiligne, H.M., Weis, M.M. Axon count and axon diameter distribution. *Ophthalmology.* 1989; 96 (9):1325-8.

26. Jonas, J.B., Naumann, G.O.H. The optic nerve: Its embryology, histology, and morphology. In: Varma, R., Spaeth, G.L., Parker, K.W.,ed. *The optic nerve in glaucoma*, J. Philadelphia: J. B. Lippincott Company, 1993; 1: 3-26.

27. Balazsi, A.G., Rootman, J., Drance, S.M., Schulzer, M., Douglas, G.R. The effect of age on the nerve fiber population of the human optic nerve. *Am J Ophthalmol.* 1984; 97: 760-6.

28. Spalton, D.J., Hitchings, R.A., Hunter P.A. *Atlas of clinical ophthalmology.* 2nd ed. London: Mosby- Year Book Europe (Wolfe), 1994.

29. Airaksinen, P.J., Tuulonen, A. Retinal nerve fiber layer evaluation. In: Varma, R., Spaeth, G.L., Parker, K.W.,ed. *The optique nerve in glaucoma*, J. Philadelphia: J. B. Lippincott Company, 1993; 18: 277-87.

30. Varma, R., Skaf, M., Barron, E. Retinal nerve fiber layer thickness in normal human eyes. *Ophthalmology.* 1996; 103 (12): 2114-9.

31. Drake, M.V. Glaucomatous visual field loss. In: Moses, R.A., Hart, W.M., ed. *Adler's physiology of the eye: Clinical application.* 9th ed. Saint-Louis: Mosby Year Book, 1992; 113: 1301-10.

32. Lewis, T.L., Chronister, C.L. Etiology and pathophysiology of primary open-angle glaucoma. In: Lewis, T.L., Fingeret, M., ed. *Primary care of the glaucomas.* Norwalk: Appleton & Lange,1993; 5: 65-77.

33. Nesterov, A.P, Egorov, E.A. Pathological physiology of primary open-angle glaucoma: the optic nerve changes. In: Cairns, J.E., ed. *Glaucoma.* Vol 1. London: Grune & Stratton, 1986; 18: 369-90.

34. Langham, M.E. Ocular blood flow and vision in healthy and glaucomatous eyes. *Survey Ophthalmol.* 1994; 38 Suppl: S161-8.

35. Manni, G., Lambiase, A., Centofanti, M., Mattei, E., De Gregorio, A., Aloe, L., de Feo, G. Histopathological evaluation of retinal damage during intraocular hypertension in rabbit: involvement of ganglion cells and nerve

fiber layer. *Graefes Arch Clin Exp Ophthalmol.* 1996; 234 Suppl 1: S209-13.

36. Caprioli, J., Prum, B., Zeyen, T. Comparison of methods to evaluate the optic nerve head and nerve fiber layer for glaucomatous change. *Am J Ophthalmol.* 1996; 121(6): 659-67.

37. Eid, T.M., Spaeth, G.L., Katz, L.J., Azuara-Blanco, A., Agusburger, J., Nicholl, J. Quantitative estimation of retinal nerve fiber layer height in glaucoma and the relationship with optic nerve head topography and visual field. *J Glaucoma.* 1997; 6 (4): 221-30.

38. Schuman, J.S., Hee, M.R., Puliafito, C.A., Wong, C., Pedut-Kloizman, T., Lin, C.P., Hertzmark, E., Izatt, J.A., Swanson, E.A., Fujimoto, J.G. Quantification of nerve fiber layer thickness in normal and glaucomatous eyes using optical coherence tomography. *Arch Ophthalmol.* 1995; 113 (5): 586-96.

39. Schuman, J.S., Pedut-Kloizman, T., Hertzmark, E., Hee, M.R., Wilkins, J.R., Coker, J.G., Puliafito, C.A., Fujimoto, J.G., Gloor, B. Value of scanning laser ophthalmoscopy and polarimetry compared with perimetry in evaluating glaucomatous changes in the optic papilla and nerve fiber layer. *Ophthalmologe.* 1996; 93 (5): 520-6.

40. Uchida, H., Tomita, G., Onda, E., Sugiyama, K., Kitazawa, Y. Relationship of nerve fiber layer defects and parafoveal visual field defects in glaucomatous eyes. *Japanese J Ophthalmol.* 1996; 40 (4): 548-53.

41. Weinreb, R.N., Shakiba, S., Sample, P., Shahrokni, S., van Horn, S., Garden, V.S., Asawaphureekorn, S., Zangwill, L. Association between quantitative nerve fiber layer measurement and visual field loss in glaucoma. *Am J Ophthalmol.* 1995; 120: 732-8.

42. Quigley, H.A., Enger, C., Katz, J., Sommer, A., Scott, R., Gilbert, D. Risk factors for the development of glaucomatous visual field loss in ocular hypertension. *Arch Ophthalmol.* 1994; 112 (5): 644-9.

43. Tuulonen, A., Lehtola, J., Airaksinen, P.J. Nerve fiber layer defects with normal visual fields. Do normal optic disc and normal visual field indicate absence of glaucomatous abnormality? *Ophthalmol.* 1993; 100 (5): 587-97; discussion 597-8.

44. Wang, F., Quigley, H.A., Tielsch, J.M. Screening for glaucoma in a medical clinic with photographs of the nerve fiber layer. *Arch Ophthalmol.* 1994; 112 (6): 796-800.

45. Tjon-Fo-Sang, M.J., Lemij, H.G. The sensitivity and specificity of nerve fiber layer measurements in glaucoma as determined with scanning laser polarimetry. *Am J Ophthalmol.* 1996; 123: 62-9.

46. Weinreb, R.N., Shakiba, S., Zangwill, L. Scanning laser polarimetry to measure the nerve fiber layer of normal and glaucomatous eyes. *Am J Ophthalmol.* 1994; 119: 627-36.

47. Bill, A. Vascular physiology of the optic nerve. In: Varma, R., Spaeth, G.L., Parker, K.W.,ed. *The optic nerve in glaucoma.* Philadelphia: J. B. Lippincott Company, 1993; 3: 37-50.

48. Hayreh, S.S. Blood supply of the optic nerve head in health and disease. In: Lambrou, G.N., Greve, E.L, ed. *Ocular blood flow in glaucoma: Means , methods and measurements.* Berkeley: Kugler & Ghedini Publications, 1989: 3-48.

49. Apple, D.J. *Ocular pathology: Clinical applications and self-assessment.* 3rd ed. Saint-Louis: The C.V. Mosby Company, 1985.

50. Alm, A., Bill, A. Ocular circulation. In: Moses, R.A., Hart, W.M., ed. *Adler's physiology of the eye: Clinical application.* 9th ed. Saint-Louis: Mosby Year Book, 1992; 6: 198-224.

51. Wise, G. N., Dollery, C.T., Hendkind, P., *The retinal circulation.* 1st ed. New York: Harper & Row, 1971.

52. Henkind, P., Hansen, R.I., Szalay, J. Ocular circulation. In: Duane, T.D., Jaeger, E.A., ed. *Biomedical foundation of ophthalmology.* Vol 2. Philadelphia: Lippincott Company, 1988; 5: 1-53.

53. Kuwabara, T. Blood vessels in the normal retina. In: Straatsma, B.R., Hall, M.O., Allen, R.A. and Crescitelli, F., ed. *The retina: Morphology, function and clinical characteristics.* UCLA Forum Med. Sci. No.8, Los Angeles: University of California Press, 1969; 163-76.

54. Funk, R.H.W. Blood supply of the retina. *Ophthalmic Res.* 1997; 29: 320-5.

55. Hayreh, S.S. Blood supply and vascular disorders of the optic nerve. In: Cant, J.S., ed. *The optic nerve.* Saint-Louis: The C.V. Mosby Company, 1972: 59-67.

56. Müller, H. Anatomische Beitrage zur ophthalmologie: Ueber Nervean-Veran-deungen ander Eintrittsstelle des Scherven. *Arch Ophthalmol.* 1958; 4: 1.

57. von Jaeger, E. Ueber Glaucom und sein Heilung durch iridectomie. *Z Ges der Aerztezuwren.* 1858; 14: 465-84.

58. Spaeth, G.L. *The pathogenesis of nerve damage in glaucoma: Contribution of fluorescein angiography.* New York: Grune & Stratton, 1977.

59. Van Buskirk, E.M. Is glaucoma a pressure disease? In: Ball, S.F., Franklin, R.M., ed. *Glaucoma: Diagnosis and therapy.* New Orleans: New Orleans Academy of Ophthalmology, 1993: 51-7.

60. Quigley, H.A., Flower, R.W., Addicks, E.M., Mc Leod, D.S. The mechanism of optic nerve damage in experimental acute intraocular pressure elevation. *Invest Ophthalmol Vis Sc.* 1980; 19: 505.

61. Brooks, D.E., Garcia, G.A., Dreyer, E.B., Zurakowski, D., Franco-Bourland R.E. Vitreous body glutamate concentration in dogs with glaucoma. *Am J Vetenerinary Res.* 1997; 58(8): 864-7.

62. Dreyer, E.B., Zurakowski, D., Schumer, R.A., Podos, S.M., Lipton, S.A. Elevated glutamate levels in the vitreous body of humans and monkeys with glaucoma. *Arch Ophthalmol.* 1996; 114 (3): 299-305.

63. Nickells, R.W. Retinal ganglion cell death in glaucoma: the how, the why, and the maybe. *J Glaucoma.* 1996; 5 (5): 345-56.

64. Hamard, P., Hamard, H., Dufaux, J. Blood flow rate in the microvasculature of the optic nerve head in primary open angle glaucoma. *Survey Ophthalmol.* 1994; 38 Suppl: S87-93; Discussion S94.

65. Hamard, P., Hamard, H., Dufaux, J., Quesnot, S. Optic nerve head blood flow using a laser Doppler velocimeter and haemorheology in primary open angle glaucoma and normal pressure glaucoma. *Br J Ophthalmol.* 1994; 78 (6): 449-53.

66. Butt, Z., McKillop, G., O'Brien, C., Allan, P., Aspinall, P. Measurement of ocular blood flow velocity using color Doppler imaging in low tension glaucoma. *Eye.* 1995; 9 (Pt 1): 29-33.

67. Butt, Z., O'Brien, C., McKillop, G., Aspinall, P., Allan, P. Color Doppler imaging in untreated high- and normal-pressure open-angle glaucoma. *Invest Ophthalmol Vis Sc.* 1997; 38 (3): 690-6.

68. Galassi, F., Nuzzaci, G., Sodi, A., Casi, P., Cappelli, S., Vielmo, A. Possible correlations of ocular blood flow parameters with intraocular pressure and visual-field alterations in glaucoma: a study by means of color Doppler imaging. *Opthalmologica.* 1994; 208 (6): 304-8.

69. Michelson, G., Groh, M.J., Groh, M.E., Grundler, A. Advanced primary open-angle glaucoma is associated with decreased ophthalmic artery blood-flow velocity. *German J Ophthalmol.* 1995; 4 (1): 21-4.

70. Nasemann, J.E., Carl, T., Pamer, S., Scheider, A. Perfusion time of the central retinal artery in normal pressure glaucoma. Initial results. *Ophthalmologe.* 1994; 91 (5): 595-601.

71. Quaranta, L., Manni, G., Donato, F., Bucci, M.G. The effect of increased intraocular pressure on pulsatile ocular blood flow in low tension glaucoma. *Survey Ophthalmol.* 1994; 38 Suppl: S177-81; Discussion S182.

72. Ravalico, G., Pastori, G., Toffoli, G., Croce, M. Visual and blood flow responses in low-tension glaucoma. *Survey Ophthalmol.* 1994; 38 Suppl: S173-6.

73. Wolf, S., Arend, O., Haase, A., Schulte, K., Remky, A., Reim, M. Retinal hemodynamics in patients with chronic open-angle glaucoma. *German J Ophthalmol.* 1995; 4 (5): 279-82.

74. Tielsch, J.M., Katz, J., Sommer, A., Quigley, H.A., Javitt, J.C. Hypertension, perfusion pressure, and primary open-angle glaucoma. A population-based assessment. *Arch Ophthalmol.* 1995; 113 (2): 216-21.

75. Kiel, J.W., van Heuvan, W.A.J. Ocular perfusion pressure and choroidal blood flow in the rabbit. *Invest Ophthalmol Vis Sc.* 1995; 36 (3): 579-85.

76. Lovasik, J.V. Evidence for autoregulation of blood flow in the human choroidal vasculature. *Opto Vis Sc.* 1996; 73 (12): 76

77. Anderson, D.R. Glaucoma, capillaries and pericytes. 1. Blood flow regulation. *Ophthalmologica.* 1996; 210 (5): 257-62.

78. Brown, S.M., Jampoli, L.M. New concepts of regulation of retinal vessel tone. (Review). *Arch Ophthalmol.* 1996; 114 (2): 199-204.

79. Haefliger, I.O., Meyer, P., Flammer, J., Luscher, T.F. Endothelium-dependent vasoactive factors. In: Kaisers, H.J., Flammer, J., Hendrickson, Ph., ed. *Ocular blood flow. New insights into the pathogenesis of ocular diseases.* Switzerland: Karger, 1996: 51-63.

80. Meyer, P., Haefliger, I.O., Flammer, J., Luscher, T.F. Endothelium-dependent regulation in ocular vessels. In: Kaisers, H.J., Flammer, J., Hendrickson, Ph., ed. *Ocular blood flow. New insights into the pathogenesis of ocular diseases.* Switzerland: Karger, 1996: 64-73.

81. Pournaras, C.J. Autoregulation of ocular blood flow. In: Kaisers, H.J., Flammer, J., Hendrickson, Ph., ed. *Ocular blood flow. New insights into the pathogenesis of ocular diseases.* Switzerland: Karger, 1996: 40-50.

82. Schulte, K., Wolf, S., Arend, O., Harris, A., Henle, C., Reim, M. Retinal hemodynamics during increased intraocular pressure. *German J Ophthalmol.* 1996; 5 (1): 1-5.

83. Adachi, M., Takahashi, K., Nishikawa, M., Miki, H., Uyama, M. High intraocular pressure-induced ischemia and reperfusion injury in the optic nerve and retina in rats. *Graefes Arch Clin Exp Ophthalmol.* 1996; 234 (7): 445-51.

84. Orgül, S., Cioffi, G.A. The vasomotor effect of arterial oxygen on the optic nerve microvasculature. In: Kaisers, H.J., Flammer, J., Hendrickson, Ph., ed. *Ocular blood flow. New insights into the pathogenesis of ocular diseases.* Switzerland: Karger, 1996: 87-92.

85. Harris, A., Anderson, D.R., Pillunat, L., Joos, K., Knighton, R.W., Kagemann, L., Martin, B.J. Laser Doppler flowmetry measurement of changes in human optic nerve head blood flow in response to blood gas perturbations. *J Glaucoma.* 1996; 5 (4): 258-265.

86. Haefliger, I.O., Anderson, D.R. Pericytes and capillary blood flow modulation. In: Kaisers, H.J., Flammer, J., Hendrickson, Ph., ed. *Ocular blood flow. New insights into the pathogenesis of ocular diseases.* Switzerland: Karger, 1996: 74-78.

87. Harris, A., Arend, O., Wolfe, S., Cantor, L.B., Martin, B.J. CO_2 dependence of retinal arterial and capillary blood velocity. *Acta Ophthalmol Scand.* 1995; 73: 421-4.

88. Arend, O., Harris, A., Martin, B.J., Holin, M., Wolf, S. Retinal blood velocities during carbogen breathing using scanning laser opthalmoscopy. *Acta Ophthalmol.* 1994; 72: 332-6.

89. Sponsel, W.E., De Paul, K.L., Zetlan, S.R. Retinal hemodynamic effects of carbon dioxide, hyperoxia, and mild hypoxia. *Invest Ophthalmol Vis Sc.* 1992; 33: 1864-9.

90. Sperber, G.O., Bill A. The 2-deoxyglucose method and ocular blood flow. In: Lambrou, G.N., Greve, E.L, ed. *Ocular blood flow in glaucoma: Means , methods and measurements.* Berkeley: Kugler & Ghedini Publications, 1989: 73-80.

91. Buerk, D., Riva, C.E., Cranstoun, S. Mechanisms underlying the change in cat optic nerve blood flow induced by diffuse flicker. In: Messmer, K., Kübler, W.M., ed. Sixth World Congress for microcirculation. Munich: Monduzzi, 1996: 283-7.

92. Mendel, M., Riva, C.E., Petrig, B.L. Regulation of optic nerve blood flow: effect of diffuse luminance flicker. In: Fourth International Symposium on ocular circulation and neovascularization. Budapest: 1995: May 22-26.

93. Hill, D.W., Young, S. Regional retinal blood flow in the cat. In: Cant, J.S, ed. *Vision and circulation* . London: The C.V. Mosby Company, 1974: 60-65.

3. CORRELATING NERVE FIBER LAYER THICKNESS WITH BLOOD FLOW IN THE NORMAL HUMAN EYE

Catherine Ieraci and John V. Lovasik

Various aspects of this research project have been presented at the following refereed vision science symposia:

Ieraci, C., Lovasik, J.V. Correlating nerve fiber layer thickness with blood flow in the human eye. *ARVO Annual meeting.* Forth Lauderdale, Florida. May 1997. *Invest Ophthalmol Vis Sc.* 1997; 38 (4): abstract 4895.

Ieraci, C., Lovasik, J.V. Laser Doppler flowmetry and laser scanning polarimetry correlates for the human eye. *AAO meeting.* San Antonio. Dec. 1997. *Optom Vis Sc.* 1997; 74 (12): 123.

Ieraci, C., Lovasik, J.V. Is the peripapillary nerve fiber layer in healthy humans uniformly perfused by the ocular vasculature? *Fifth Canadian Universities Optometry Conference.* Montréal, Québec, Canada. Oct 1997.

Ieraci, C., Lovasik, J.V. Correlating the nerve fiber layer thickness with blood flow in the human eye. *Réseau de recherche en vision.* Québec. Oct. 1997.

3.1 RÉSUMÉ

Objectif. Déterminer s'il existe une corrélation entre l'épaisseur de la couche de fibres nerveuses dans les quatre quadrants principaux de l'aire péripapillaire et le flot sanguin de sites rétiniens correspondants.

Méthodes. Vingt-quatre (24) jeunes adultes (âge moyen 21.5± 2.8 années) ont participé à cette étude. L'épaisseur de la couche de fibres nerveuses a été mesurée au niveau de quatre sites rétiniens, localisés dans les quadrants supérieur, inférieur, nasal et temporal d'une zone péripapillaire située à 1.75DD du centre du nerf optique. Les mesures ont été réalisées à l'aide d'un polarimètre à balayage au laser, le *Nerve Fiber Analyser* (NFA) de Laser Diagnostic Technologies. Un système au laser utilisant le principe de l'effet Doppler, le *Laser Doppler Flowmeter* (Oculix LDF System, 670nm), a été utilisé pour quantifier le flot sanguin au niveau des aires rétiniennes correspondant aux sites de mesures de l'épaisseur de la couche de fibres nerveuses.

Résultats. L'épaisseur de la couche de fibres nerveuses rétiniennes (CFNR) a démontré des différences significatives à travers les quadrants ($p < 0.001$). Les aires péripapillaires échantillonnées dans les quadrants supérieur et inférieur (respectivement 102.5 et 91.7µm) ont en moyenne démontré une épaisseur de CFNR plus grande que les aires nasale et temporale (respectivement 55.6 et 49.6 µm). Le flot sanguin n'a pas démontré de différence significative à travers les quadrants. Aucune corrélation n'a été trouvée entre l'épaisseur de la couche de fibres nerveuses et le flot sanguin d'aires péripapillaires correspondantes ($p = 0.38$, $r = 0.09$).

Conclusions. Chez des jeunes sujets de santé oculaire normale, le flot sanguin rétinien semble se répartir uniformément à travers des couches de fibres nerveuses d'épaisseur significativement différentes autour du nerf optique. Il est probable qu'une chute globale du flot sanguin durant tout

processus pathologique puisse conduire à une plus grande susceptibilité d'ischémie pour les couches les plus épaisses de fibres nerveuses rétiniennes nécessitant un apport métabolique supérieur.

Mots clés: *fibres nerveuses rétiniennes, flot sanguin, polarimètre à balayage au laser, fluxmétrie à laser Doppler.*

3.2 ABSTRACT

Purpose. To determine whether the differential thickness of the retinal nerve fiber layer (NFL) along the vertical and horizontal quadrants are differentially perfused by the retinal vasculature.

Methods. Scanning laser polarimetry and laser Doppler flowmetry (LDF) were performed on the right eye of twenty four (24) healthy adult volunteers (mean age 21.5 ± 2.8 years). A Laser Diagnostic Technologies Nerve Fiber Analyser (NFA) was used to assess the NFL thickness over a scan angle of 15 ° around the optic nerve head (ONH). NFL thickness measurements were made in the vertical and horizontal quadrants, 1.75 DD away from the ONH center. An Oculix Laser Doppler Flowmetry System (LDF, 670 nm), was subsequently used to quantify blood flow at a selected NFL thickness site in each quadrant to correlate blood flow with focal NFL thickness measurements.

Results. The group average NFL thickness in the superior (102.5 μm) and inferior (91.7μm) quadrants were significantly greater ($p<0.0001$) than the nasal (55.6 μm) and temporal (49.6 μm) quadrants. This resulted in a characteristic M-shaped NFL thickness distribution along the reference ellipse surrounding the ONH. Local measurements of blood flow did not vary significantly across quadrants ($p>0.05$). There was no correlation between local NFL thickness and blood flow measurements ($p=0.38$, $r=0.09$).

Conclusions. In normal young subjects, blood flow for a retina exposed to a constant luminous background is uniform across the fundus even though the NFL thickness varies systematically around the ONH. Because of this relationship between neural structure and blood flow, ocular diseases that impair blood flow globally may place the nerve fibers in the vertical meridian at greater risk for physiological dysfunction or death.

Key words: nerve fiber layer thickness, blood flow, scanning laser polarimetry, laser doppler flowmetry.

3.3 INTRODUCTION

Glaucomatous optic neuropathy is characterized by a progressive loss of retinal ganglion cells and axons, with preferential loss of nerve fibers at the vertical poles of the nerve head. This sectorial progression of the atrophy has suggested that study of regional function or anatomy might provide clues to pathogenesis. The principal objective of this study was to determine whether, in the normal human eye, the varying thickness of the retinal nerve fiber layer (NFL) around the optic nerve head (ONH) is differentially perfused by the retinal vasculature.

It is well known from histological studies that the retinal ganglion cell and nerve fiber layers of the eye show distributional differences in thickness across the fundus. The nerve fiber layer progressively increases in thickness from the ora serrata toward the optic nerve head, around which sectorial differences are also present: Varma et al (1) found a decreasing nerve fiber layer thickness starting with the superior disc margin, the inferior, the nasal and finally the temporal disc margin showing the thinnest nerve fiber layer. Since the thickness of the retinal nerve fiber layer is proportional to the number of axons, we can assume that regions of thicker nerve fiber layers represent the projections of proportionately larger retinal surface areas, or of greater neuronal activity, than regions of thinner nerve fiber layers. We also know from the anatomy of the eye that retinal capillary beds tend to become multilayered in regions of increased nerve fiber layer thickness (2, 3, 4), which is consistent with possibly greater metabolic demands in those regions. A study using scanning laser Doppler flowmetry revealed that blood flow in the neuroretinal rim area was significantly higher than that of the thinner juxtapapillary retinal area, with POAG patients showing a decreased blood flow in both regions compared with healthy subjects (5).

Most theories on the physiopathology of glaucoma tend to regard the optic nerve head, and particularly the lamina cribrosa, as the principal site of injury to

the ganglion cell axons. This presumption has disregarded the possibility that injury to the retinal ganglion cell may in fact be closer to its origin in the retinal nerve fiber layer. Studies have shown evidences of possible vascular disturbances at the retinal level in glaucoma (6). For instance, the early stages of glaucoma are associated with instability of the differential light sensitivity (DLS) at discrete retinal points, which develops prior to visual loss. In healthy subjects, the DLS remains stable despite substantial lowering of the perfusion pressure resulting from increased intraocular pressure. This stability of vision was attributed to an autoregulation of blood flow to the retinal ganglion cell axons, which might be absent or deficient in glaucoma patients (6). Also, in old rhesus monkeys with artificially reduced perfusion pressure (by elevation of the IOP), ischemic reactions were observed in the inner and outer layers of the retina as well as in the optic nerve head (7). An enhanced glucose uptake in these regions indicated that a compromised oxygen supply had resulted in anaerobic glycolysis. The same reaction was not seen in young healthy monkeys, indicating that efficient autoregulation of the blood flow maintained essentially normal glucose consumption during increases in intraocular pressure.

The anatomy shows that retinal ganglion cells and axons are surrounded by supportive glial tissue and vascular elements, which regulate vital exchanges of nutrients and wastes to the cells at all points of their course toward the optic nerve head. It is reasonable to think that a vascular disturbance at any point of this course may interfere with the normal metabolic functions of the whole cell and potentially lead to its death if such vascular disturbances are not reversed by autoregulatory mechanisms. The preferential loss of retinal ganglion cell axons projecting in the vertical poles of the optic nerve may be the consequence of sectorial vascular insufficiencies.

The superior and inferior poles of the disc are the sites of important neuronal activity, which may result in higher metabolic demands, and consequently a need for greater blood supply. We designed a study to

determine whether, in young healthy subjects, peripapillary retinal areas of different nerve fiber layer thickness are accompanied by proportional changes in blood flow. Quantifications of the nerve fiber layer thickness and blood flow measurements were made using non-invasive techniques, scanning laser polarimetry and laser Doppler flowmetry, respectively.

3.4 MATERIALS AND METHODS

3.4.1 Subjects

Measurements were performed on twenty-four (24) healthy volunteers (19 women and 5 men) ranging in age from 16 to 29 years (21.3 ± 2.6 years, mean ± 1SD). The right eye for each subject was used as the test eye. Subjects had no history of systemic or ocular disease and results of there ocular examinations were normal. Refraction expressed in equivalent sphere ranged between -5.50 and +0.25 diopters, and corneal curvature ranged between 7.15 and 8.15 mm (Canon AE 5000 autorefractor). Intraocular pressure (IOP) was recorded after pupillary dilation using the Tomey Pro Ton tonometer and was < 18 mm Hg in all subjects (14.1 ± 2.4 mm Hg, mean ± 1SD). Informed consent, based on the tenets of the Helsinky declaration for the use of humans in experimentation, was obtained from all subjects, for all experimental procedures. All subjects were informed of their right to withdraw from the study at any time, for any reason of their choosing, without prejudice.

3.4.2 Nerve fiber layer thickness measurements by scanning laser polarimetry

A scanning laser polarimeter (the Nerve Fiber Analyser I, Laser Diagnostic Technologies, Inc, San Diego, California) was used to quantitatively assess the peripapillary retinal nerve fiber layer thickness. Figure 17 schematically illustrates the optical principles underlying the *in vivo* measurement of the NFL thickness in human eyes. The SLP technique is based on the birefringent

property of the retinal nerve fiber layer which is explained by the cylindrical parallel structure of the nerve fibers (12). When a polarized, near infra-red laser light (780 nm) is focused onto one point of the retina and partially reflected from deeper layers, its state of polarization is changed; the amount of phase shift of the exiting light is referred to as *retardation* and is proportional to the thickness of the layer. In their study on postmortem monkey eyes, Weinreb et al (12) found that 1 degree of retardation corresponded to a retinal nerve fiber layer thickness of approximately 7.4 μm. The applicability of scanning laser polarimetry (SLP) to the human eye has been demonstrated (9, 11).

The theory and applications of scanning laser polarimetry has been described in detail by Weinreb et al (12). In brief, the Nerve Fiber Analyser (NFA) is a confocal scanning laser ophthalmoscope with a polarization modulator, a cornea polarization compensator and a polarization detection unit. (11). A nonpolarizing beam splitter separates the incident and reflected lights. The polarization state of the light emerging from the eye is consequently analysed by the polarization detection unit. A scan unit deflects the illuminating laser beam to an adjacent retinal position where the preceding procedure is repeated. A polarization compensation algorithm is used to neutralize the polarization effects of the birefrigent cornea and lens of the human eye. With the NFA, a retardation map consisting of 256 X 256 individual retinal positions is created, with each pixel corresponding to the amount of retardation at each location within a field of view of approximately 15 degrees. Figure 18 presents a sample printout of a NFL thickness map, as well as the general experimental setting used for the NFL measurements by scanning laser polarimetry. The left side of the sample printout presents a reflectivity image of the ONH and peripapillary area, while the right side presents a color-coded NFL thickness map: the white- and blue-end of the color scale represent areas of thickest and thinnest NFL, respectively.

In the present study, all polarimetric recordings were obtained under the following conditions: each subject's head was stabilized within a chin and

forehead rest during NFL measurements, pupils were left undilated, and normal room light was maintained. For archival purposes, the refractive status and corneal curvature of the tested eye were measured (Canon AE 5000 autorefractor) and tabulated into the calculation program of the NFA. All measurements were made by the same well-trained examiner to avoid inter-observer variations. A movable "X" located approximately 1.5 meters away from the instrument served as a fixation point and alignment target for the non-test eye. The optic nerve head of the test eye was directed into the center of the SLP monitor using the fixation target for the fellow eye. The focus, alignment, fundus illumination and intensity were adjusted optimally prior to each NFL image. A minimum of five separate NFL scans per subject were obtained and the best three images were averaged to derive a baseline phase retardation NFL thickness map which was used for data analysis.

For data analysis, we applied the squares-calculation method described by Tjon-Fo-Sang et al (9). Using the native software, the retardation map was divided in 16 X 16 squares of 256 pixels each, corresponding to a retinal area of approximately 56 X 56 min. arc. A mean value of NFL thickness was automatically calculated by the software for each square, using the 256 individual values of NFL thicknesses comprising the selected square. A peripapillary ellipse of 1.75 DD was located concentric to the margins of the optic disc, and the retardation map was divided into four retinal regions: a superior and inferior regions of 120° each, a temporal region of 50°, and a nasal region of 70°.

Subsequently, one square was selected in each of the four major quadrants (superior, inferior, temporal and nasal) for comparison with blood flow measurements. All squares were located approximately 1.75DD away from the optic disc center, in areas free of retinal blood vessels and choroidal atrophy. For the superior and inferior regions, the areas showing the thickest portion on the nerve fiber layer of the retardation map were selected; while the thinnest

NFL retinal sites were selected for the temporal and nasal regions. Subsequent blood flow measurements were carried out in these retinal areas by referring to a polaroid picture of the fundus. Figure 19 illustrates how retinal sites were selected for analysis and how blood flow measurements were matched to corresponding NFL thickness measurements.

The mean absolute values of the nerve fiber layer thickness inside each square were obtained using the thickness grid native to the NFA program. Relative ratios for the superior, inferior and temporal NFLs were also computed by dividing superior, inferior and temporal values by the nasal value (respectively referred to as superior NFL, inferior NFL and temporal NFL).

3.4.3 Blood flow measurements by laser Doppler flowmetry

A Laser Doppler Flowmeter, the Oculix, LDF 5000 system, was used to measure relative peripapillary blood flow. A diode laser beam (λ=670 nm, 50-90 μW at the cornea) was delivered to the eye through the illumination pathway of a modified fundus camera (Topcon, model TRC - 50V/50VT). The principles of laser Doppler flowmetry have been described in detail in the literature (10). In brief, this method is based on the optical Doppler effect, which is schematically illustrated in Figure 20: laser light scattered by a moving particle is shifted in frequency by an amount Δf, referred to as the *Doppler shift*, dependent on the velocity of the moving particle and on the angle of incidence (13).

In a capillary bed, red blood cells (RBCs) move in many different directions, and the incident light undergoes several scattering events with static scatterers in the tissue, as well as other RBCs, before it is finally scattered back. Each of these scattering events alters the direction of the light leaving the tissue in the direction of the detector. The result is a broadening of the scattered spectrum (also referred to as the *Doppler shift power spectrum* (DSPS)) rather than a

simple shift in frequency. A model for light scattering in a capillary bed is presented in Figure 21.

In the LDF system, a spectrum analysis of the collected light is performed using a fast Fourier transform algorithm, which was developed based on the theory of Bonner and Nossal (14). Three important LDF parameters are derived from the analysis: (a) "volume" of blood in a tissue (number of red blood cells); (b) "velocity", the average relative speed of moving red blood cells and (c) "flow", the product of volume and velocity which is proportional to the blood flow through the tissue. *Flow* describes the distance covered by all moving cells inside the sample volume per unit time (15). Figure 22 illustrates the general experimental set-up for peripapillary blood flow measurements, as well as a sample printout of a LDF recording.

In preparation for the blood flow measurements taken after NFL thickness measurements, the right pupil of each subject was dilated using a combination of drops: proparacaine hydrochloride 0.5%, tropicamide 1% and phenylephrine hydrochloride 2.5%. A blood flow sensor was clipped onto the subject's left ear lobe for simultaneous recording of the cardiac pulse, that is needed for calculation of various blood flow parameters. An opaque patch was placed over the left eye to facilitate steady fixation by the test eye on a fixation probe. During blood flow measurements the head of each subject was steadied by chin and forehead rest. A polaroid fundus picture was taken prior to all LDF recordings and the sites of blood flow measurements were marked using anatomical structures (eg. course of vessels) as fiduciary areas that matched the sites of local NFL thickness measurements.

The probing laser diode beam of the LDF system was focused away from visible vessels at retinal sites in the peripapillary region of the fundus, about 1.75DD away from the optic disc center. The stationary probing laser was directed towards the retinal area of interest by having the test eye follow a separate movable fixation probe. A minimal 60 sec. continuous recording of

blood flow was taken in the superior, inferior, temporal, and nasal quadrant, respectively. The measurements were taken along the vertical and horizontal axis, in fundus areas corresponding to the sites shown on the retardation maps to have the thickest NFL in the superior and inferior quadrants, and the thinnest NFL in the temporal and nasal quadrants. During each 60 sec. recording session, the subject was asked to fixate first the center of the fixation probe and then the 12, 3, 6 and 9 o'clock edges of the probe circumference before refixating the probe center. The latter consisted of a miniature 670 nm pencil composed of a fine bundle of fiber optics encassed in a 1.2 mm stainless steel cannula. Figure 23 illustrates typical mean blood flow changes in accordance with slight voluntary changes in fixation around the fixation probe. This procedure minimized blood flow measurement discrepancies caused by slight differences in the retinal recording site by averaging blood flow in a small locus of retinal points. For the viewing conditions of this study, the fixation probe subtended approximately 40 minarc at the retina.

All digitally stored LDF recordings were subsequently analysed to remove from analysis any segment of the blood flow recordings without discernable pulsatility related to the cardiac pulse, and those records contaminated with large eye movements or blink artefacts. The artefact free blood flow recording was then averaged over the 60 sec. recording interval using the data averaging function in the Oculix LDF analysis program and expressed as flow in arbitrary units (AU). The same analysis procedure was followed for each of the sites in the four quadrants where blood flow measurements were made.

3.4.4 Statistical analysis

In order to compare data across subjects and eliminate the large inter-subject differences in baseline blood flow values, absolute blood flow data within subjects was compared to the flow values obtained in the nasal quadrant. The nasal sector was selected as the reference site because the nasal fibers are the most stable in glaucoma. Relative ratios for the superior, inferior, and

temporal LDFs were thus computed by dividing superior, inferior, and temporal LDF values by the nasal value (respectively referred to as superior LDF, inferior LDF and temporal LDF). As previously mentionned, the same procedure was applied to the mean absolute NFL thickness values.

Analyses of Variance (ANOVA) procedures were used to determine whether the mean absolute values of NFL thickness and blood flow differed across quadrants. ANOVA's were also applied to the NFL thickness and LDF measurements expressed in ratios-to-nasal. An alpha value of 0.05 was used to qualify any differences as statistically significant. The correlation between the LDF and NFL thickness measurements was evaluated using linear regression techniques, on both the absolute values and ratio-to-nasal values. A p-value of less than 0.05 was considered statistically significant.

3.5 RESULTS

The group averaged absolute and ratio-to-nasal data for the NFL thickness and LDF measurements are summarized in Table I. Analyses showed that there was a significant difference between the mean NFL thickness measured in the superior, inferior, temporal and nasal sections of the peripapillary retina ($p < 0.0001$). Figure 24 illustrates for each retinal quadrant, the distribution of individual NFL thickness values, in ascending order across subjects. On average, the NFL test sites in the superior (102.5 μm) and inferior (91.7μm) quadrants were thicker than the nasal (55.6 μm) and temporal (49.6μm) NFL test sites.

In contrast, the LDF values did not differ across quadrants ($p = 0.97$). The right hand data column in Table I for the LDF ratios-to-nasal shows that all LDF ratios were close to a value of 1, thereby indicating the same relative blood flow across retinal quadrants. Figure 25 illustrates for each retinal quadrant, the distribution of individual absolute LDF values, in ascending order across subjects. This schematical presentation of the LDF data highlights a great

intersubject variability in blood flow levels, and comparable LDF values across quadrants.

Figure 26 illustrates the relationship between the absolute LDF and NFL thickness values. Focal LDF readings did not correlate with local NFL thickness measurements of corresponding fundus areas ($p = 0.38$, $r = 0.09$). For each subject, the local NFL thickness and flow values were expressed as ratios by dividing each NFL and LDF mean value by the NFL or LDF value obtained in the nasal section for the same subject. Once again, statistical analyses showed that the LDF ratio did not correlate with the NFL ratio for the same fundus site ($p= 0.17$, $r=0.14$).

Table I

Retinal nerve fiber layer thickness and blood flow changes across quadrants in defined peripapillary sites (n=24) (Mean ± SD)

Retinal area	NFL (μm)	NFL Ratio (NFL/nasal)	LDF (au)	LDF Ratio (LDF/nasal)
Superior	102.5±19.1	1.87±0.2	34.9±13.0	1.03±0.4
Inferior	91.7±18.2	1.67±0.2	32.6±12.4	0.96±0.4
Temporal	49.6± 9.4	0.91±0.1	35.7±22.0	0.97±0.3
Nasal	55.6±11.8	1.00±0.0	37.1±18.3	1.00±0.0
ANOVA	(p<0.0001)	(p<0.0001)	(p=0.97)	(p=0.82)

In order to qualify the relationship between the average blood flow in the vertical quadrants and the average blood flow in the horizontal quadrants, a normalized blood flow ratio (BFR) was also calculated for each individual. This was computed according to the equation below i.e. dividing the average mean flow in the vertical meridian by the average mean flow in the horizontal meridian:

$$\mathbf{BFR = average\ LDF_{vert} / average\ LDF_{horiz}}$$

$$\mathbf{BFR = (LDF_{sup} + LDF_{inf}) / (LDF_{temp} + LDF_{nas})}$$

Using this analytical approach, two subgroups were derived: subjects showing a **BFR >1** were arbitrarily placed into **Group 1**, where the average vertical flow was significantly greater than the average horizontal flow (ANOVA $p < 0.01$). Subjects showing a **BFR <1** were arbitrarily placed into **Group 2**, where the average vertical flow was significantly lower than the average horizontal flow (ANOVA $p < 0.05$). Interestingly, the subject population was roughly divided in half by this classification; thirteen (13) subjects qualified for group 1 and eleven (11) subjects qualified for group 2. This fallout of data suggests that there is no physiological significance to this classification since it could occur entirely by chance.

The mean BFR was 1.22 ± 0.18 and 0.75 ± 0.13 for group 1 and group 2, respectively (ANOVA $p < 0.0001$). The refractive error and IOP were not significantly different between the two groups. Furthermore, the overall correlation between the focal LDF and NFL thickness values did not reach the 95% significance level for either groups when considered separately ($p=0.10$ for group 1, and $p=0.47$ for group 2).

Fig. 17

PRINCIPLE OF SCANNING LASER POLARIMETRY FOR NFL THICKNESS MEASUREMENTS

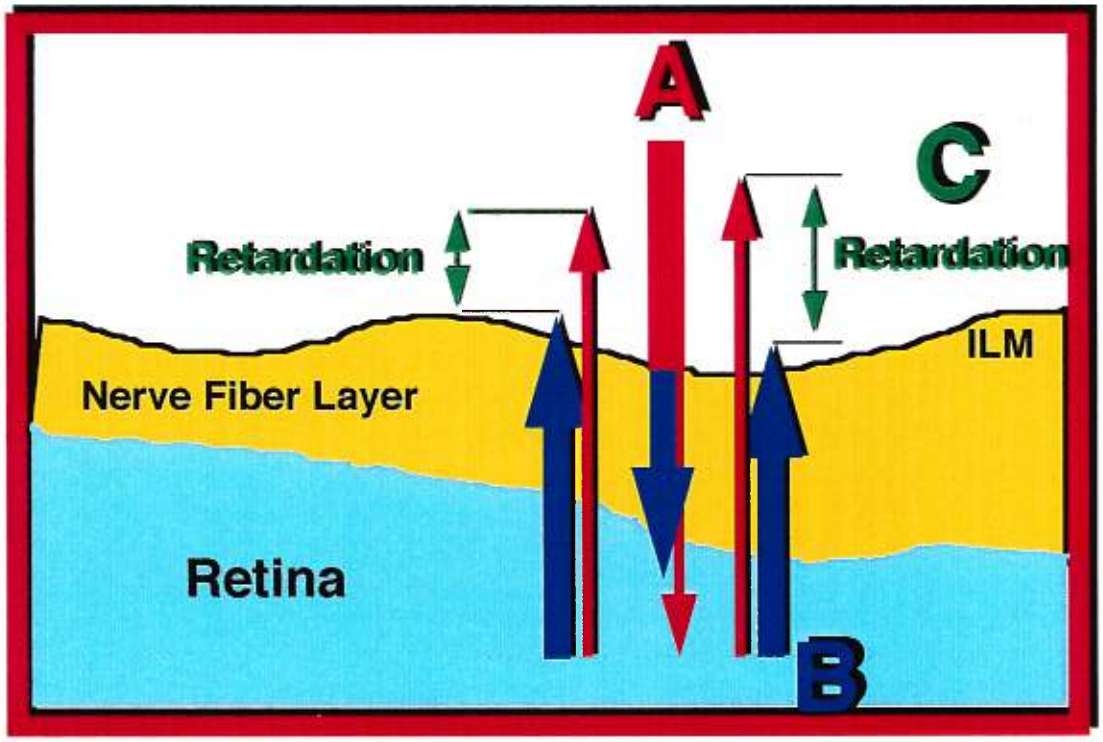

A. Birefringence of NFL splits polarized laser light into two parallel rays travelling at different speed (retardation). **B.** Exiting parallel rays traverse NFL in different times. Retardation between exiting rays **C**, is linearly related to the thickness of the NFL.

Fig. 18

SCANNING LASER POLARIMETRY ...measurement of NFL thickness

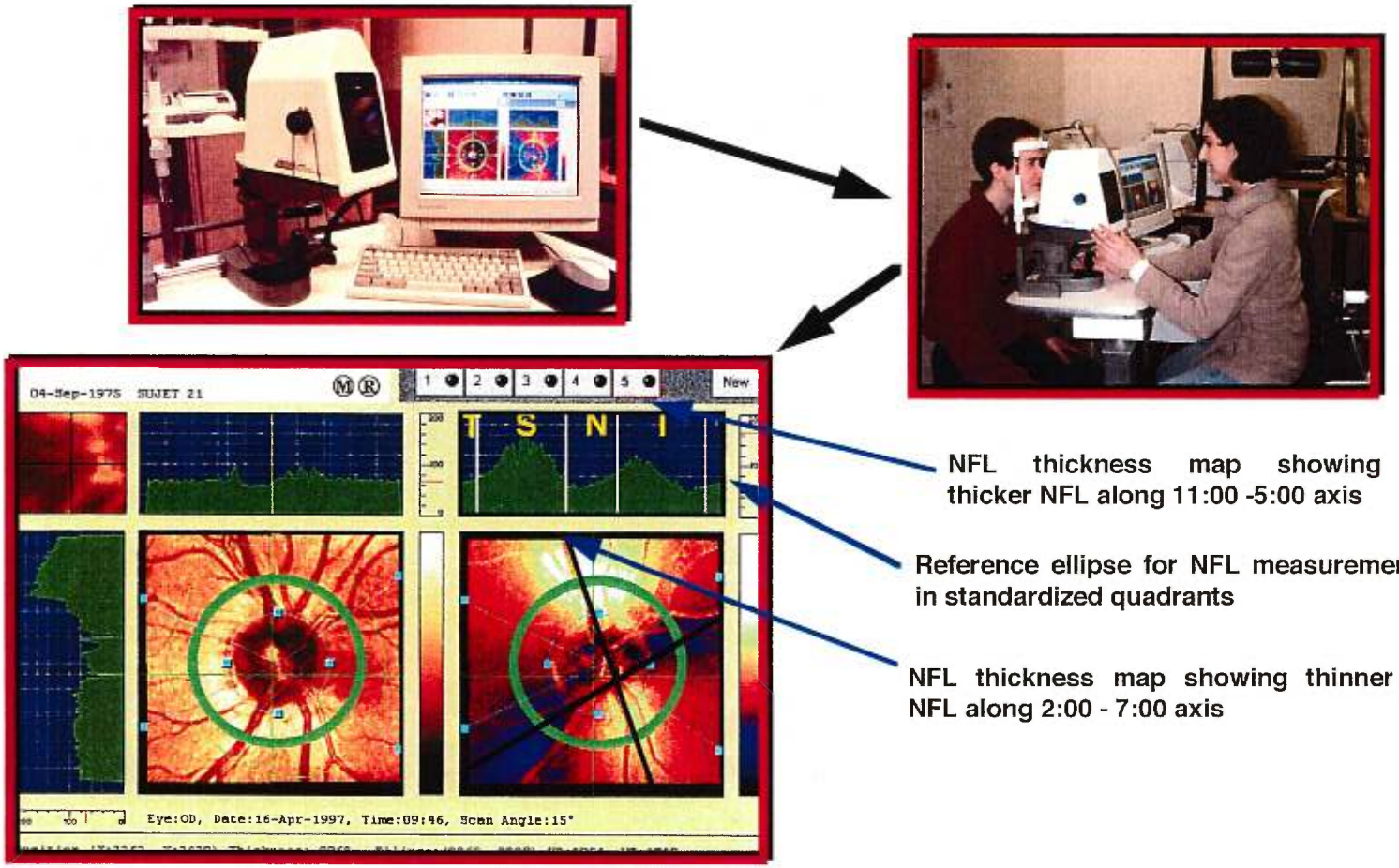

- A Laser Diagnostic Technologies Nerve Fiber Analyser was used to measure the NFL thickness over a scan angle of 15° about the ONH in subjects with non-dilated pupils.
- An average of 3 well focussed NFL scans provided our baseline NFL distribution values.
- A printout of NFL thickness distribution maps was used to determine ideal sites for blood flow measurements (i.e. thickest zones typically along vertical meridian; thinnest zones typically along horizontal meridian).

Fig. 19

MATCHING FOCAL NFL AND LDF MEASUREMENT SITES

Polaroid fundus picture

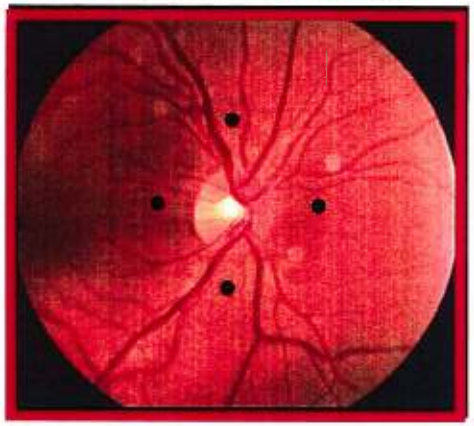

- Site of blood flow measurement is marked on a polaroid fundus picture with a pen (black dots).
- The LDF sites correspond to sites where the NFL is most thick and thin within a thickness grid.
- The average thickness in a single square of the grid (equal to 56 minarc) is used for correlational analysis with blood flow.

Grid of NFL thickness values (15 ° x 15 ° field)

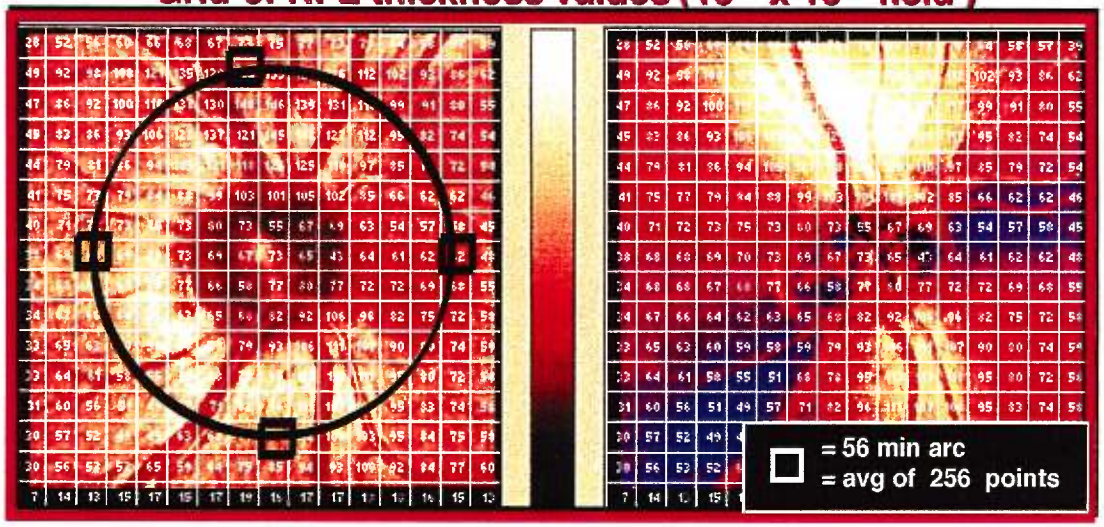

Fig. 20

Doppler Shift by RBCs in blood vessels

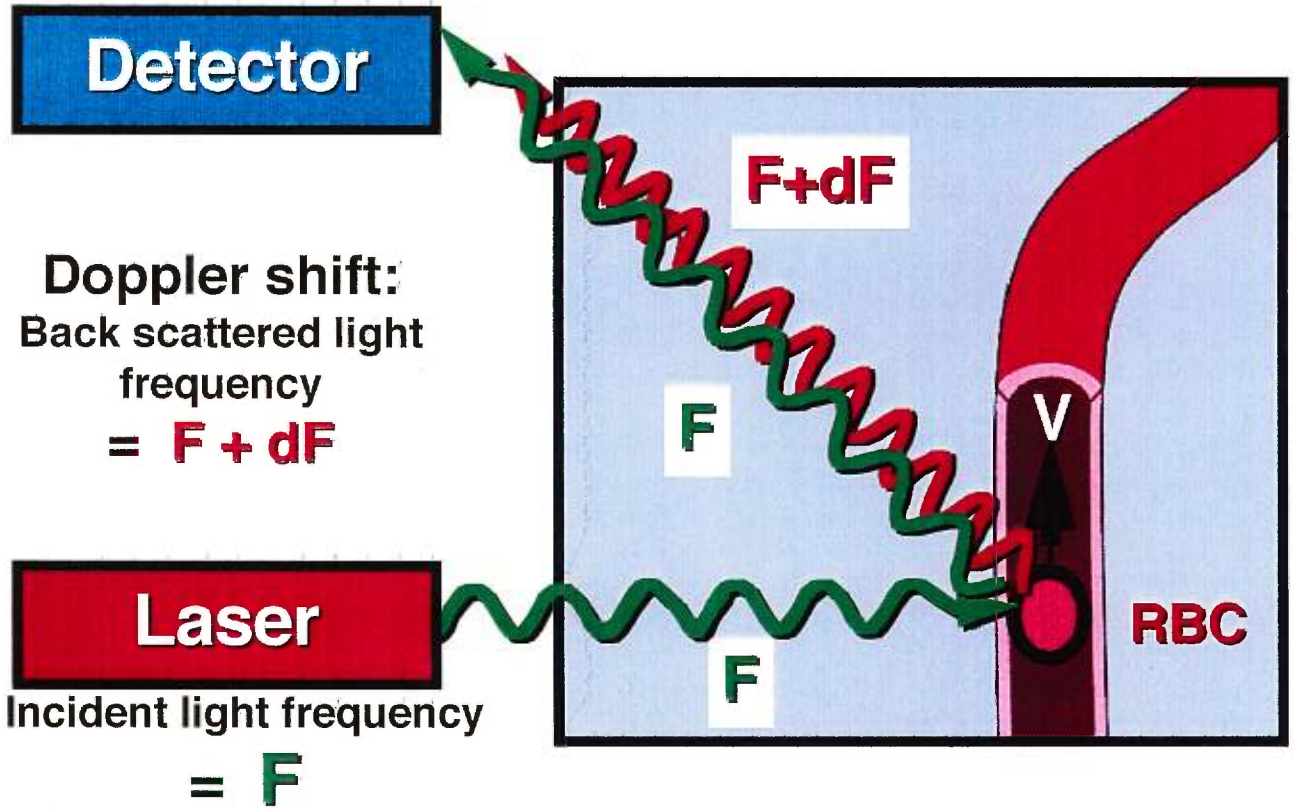

- A coherent light source of specific wavelength or frequency F illuminates both the vessel wall and the RBCs moving in the vessel. Some light is reflected from the vessel wall without frequency change, i.e. F.
- Moving RBCs cause a slight change in the wavelength or frequency of the original laser light and reflect it at the frequency F + dF.
- Backscattered frequencies F and F+ dF interfere to produce a frequency "beat". This variation in backscattered light is converted into a frequency spectrum (FFT) to derive blood flow parameters.

Fig. 21

LIGHT SCATTER MODEL FOR LASER DOPPLER FLOWMETRY

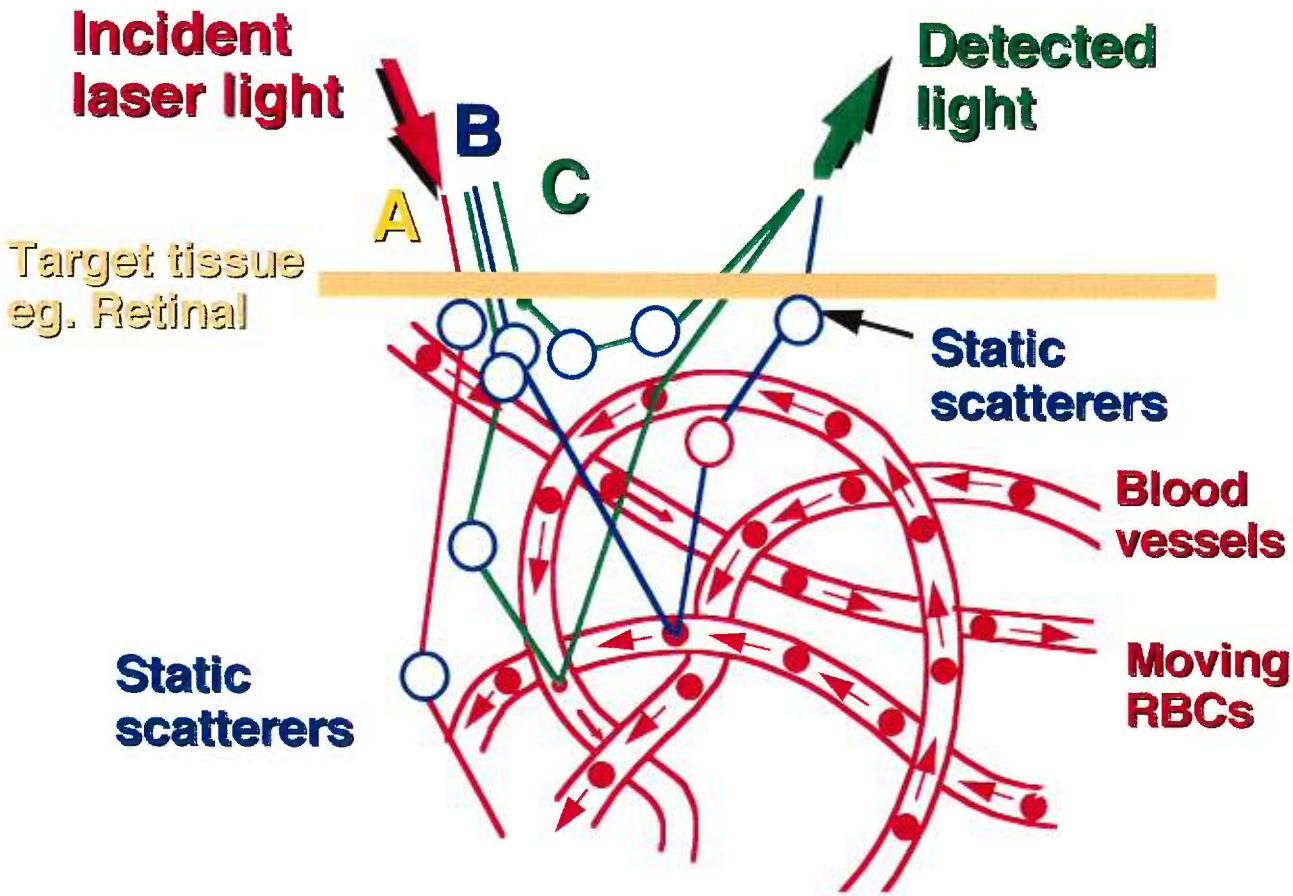

Laser light incident on the ONH is scattered mainly by static scatterers (optic nerve tissue) and some RBCs in the resident capillaries. Some of the light scattered by tissue and RBCs eventually reaches a light detection system for determination of the Doppler shift and derivation of blood flow parameters.

Fig. 22

LASER DOPPLER FLOWMETRY.. measurement of blood flow

LDF system

- Subjects' pupils were dilated with Tropicamide and Phenylephrine
- An Oculix LDV 5000 system was used to measure the blood flow at four sites in each major quadrant along the vertical and horizontal meridians about 1DD from the disc margin.
- At each site a minimal 60 second record of flow was made following a fixation routine.
- Heart rate was monitored with an ear sensor

Sample LDF recording for one quadrant site

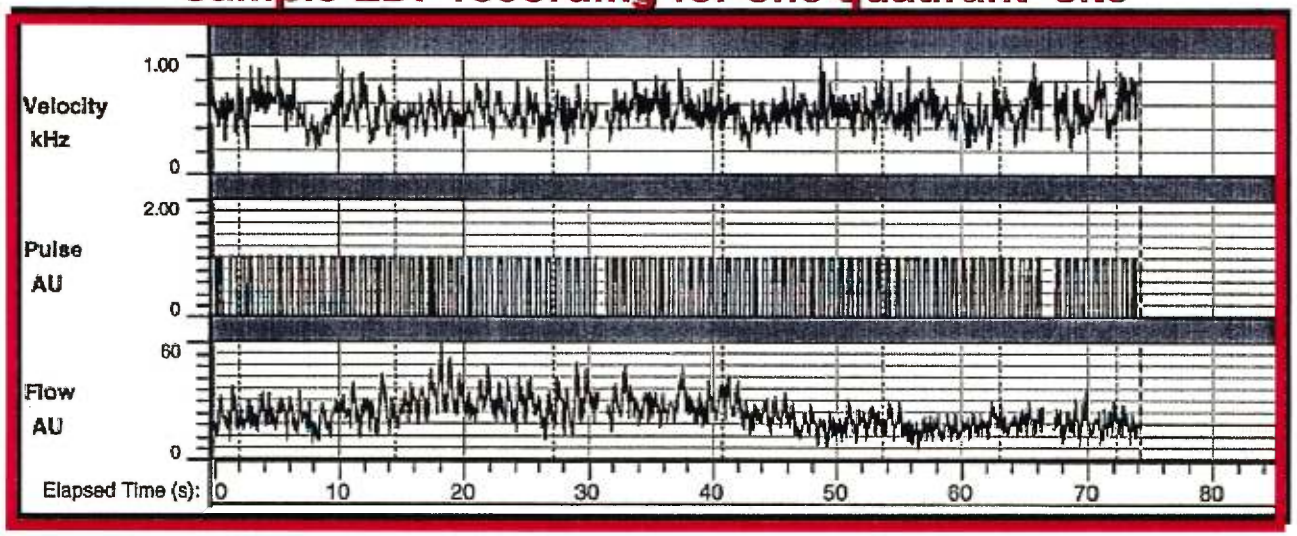

Fig. 23

Fixation protocal for focal LDF measurements at selected quadrantal sites

Head-on view of fixation laser probe

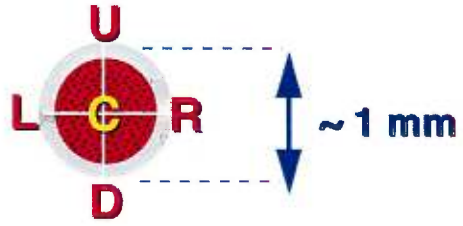

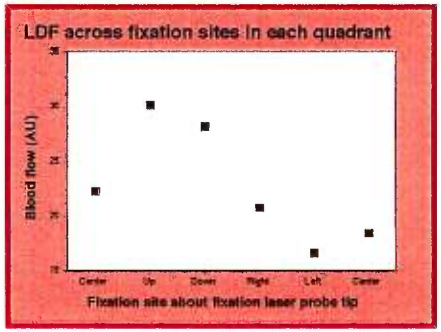

Focal measurements made in sample temporal quadrant
- LDF parameters vary slightly with deliberate fixation changes -

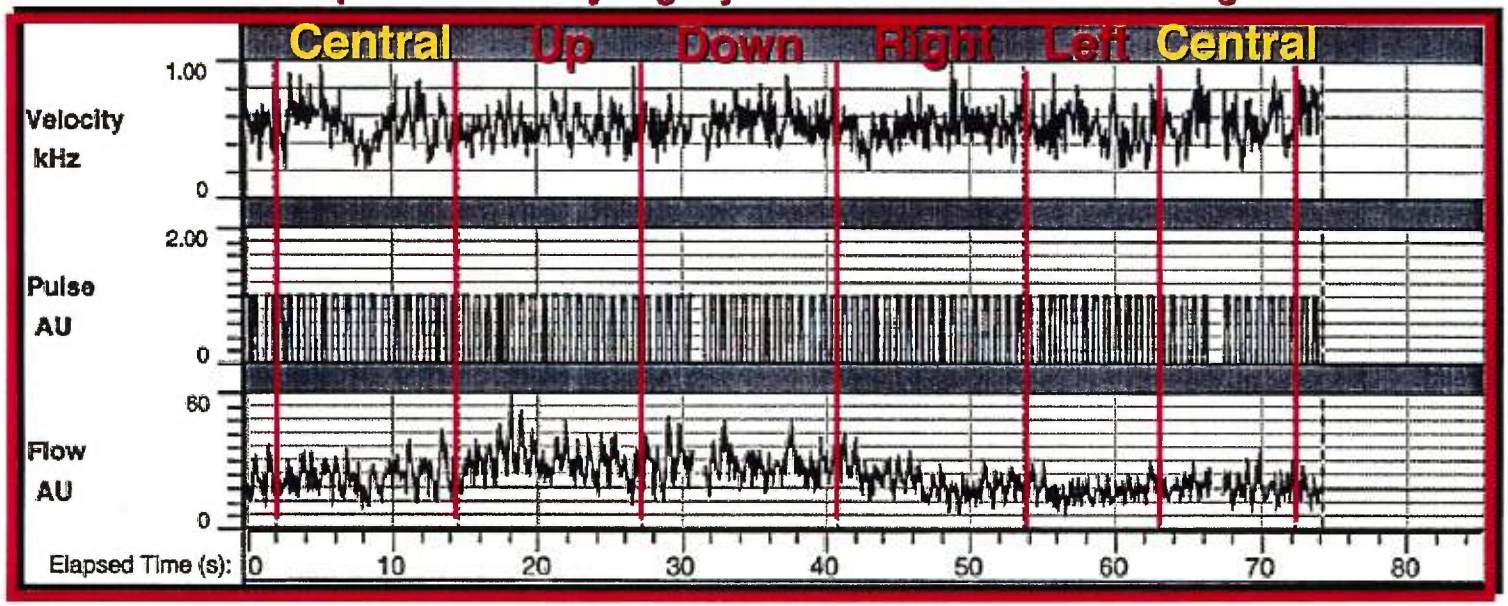

Fig. 24

DISTRIBUTION OF FOCAL NERVE FIBER LAYER THICKNESSES IN ASCENDING ORDER ACROSS SUBJECTS AND QUADRANTS ABOUT THE OPTIC NERVE HEAD

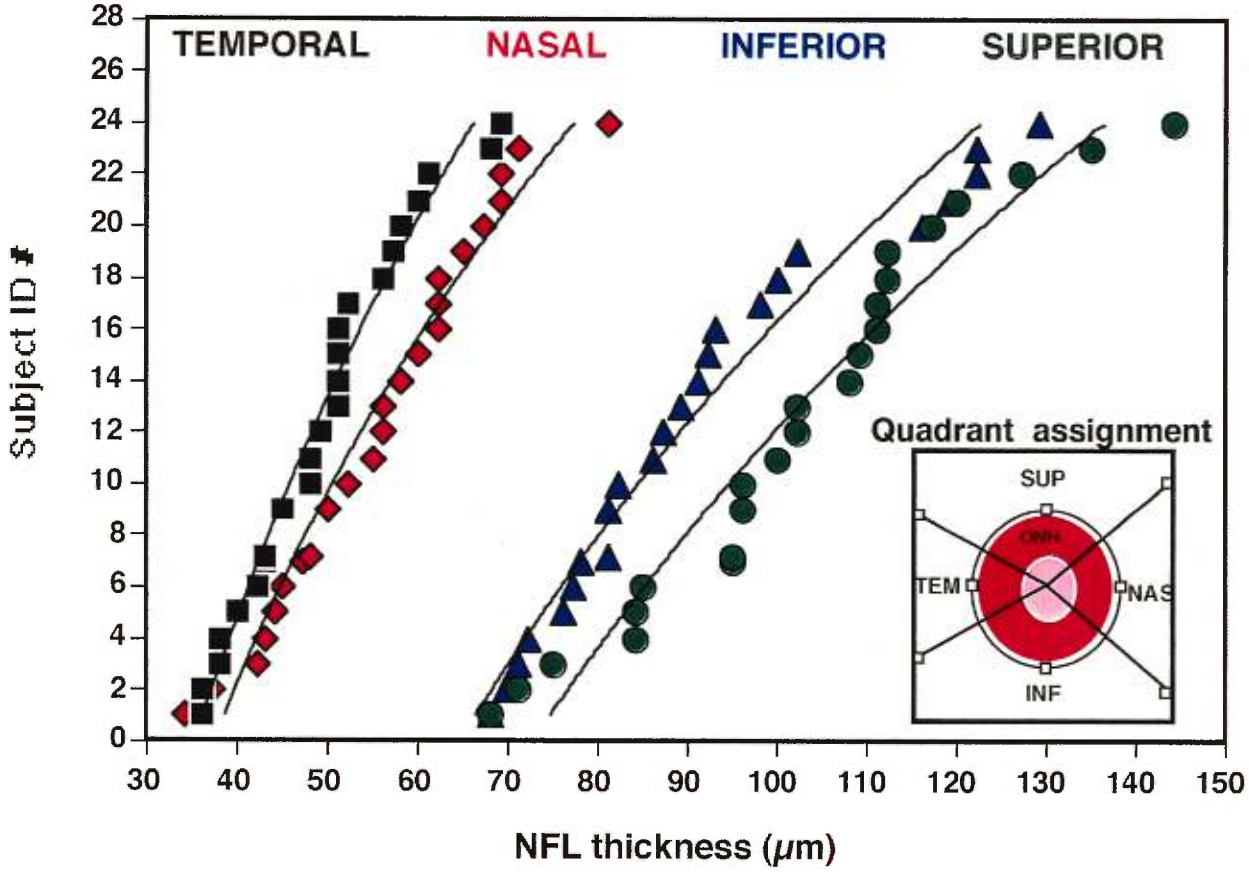

For these 24 subjects, the NFL sites measured in the Vertical axes were THICKER than the NFL sites measured along the Horizontal axes (ANOVA, $p < 0.0001$).

Fig. 25

DISTRIBUTION OF FOCAL BLOOD FLOW IN ASCENDING ORDER ACROSS SUBJECTS AND QUADRANTS ABOUT THE OPTIC NERVE HEAD

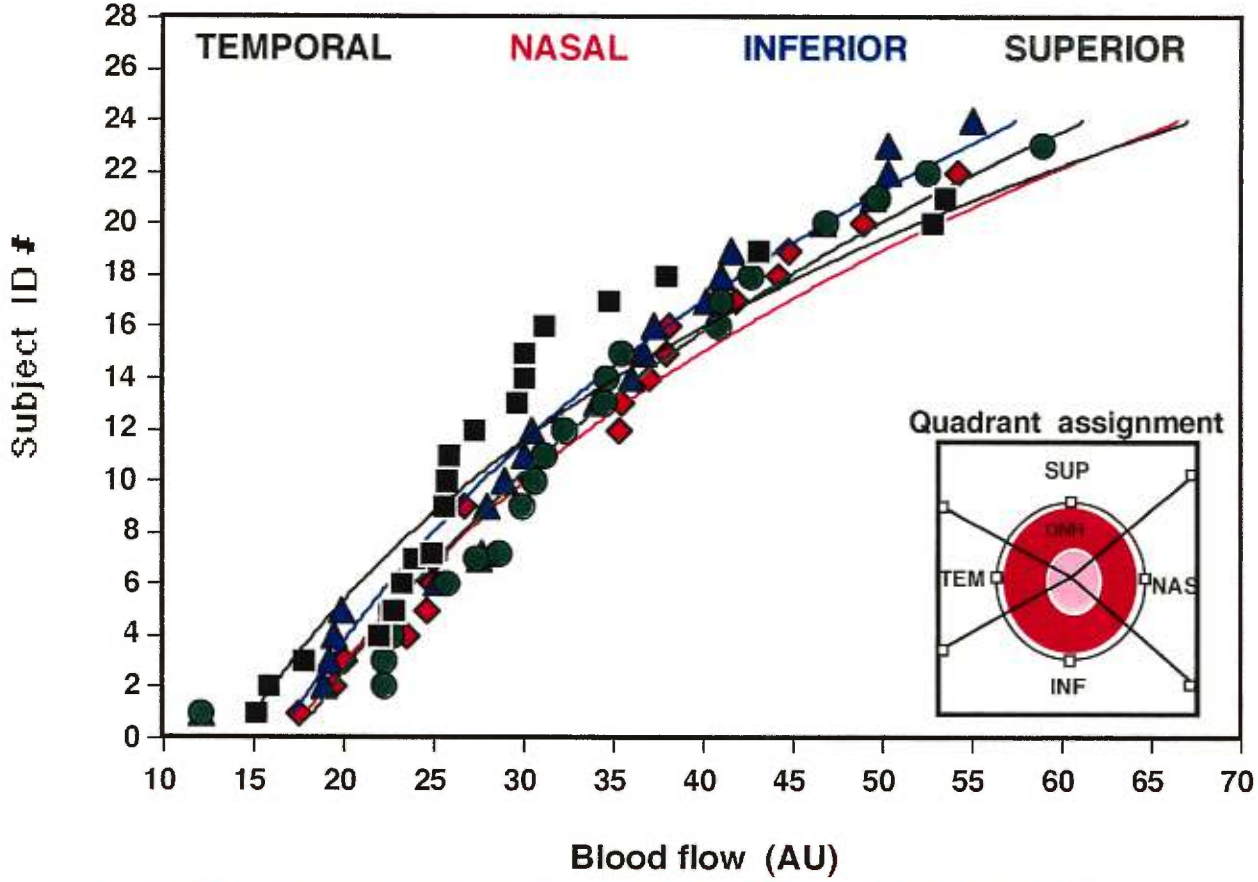

For these 24 subjects, blood flow did not differ across the fundus quadrants combined (ANOVA , p= 0.97)

Fig. 26

FOCAL BLOOD FLOW AS A FUNCTION OF FOCAL NERVE FIBER LAYER THICKNESS ACROSS SUBJECTS AND QUADRANTS ABOUT THE OPTIC NERVE HEAD

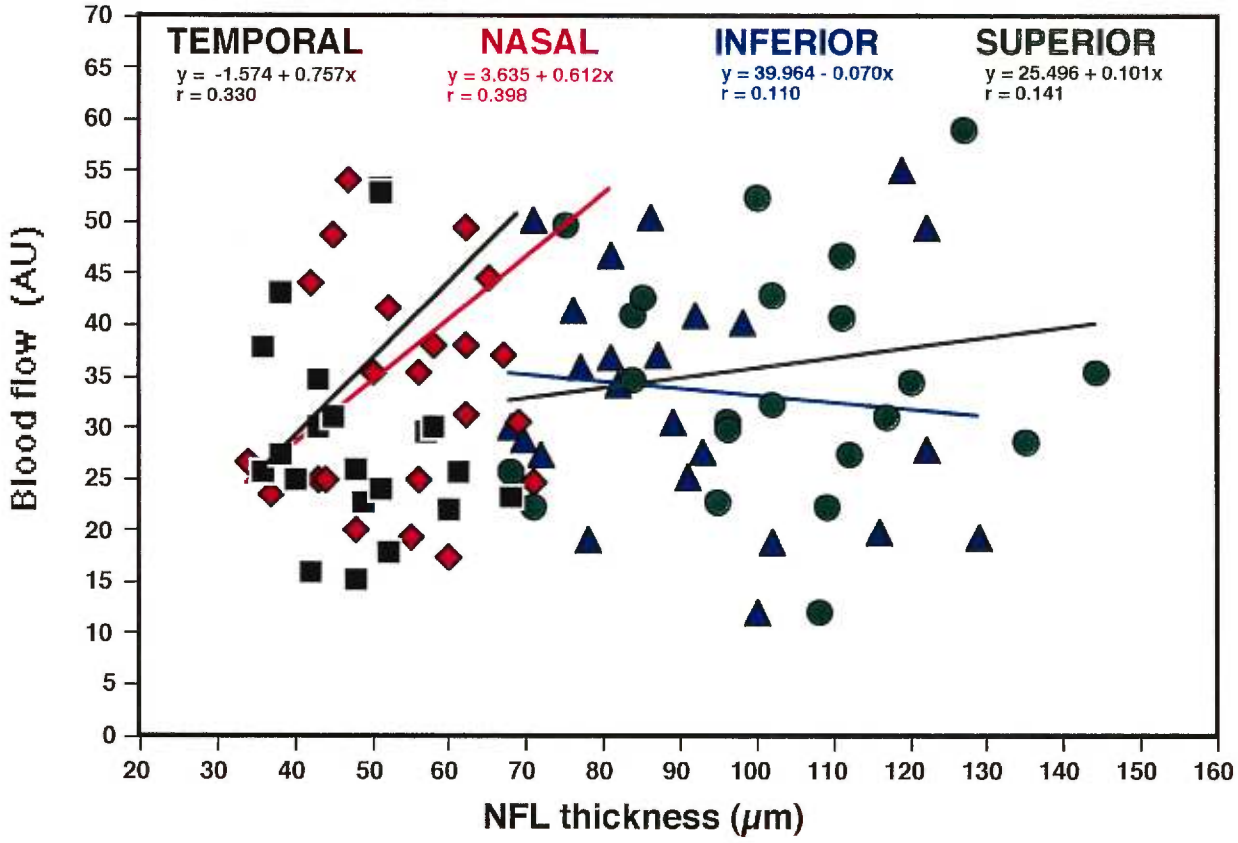

For these 24 subjects, blood flow did not correlate with the NFL thickness globally (p=0 .38, r=0.09).

3.6 CONTROL STUDY FOR REPEATABILITY OF BLOOD FLOW MEASUREMENTS USING THE 670 nm LDF SYSTEM

3.6.1 Materials and methods

To investigate the reproducibility of the LDF measurements across time with the Oculix LDF system, multiple LDF recordings were taken on one well-trained subject, in three protocols. All measurements were made in a temporal peripapillary site of the right eye, located about 1.75 DD away from the optic disc center, in a retinal area free of large vessels.

1) *LDF reproducibility over a one minute interval*

The subject was asked to alternately open and close the test eye at 10 second intervals to obtain an arbitrary total of seven consecutive blood flow records at the same NFL site. During the procedure, the subject's head position, alignment of the instrumentation, and position of the probing laser were unchanged so as to derive blood flow records that maximally represented the physiological variation in blood flow over time at a single NFL site.

Data analysis consisted of dividing each of the seven continuous LDF recordings into 10 one second intervals. An average blood flow value was then obtained for each interval using the native analysis software. The mean flow and SD for all seven LDF recordings were calculated using the 10 individual flow values. Altogether, 70 segments were used in this analysis of repeatability of blood flow measurements over a short interval.

2) *LDF reproducibility over a one hour measurement interval*

In this control study, a 30 second LDF record of blood flow was made every 10 minutes, within about a one hour period to yield seven 30 second records of dynamic changes in blood flow at a single NFL site. Just prior to each thirty second LDF recording, the subject repositioned his head in the Oculix system where the alignment between the measurement and fixation lasers was kept

constant to help insure that blood flow measurements were made at the same retinal site. When needed, the focus of the fundus image was adjusted to maintain a criterion clear view of fine retinal vessels close to the NFL measurement site.

Data analysis consisted of dividing each of the seven 30 second LDF recordings into ten, 3 second intervals and then averaging the blood flow parameters over each interval using the appropriate Oculix averaging analysis protocol. Subsequently, the mean blood flow with standard deviation values were calculated for each of the seven, 30 second LDF recordings using the blood flow values derived for each of the ten, 3 second intervals. Thus, in all, 70 segments of continuous blood flow were used in the present analysis.

3) *LDF reproducibility over a one day test interval*

In order to determine the variability in blood flow measurements that principally reflected diurnal changes in blood flow over the course of a normal day, 30 second samples of moment-to-moment changes in blood flow were taken hourly starting at 8:00AM, and ending with a final 30 second sample at 6:00PM. Overall, this provided eleven LDF recordings, each 30 seconds or more in duration. Just prior to each recording session after the first 30 second blood flow measurement, the subject repositioned his head into the Oculix system that remained unchanged from the initial laser alignments and fundus focus. The subject was allowed to proceed with his normal activities (including eating) between hourly recording sessions.

Data analysis consisted of dividing each of the eleven blood flow sessions into ten 3 second intervals for which average blood flow values were measured by the appropriate Oculix analysis software. The mean flow and standard deviation (SD) of the eleven LDF recordings were calculated using the 10 individual blood flow values. In all, 110 measurement segments were used for determining blood flow reproducibility over the ten hour test interval.

3.6.1 Results

The variations of LDF measurements across time are illustrated in Figure 27. For the control study examining blood flow measurement reproducibility over one minute (Figure 27, graph A), an average coefficient of variation of 7.18% was found within each 10 second blood flow recording. A coefficient of variation of 7.06% (Mean flow =34.51AU ± 2.44, n=7) was calculated over a one minute interval. An analysis of variance (ANOVA) indicated a statistically significant difference between the seven average blood flow values obtained every 10 seconds ($p < 0.0001$). A post hoc analysis revealed that five out of seven average LDF values were identical to each other (Scheffe F-test, $p > 0.05$); only the first and the second LDF values differed from the remaining blood flow estimates, and differed from each other (see letter notation to show identical and different data points). The 95% confidence interval for mean blood flow over one minute was ±6.53%. Overall these data indicated a high reproducibility of blood flow measurements at a single retinal site when fixation and recording sites were kept constant.

For the study examining the reproducibility of blood flow over a one hour interval (Figure 27, graph B), an average coefficient of variation of 5.75% was calculated within each 30 sec. LDF recording. The overall coefficient of variation was 7.59% when considering the mean flow values obtained for each of the seven recordings over a period of one hour (Mean flow=34.72 ± 2.64, n=7). ANOVA testing indicated that there was some difference in the mean blood flow values across the 7 data sets ($p<0.0001$). Once again, a post hoc analysis revealed that five out of seven values did not differ from each other; data sets for the first and seventh trials differed from the rest of the mean LDF values but were identical to one another (see letter notation to show identical and different data points). The 95% confidence interval for mean blood flow over one hour was ±7.14%. This data set also indicated a high reproducibility of blood flow measurements.

For the control study examining the variability in blood flow measurements at a single retinal site over one day (Figure 27, graph C), an average coefficient of variation of 7.16% was found for each 30 sec. recording of blood flow. The coefficient of variation for the data acquired hourly over the 10 hour test session was 16.1% (Mean flow =29.86 ± 4.806, n=11). There was a statistically significant difference between the eleven average blood flow values obtained every hour (ANOVA, $p<0.0001$). Here a post hoc analysis clearly showed that groups of LDF values differed from each other over time (see letter notation to show identical and different data points). A visual inspection showed that there was an overall tendency for the blood flow values to increase progressively in the first half of the day (8 AM to 1 PM), and a slight decline or a tendency to maintain a plateau between noon time and 6 PM. However, since these data are for one subject only, no exact prediction about diurnal trends can be made. What is seen in this case is that there is an increased variability in blood flow measures with longer inter-trial intervals. The 95% confidence interval for mean blood flow over one day was ±10.71%.

3.7.3 Interpretation

This study demonstrates good reproducibility of the blood flow measurements with the Oculix 670 nm, LDF system when specific conditions are met: steadiness of the subject's head position and fixation, constancy of the angle of incidence of the probing laser at the retinal test site, and minimal time between consecutive measurements.

A 95% confidence interval of ±6.53% was found for the mean blood flow measured over a 60 sec. period. This confidence interval was slightly greater than that reported earlier by Riva et al (16) where a 95% confidence interval of ±4% was recorded for ten choroidal blood flow recordings of 15 sec. duration over a four minute interval , using an LDF Oculix system with a 811nm diode. This difference may be due to the typically clearer blood flow signal that is

obtained in LDF measurements of choroidal blood flow. The latter has a clearer and larger pulsatility and thus would yield better repeatability measures than those obtained from the sparser and less dense retinal capillaries measured in the present study.

In the present study, the variation of mean blood flow measurements over the same retinal site tended to increase with greater intervals between measurements. This latter observation may reflect real blood flow changes over time caused by the physical state of the subject (eg. hunger, anxiety, etc.) or differences caused by slight variations in measurement conditions such as minute changes in target fixation, tremor of the eye, or a combination of these factors.

The testing conditions for the present study examining the correlation between blood flow and the retinal nerve fiber layer thickness were most similar to data acquisition parameters in the control study examing LDF variability over a one hour interval; the subject's head remained in the head/chin support of the LDF system between measurements of blood flow in each of the fundus quadrants, the duration of each blood blow recording was about 60 seconds, and the interval between each recording was less than ten minutes. However, because of the objective of the experiment, the fixation and measurement lasers were necessarily readjusted between recording sessions. Such changes in the angle of incidence of the measurement laser could introduce some variation in blood flow values that do not solely represent actual changes in blood flow across segments. Therefore, a 95% confidence interval of 7.14% obtained during the control study without a change in the angle of the measurement probe would not be surprising. This means that, if the nasal blood flow was considered as baseline, a change greater than 14.28% in mean blood flow for the other quadrants would be considered significant at $p < 0.05$.

Fig. 27 **Repeatability of blood flow measurements over time**

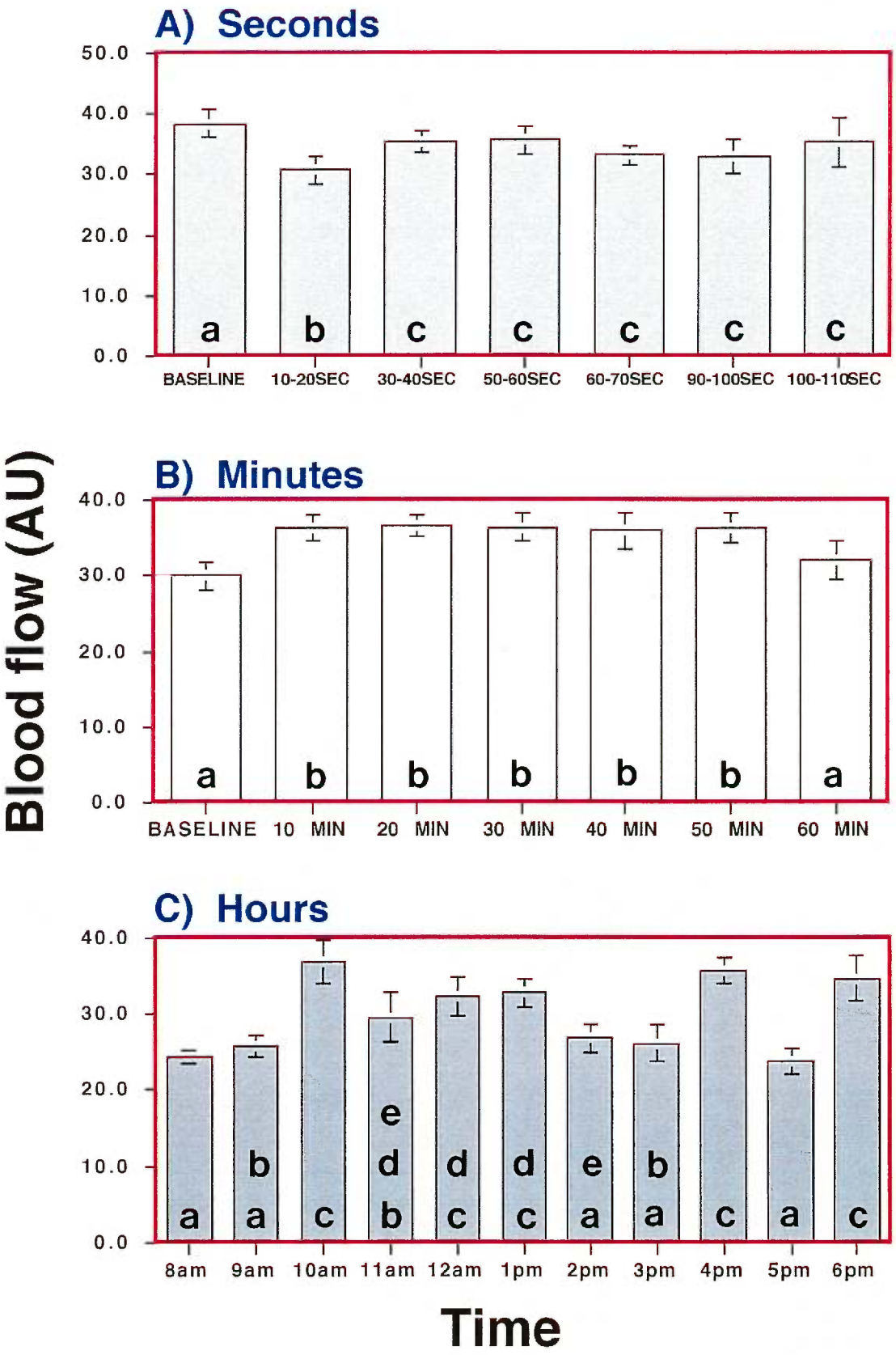

3.7 CONTROL STUDY: DOES THE CHOROIDAL BLOOD FLOW CONTRIBUTE TO THE LDF MEASUREMENTS AT PERIPAPILLARY SITES USING THE 670 nm LDF SYSTEM?

In their study of spectral absorption by the retina, Geeraets et al (17) showed that the percent transmission of the human retinal pigment epithelium for a 670nm light was less than 80%. Levels of transmission greater than 80% were found for wavelengths of 800nm and over. Riva et al (16) were able to measure local, relative choroidal blood flow in humans using a noninvasive 811nm LDF system. The foveal region of the fundus was chosen as the measuring site for the obvious reason that it is free of retinal vessels. Among other findings, Riva et al demonstrated that the choroidal blood flow (ChBF) was pulsatile i.e. demonstrated a rhythmical waveform with wavelets synchronous with the cardiac cycle.

In the present study, a separate control study was carried out to determine whether the blood flow measurements made with a 670nm laser diode could have included signals of choroidal origin.

3.7.1 Materials and methods

Three (3) healthy volunteers (age 15, 17 and 45 years of age) participated in this control study. The ages of the subjects were selected to represent healthy, young and middle age eyes. For each of the subjects, blood flow recordings were taken with a 670nm probe at the fovea, and also at a temporal peripapillary site, some 1.75DD away from the ONH center. The blood flow recordings for the fovea were also taken with an 811nm laser probe. All peripapillary blood flow recordings were taken under the same procedures described in the body of this report. Foveal blood flow measurements however, involved direct fixation of the probing laser by the subject to insure recording from the central macula which is free of retinal vessels. A minimal 30 sec. recording was taken for each of the three blood flow measurements. Sample

waveforms of blood flow patterns obtained with the 811nm probe in the macula and the 670nm probe in the macula and peripapillary NFL site are shown in Figure 28, plates A, B, and C respectively.

3.7.1 Results

The sample blood flow recordings for the foveo-macular area taken with an 811nm probe revealed a very regular sinusoidal-like pattern of wavelets time-locked to the cardiac pulse that was measured with an ear sensor. Averaging of the wavelets for the foveo-macular flow revealed a sawtooth pattern with the steeper portion corresponding to the systolic phase of the cardiac cycle (see frame A, Figure 28).

An assessment of foveo-macular flow using a 670nm probe yielded a pulsatile waveform with larger amplitude oscillations than that obtained with the 811nm probe. However, careful inspection of the blood flow pattern revealed that the wavelets were not universally linked to the cardiac pulse. Several wavelets could be found in the absence of a cardiac pulse as shown by the inverted arrows in frame B, Figure 28. By averaging the blood flow wavelets over a sample 12 second recording, objective confirmation was obtained to show that the wavelets had an irregular periodicity, and were only loosely linked to the cardiac pulse. That is, some of the wavelets were time-locked to the cardiac pulse, but others were not. As a result, the averaged flow waveform shown in the right hand panel of Frame B in Figure 28 did not have a characteristic sawtooth profile as did the waveform for the 811nm foveo-macular recording. This was interpreted as indicating that the wavelets seen in the blood flow record were not clearly linked to a pulsatile blood flow per se.

Furthermore, since the absolute flow value obtained by the 670nm probe in the foveo-macular area was on average three times greater than that seen for the 811 nm foveo-macular recordings across all three control subjects, it was concluded that the 670nm blood flow wavelets represented mainly light reflected from the NFL and blood vessel free, mirror-like vitreo-retinal interface

at the foveo-macular zone. The pulsatility in the blood flow pattern was mainly caused by light scattering events involving the static non-vascular elements of the retinal tissue itself. Specifically, the wavelets are interpreted to be due to the cardiac pulse present throughout the choroidal vasculature which rhythmically displaced the overlying retinal pigment epithelium and neural retina more or less in tandem with the heart beat and thus caused a phase shift in the laser light to produce the wavelets. It is further presumed that only a very small portion of the 670nm light likely penetrated the RPE, was then phase shifted by the moving blood cells in the choriocapillaris, and was ultimately back-scattered back through the RPE to the light measuring sensor in the LDF system.

The sample 670nm recording for the peripapillary NFL area shown in plate C of Figure 28 demonstrates a clear pulsatile waveform that is invariably linked to the cardiac pulse. It was also noted that the group averaged blood flow pattern obtained in the peripapillary zone with the 670 nm probe differed significantly from that obtained with the same probe from the foveo-macular area. The group averaged peripapillary recording shown in the right hand window of plate C in Figure 28 has a regular sawtooth waveform, with the steep rising phase clearly time-locked with the rising phase of the averaged cardiac pulse which correlates with the systolic component of the cardiac cycle.

An objective quantifiable measurement of the blood flow waveform is the so called "Pulsatility index". This parameter defines the modulation depth of the regular fluctuations in blood flow (i.e. wavelets) seen in an LDF record. The pulsatility is calculated according to the formula below:

$$\textbf{Pulsatility} = 1 - \frac{(\text{Flow}_{\text{Systole}} - \text{Flow}_{\text{Diastole}})}{(\text{Flow}_{\text{Systole}} + \text{Flow}_{\text{Diastole}})}$$

This pulsatility index for each control blood flow recording is presented in Table II. It is noted that the pulsatility for the blood flow measurements made in the fovea with the 811nm vs the 670nm probe is about double in all subjects for the 811nm recordings, indicating that these were strongly linked to the cardiac

pulse whereas the 670nm foveo-macular recordings had only a much lower correlation with the heart beat. Furthermore, in comparison to the foveo-macular blood flow made with the 670nm probe, the pulsatility index tripled in two subjects when the 670nm recordings were made in the peripapillary zone. This indicated a close linkage with the heart beat for these latter recordings.

Table II

Relative blood flow and pulsatility values for LDF recordings at a peripapillary site and foveo-macular region, using the 670nm and 811nm laser probes

Subject (Age)	Test site	Blood Flow (AU)	Pulsatility index
Subject 1 (45)	Peripapillary (670nm)	79.56	0.33
	Fovea (670nm)	36.67	0.10
	Fovea (811nm)	16.83	0.25
Subject 2 (17)	Peripapillary (670nm)	57.53	0.18
	Fovea (670nm)	35.50	0.19
	Fovea (811nm)	08.41	0.33
Subject 3 (15)	Peripapillary (670nm)	25.94	0.44
	Fovea (670nm)	47.41	0.15
	Fovea (811nm)	11.08	0.31

3.7.3 Interpretation

Based on all the above-mentioned findings, it is concluded that the blood flow pattern measured with the 670nm probe in the peripapillary region was caused by a fluid network that was exclusively linked with the cardiac cycle, and was located in a retinal plane before the photoreceptor-RPE complex. Collectively, this logic isolated the retinal vasculature as the sole anatomical

possibility for a source of blood as measured by the 670nm probe in the peripapillary region.

Fig. 28

VARIABLES INFLUENCING LASER DOPPLER FLOWMETRY

Blood flow, waveform, and pulsatility as a function of measurement site and wavelength of laser probe

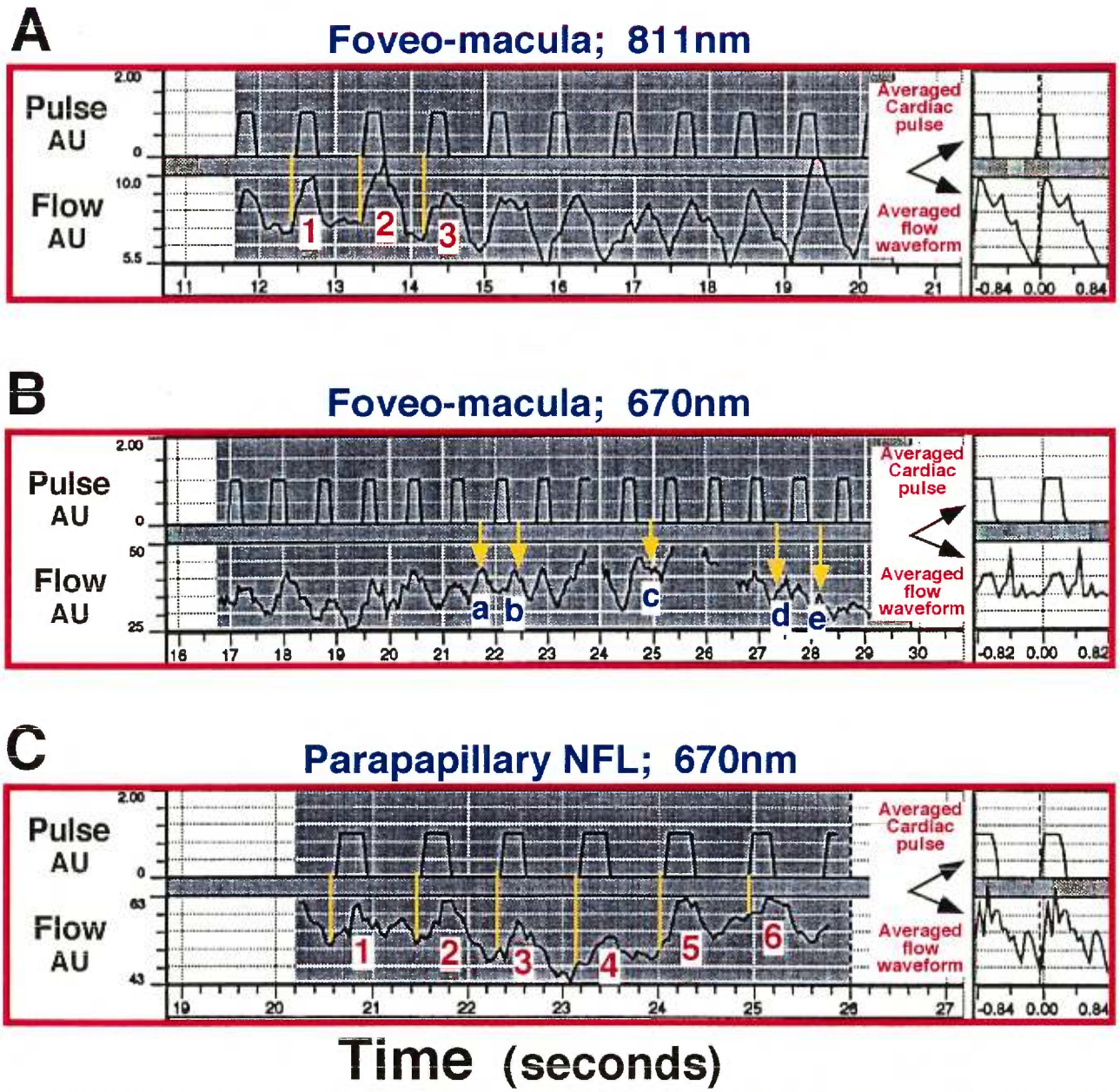

Sample traces of LDF blood flow records in the foveo-macular area using an 811nm and 670nm probe, and a peripapillary area using a 670nm probe. The greyed areas in each frame indicate the portion of each record that was group averaged to generate the averaged flow waveforms shown in the small right side panels in each frame. Note in Frame A that the wavelets are uniformly synchronized with the cardiac pulse, as shown by the alignment between wavelets 1-3 and the cardiac pulse. In Frame B, wavelets a-e identified by inverted arrows, do not correlate with the cardiac pulse while the rest do. Frame C shows a consistent correlation between wavelets 1 to 6 and the cardiac pulse.

3.8 CONCLUSIONS AND GENERAL DISCUSSION

Our results showed a significantly greater nerve fiber layer thickness in the retinal areas sampled in the superior and inferior peripapillary regions than that of the nasal and temporal areas. This finding is consistent with the anatomical distribution of the nerve fibers adjacent to the optic nerve head and with the histological findings of Varma et al (1).

The laser Doppler flowmetry (LDF) readings did not vary significantly across peripapillary sites with different nerve fiber layer thickness. The mean LDF values showed considerable intersubject differences for all retinal quadrants, which resulted in coefficients of variation more than two times greater than those found in our control study of reproducibility for the laser Doppler flowmetry (670nm). Our control study had shown coefficients of variation for mean flow between 7 and 15% over a one minute and one day period, respectively. We can assume that the variability of the LDF values across subjects is partially explained by real anatomically based individual variations in baseline blood flow distribution. This observation is supported by studies on ocular blood supply which report a marked inter-individual variation in the anatomical pattern of the intraocular vessel distribution (18).

Other factors related to the sites of blood flow measurements may have contributed to inter-individual differences in LDF values. All blood flow measurements were made about 1.75DD away from the optic disc center, in retinal areas free of visible vessels. Because of considerable differences in retinal vessel organization between subjects, some LDF recordings were taken at a reasonable distance from visible vessels, while others were taken closer to the edges of visible vessels, therefore possibly falling in the characteristic periarterial capillary-free zone described in anatomical studies. This capillary-free zone can be as large as 120μm (2), and can result in reduced mean LDF values. Also, the retinal microcirculation is organized in large capillary meshworks, leaving holes of 50 to 65μm in diameter between the capillaries (3,

4) (See Figure 12, section 2.2). If the incident laser light is directed in the center of a capillary meshwork, the corresponding blood flow measurement may appear to be lower than one taken with the laser light directly incident on a capillary. This configuration of the retinal microvasculature may explain the large variations in blood flow measurements during normal micromovements of the eye around the fixation point. In a control study, the mean blood flow was seen to vary with a coefficient of variation of only 7.06% during a one minute LDF recording with a steady fixation. Using a scanning laser doppler flowmeter, Harris (19) observed that a small change in sample volume location resulted in large differences in the flow measurement, with an average variation in flow between adjacent frame positions of 18.5% (20). In the present study, the influence of positional factors was minimized by having the subject change his fixation about the fixation probe (refer to Figure 23, section 3) and thus averaging the blood flow measurements over a larger retinal area.

Significant changes in the group averaged nerve fiber layer thickness were not correlated with the group averaged mean blood flow at the same retinal site for the twenty-four subjects who participated in the present study. The pattern of blood flow distribution for nerve fiber layers of varying thickness also showed inter-individual differences. Two subgroups were defined based on the meridian showing the greatest average blood flow. Of the 24 subjects, 13 were found to have an average vertical blood flow greater than the average horizontal blood flow, while 11 subjects showed a greater average blood flow in the horizontal meridian. However, the correlation between the local NFL thickness values and the mean LDF values did not reach the 95% significance level in either group. Also, the two groups did not show any significant difference in IOPs or refractive errors. No segregation of subjects into distinct NFL/LDF performance groups could be made by the age or sex of the subjects. As a result, data was collapsed across subjects during data analysis.

When treated as a homogenous population, the test group did not indicate a significant correlation between RNFL thickness and blood flow in

corresponding fundus areas. A possible interpretation of the uniform blood flow levels around the optic nerve head is that LDF values represented the mean blood flow in a constant volume of tissue, and did not sample the nerve fiber layer through its whole thickness. The parameter *flow* measured with the laser Doppler flowmetry technique is defined as the distance covered by all moving cells inside the sample volume per unit time. Anatomical studies show a constant ratio of capillaries to axons to glial cells in the optic nerve head that tends to be preserved during the glaucomatous process. In the retina, the capillary meshworks become multilayered in regions of thicker nerve fiber layers, which might reflect the same objective of preserving a constant ratio of capillaries to axons. If this is the case, then a fixed volume of nerve fiber tissue sampled around the optic nerve may show the same level of blood flow for baseline activity, whether it is sampled in a thick or a thin portion of the retina, because the density of capillaries in the sampled volume would be the same. All measurements of LDF were made with the receptor probe aligned immediately above the incident light. Riva (21) has suggested that putting the detection probe a little further from the laser source may yield deeper readings because of increased chances of picking up light backscattered from greater depths. Thus, it is possible that blood flow was measured only in relatively superficial retinal sites in the present study. The design of the present study did not permit an analysis of the actual depth of the LDF sampled tissue. In fact this is a critical issue in many published studies and may explain discrepancies across studies. Non-invasive studies of blood flow in the human eye, such as the present one, would benefit from complementary histological investigations on blood vessel count in the inner retina, in order to confirm whether or not the retinal vascular beds vary across peripapillary regions of different nerve fiber layer thickness.

On the other hand, if we assume that blood flow measurements actually reflect the available blood supply for any given portion of the nerve fiber layer, the observed uniformity in blood supply despite significant changes in the NFL

thickness may be representative of a baseline condition. The LDF measurements were carried out through dilated pupils, under bright, diffuse light conditions. These photopic conditions are normally associated with low glucose consumption by the photoreceptors and very little ganglion cell activity. (22, 23) Therefore, regions of thicker nerve fiber layer may have shown little difference in metabolic activity, which did not need to be compensated by increased blood flow. Studies on monkeys have shown that flashing light from a stroboscope at low temporal frequencies caused an activation of the ganglion cells which resulted in a greater glucose consumption in the inner parts of the retina as well as in the optic nerve head (18). Further investigations in man would be needed to determine whether flashing light may be an efficient stimulus to create differential increases in blood flow in the larger populations of nerve fibers.

This study has demonstrated that, in normal young subjects, blood flow for a retina exposed to a constant luminous background is uniform accross the fundus even though the NFL thickness varies systematically around the ONH. Because of this relationship between neural structure and blood flow, ocular diseases that impair blood flow globally may place the nerve fibers in the vertical meridian at greater risk for physiological dysfunction or death.

3.9 REFERENCES

1. Varma, R., Skaf, M., Barron, E. Retinal nerve fiber layer thickness in normal human eyes. *Ophthalmology.* 1996; 103 (12): 2114-9.

2. Henkind, P., Hansen, R.I., Szalay, J. Ocular circulation. In: Duane, T.D., Jaeger, E.A., ed. *Biomedical foundation of ophthalmology.* Vol 2. Philadelphia: Lippincott Company, 1988; 5: 1-53.

3. Wise, G. N., Dollery, C.T., Hendkind, P., *The retinal circulation.* 1st ed. New York: Harper & Row, 1971.

4. Funk, R.H.W. Blood supply of the retina. *Ophthalmic Res.* 1997; 29: 320-5.

5. Michelson, G., Langhans, M.J., Groh, M.J. Perfusion of the juxtapapillary retina and the neuroretinal rim area in primary open angle glaucoma. *J Glaucoma.* 1996; 5 (2): 91-8.

6. Langham, M.E. Ocular blood flow and vision in healthy and glaucomatous eyes. *Survey Ophthalmol.* 1994; 38 Suppl: S161-8.

7. Hayreh, S.S., Bill, A., Sperber, G.O. Effects of high intraocular pressure on the glucose metabolism in the retina and optic nerve in old atherosclerotic monkeys. *Graefes Arch Clin Experim Ophthalmol.* 1994; 232 (12): 745-52.

8. Niessen, A.G., van den Berg, T.J., Langerhorst, C.T., Greve, E.L. Retinal nerve fiber layer assessment by scanning laser polarimetry and standardized photography. *Am J Ophthalmol.* 1996; 121: 484-93.

9. Tjon-Fo-Sang, M.J., Lemij, H.G. The sensitivity and specificity of nerve fiber layer measurements in glaucoma as determined with scanning laser polarimetry. *Am J Ophthalmol.* 1996; 123: 62-9.

10. Petrig, B.L., Riva, C.E. Optic nerve head laser Doppler flowmetry: Principles and computer analysis. In: Kaisers, H.J., Flammer, J., Hendrickson, Ph., ed. *Ocular blood flow. New insights into the pathogenesis of ocular diseases.* Switzerland: Karger, 1996: pp 120-7.

11. Weinreb, R.N., Shakiba, S., Zangwill, L. Scanning laser polarimetry to measure the nerve fiber layer of normal and glaucomatous eyes. *Am J Ophthalmol.* 1994; 119: 627-36.

12. Weinreb, R.N., Dreher, A.W., Coleman, A., Quigley, H., Shaw, B., Reiter, K. Histological validation of Fourier-ellipsometry measurements of retinal nerve fiber layer thickness. *Arch Ophthalmol.* 1990; 108: 557-60.

13. Pillunat, L.E., Anderson, D.R., Knighton, R.W., Joos, K.M., Feuer, W.J. Effects of increased intraocular pressure on optic nerve head blood flow. In: Kaisers, H.J., Flammer, J., Hendrickson, Ph., ed. *Ocular blood flow. New insights into the pathogenesis of ocular diseases.* Switzerland: Karger, 1996: 138-44.

14. Bonner, R. F., Nossal, R. Principles of laser-Doppler flowmetry. In: Shepherd, A.P., Oberg, P.A., ed. *Laser-Doppler blood flowmetry.* Boston: Kluwer Academic Publishers, 1990: 17-45.

15. Michelson, G., Langhans, M.J., Groh, M.J.M. Clinical investigation of the combination of a scanning laser ophthalmoscope and laser Doppler flowmeter. *German J Ophthalmol.* 1995; 4: 342-9.

16. Riva, C.E., Cranstoun, J.E., Petrig, B.L. Choroidal blood flow in the foveal region of the human ocular fundus. *Invest Ophthalmol Vis Sc.* 1994; 35 (13): 4273-81.

17. Geeraets, W.J., Williams, R.C., Chang, G., Ham, W.T., Du Pont Guerry, Schmidt, F.H. The relative absorption of thermal energy in retina and choroid. *Invest Ophthalmol.* 1962; 1: 340-7.

18. Sperber, G.O., Bill A. The 2-deoxyglucose method and ocular blood flow. In: Lambrou, G.N., Greve, E.L, ed. *Ocular blood flow in glaucoma: Means , methods and measurements.* Berkeley: Kugler & Ghedini Publications, 1989: 73-80.

19. Harris, A. Measuring ocular blood flow: A technical overview. *Ocular Surgery News.* 1997; Suppl Dec: 4-6.

20. Hollo, G., van den Berg, T.J., Greve, E.L. Scanning laser Doppler flowmetry in glaucoma. *International Ophthalmol.* 1996-97; 20 (1-3): 63-70.

21. Riva, C.E., Shonat, R.D., Petrig, B.L., Pournaras, C.J., Barnes, J.B. Noninvasive measurement of the optic nerve head circulation. In: Lambrou, G.N., Greve, E.L, ed. *Ocular blood flow in glaucoma: Means , methods and measurements.* Berkeley: Kugler & Ghedini Publications, 1989: 129-34.

22. Alm, A., Bill, A. Ocular circulation. In: Moses, R.A., Hart, W.M., ed. *Adler's physiology of the eye: Clinical application.* 9th ed. Saint-Louis: Mosby Year Book, 1992; 6: 198-224.

23. Ernest, J.T. Macrocirculation and microcirculation of the retina. In: Ogden, T.E., ed. Basic science and inherited retinal disease. In: Ryan, S.J., ed. *Retina..* Vol 1. St-Louis: The C.V. Mosby Company, 1989; 7: 65-6.

24. Mendel, M., Riva, C.E., Petrig, B.L. Regulation of optic nerve blood flow: effect of diffuse luminance flicker. In: Fourth International Symposium on ocular circulation and neovascularization. Budapest: 1995: May 22-26.

4. BIBLIOGRAPHIE

Adachi, M., Takahashi, K., Nishikawa, M., Miki, H., Uyama, M. High intraocular pressure-induced ischemia and reperfusion injury in the optic nerve and retina in rats. *Graefes Arch Clin Exp Ophthalmol.* 1996; 234 (7): 445-51.

Airaksinen, P.J., Tuulonen, A. Retinal nerve fiber layer evaluation. In: Varma, R., Spaeth, G.L., Parker, K.W.,ed. *The optic nerve in glaucoma*, J. Philadelphia: J. B. Lippincott Company, 1993; 18: 277-87.

Alm, A., Bill, A. Ocular circulation. In: Moses, R.A., Hart, W.M., ed. *Adler's physiology of the eye: Clinical application.* 9th ed. Saint-Louis: Mosby Year Book, 1992; 6: 198-224.

Anderson, D.R. Glaucoma, capillaries and pericytes. 1. Blood flow regulation. *Ophthalmologica.* 1996; 210 (5): 257-62.

Anderson, D.R., Quigley, H.A. The optic nerve. In: Moses, R.A., Hart, W.M., ed. *Adler's physiology of the eye: Clinical application.* 9th ed. Saint-Louis: Mosby Year Book, 1992; 20: 616-637.

Apple, D.J. *Ocular pathology: Clinical applications and self-assessment.* 3rd ed. Saint-Louis: The C.V. Mosby Company, 1985.

Arend, O., Harris, A., Martin, B.J., Holin, M., Wolf, S. Retinal blood velocities during carbogen breathing using scanning laser opthalmoscopy. *Acta Ophthalmol.* 1994; 72: 332-6.

Balazsi, A.G., Rootman, J., Drance, S.M., Schulzer, M., Douglas, G.R. The effect of age on the nerve fiber population of the human optic nerve. *Am J Ophthalmol.* 1984; 97: 760-6.

Bill, A. Vascular physiology of the optic nerve. In: Varma, R., Spaeth, G.L., Parker, K.W.,ed. *The optique nerve in glaucoma*, Philadelphia: J. B. Lippincott Company, 1993; 3: 37-50.

Bonner, R. F., Nossal, R. Principles of laser-Doppler flowmetry. In: Shepherd, A.P., Oberg, P.A., ed. *Laser-Doppler blood flowmetry.* Boston: Kluwer Academic Publishers, 1990: 17-45.

Bour, T., Blanchard, F., Segal, A. Données épidémiologiques sur le GPAO et son traitement dans la Marne. *J Français Ophtalmol.* 1993; 16 (6-7): 367-79.

Brooks, D.E., Garcia, G.A., Dreyer, E.B., Zurakowski, D., Franco-Bourland R.E. Vitreous body glutamate concentration in dogs with glaucoma. *Am J Veterinary Res.* 1997; 58(8): 864-7.

Brown, S.M., Jampoli, L.M. New concepts of regulation of retinal vesse tone. (Review). *Arch Ophthalmol.* 1996; 114 (2): 199-204.

Buerk, D., Riva, C.E., Cranstoun, S. Mechanisms underlying the change in cat optic nerve blood flow induced by diffuse flicker. In: Messmer, K., Kübler, W.M., ed. Sixth World Congress for microcirculation. Munich: Monduzzi, 1996: 283-7.

Butt, Z., McKillop, G., O'Brien, C., Allan, P., Aspinall, P. Measurement of ocular blood flow velocity using color Doppler imaging in low tension glaucoma. *Eye.* 1995; 9 (Pt 1): 29-33.

Butt, Z., O'Brien, C., McKillop, G., Aspinall, P., Allan, P. Color Doppler imaging in untreated high- and normal-pressure open-angle glaucoma. *Invest Ophthalmol Vis Sc.* 1997; 38 (3): 690-6.

Caprioli, J., Prum, B., Zeyen, T. Comparison of methods to evaluate the optic nerve head and nerve fiber layer for glaucomatous change. *Am J Ophthalmol.* 1996; 121(6): 659-67.

Coffey, M., Reidy, A., Wormald, R., Xian, W.X., Wright, L., Courtney, P. Prevalence of glaucoma in the west of Ireland. *Br J Ophthalmol.* 1993; 77 (1): 17-21.

Dielemans, I., Vingerling, J.R., Wolfe, R.C., Hofman, A., Grobbee, D.E., de Jong P.T. The prevalence of primary open-angle glaucoma in a population-based study in the Netherlands. The Rotterdam study. *Ophthalmology.* 1994; 101 (11): 1851-5.

Drake, M.V. Glaucomatous visual field loss. In: Moses, R.A., Hart, W.M., ed. *Adler's physiology of the eye: Clinical application.* 9th ed. Saint-Louis: Mosby Year Book, 1992; 113: 1301-10.

Drance, S.M. Psychophysics and electrophysiology in glaucoma: an overview. In: Kaufman, P.L., Mittag, T.W., ed. *Glaucoma.* Vol 7. London: Mosby, 1994; I: 7.1-7.5.

Dreyer, E.B., Zurakowski, D., Schumer, R.A., Podos, S.M., Lipton, S.A. Elevated glutamate levels in the vitreous body of humans and monkeys with glaucoma. *Arch Ophthalmol.* 1996; 114 (3): 299-305.

Eid, T.M., Spaeth, G.L., Katz, L.J., Azuara-Blanco, A., Agusburger, J., Nicholl, J. Quantitative estimation of retinal nerve fiber layer height in glaucoma and

the relationship with optic nerve head topography and visual field. *J Glaucoma.* 1997; 6 (4): 221-30.

Ekstrom, C. Prevalence of open-angle glaucoma in central Sweden. The Tierp Glaucoma Survey. *Acta Ophthalmologica Scandinavica.* 1996; 74 (2): 107-12.

Ernest, J.T. Macrocirculation and microcirculation of the retina. In: Ogden, T.E., ed. Basic science and inherited retinal disease. In: Ryan, S.J., ed. *Retina..* Vol 1. St-Louis: The C.V. Mosby Company, 1989; 7: 6

Flammer, J. To what extent are vascular factors involved in the pathogenesis of glaucoma? In: Kaisers, H.J., Flammer, J., Hendrickson, Ph., ed. *Ocular blood flow. New insights into the pathogenesis of ocular diseases.* Switzerland: Karger, 1996: 12-39.

Foster, P.J., Baasanhu, J., Alsbirk, P.H., Munkgbayar, D., Uranchimeg, D.,Johnson, G.J. Glaucoma in Mongolia. A population-based survey in Hovsgol province, northern Mongolia. *Arch Ophthalmol.* 1996; 114 (10): 1235-41.

Funk, R.H.W. Blood supply of the retina. *Ophthalmic Res.* 1997; 29: 320-5.

Galassi, F., Nuzzaci, G., Sodi, A., Casi, P., Cappelli, S., Vielmo, A. Possible correlations of ocular blood flow parameters with intraocular pressure and visual-field alterations in glaucoma: a study by means of color Doppler imaging. *Opthalmologica.* 1994; 208 (6): 304-8.

Geeraets, W.J., Williams, R.C., Chang, G., Ham, W.T., Du Pont Guerry, Schmidt, F.H. The relative absorption of thermal energy in retina and choroid. *Invest Ophthalmol.* 1962; 1: 340-7.

Haefliger, I.O., Anderson, D.R. Pericytes and capillary blood flow modulation. In: Kaisers, H.J., Flammer, J., Hendrickson, Ph., ed. *Ocular blood flow. New insights into the pathogenesis of ocular diseases.* Switzerland: Karger, 1996: 74-78.

Haefliger, I.O., Meyer, P., Flammer, J., Luscher, T.F. Endothelium-dependent vasoactive factors. In: Kaisers, H.J., Flammer, J., Hendrickson, Ph., ed. *Ocular blood flow. New insights into the pathogenesis of ocular diseases.* Switzerland: Karger, 1996: 51-63.

Hamard, P., Hamard, H., Dufaux, J. Blood flow rate in the microvasculature of the optic nerve head in primary open angle glaucoma. *Survey Ophthalmol.* 1994; 38 Suppl: S87-93; Discussion S94.

Hamard, P., Hamard, H., Dufaux, J., Quesnot, S. Optic nerve head blood flow using a laser Doppler velocimeter and haemorheology in primary open

angle glaucoma and normal pressure glaucoma. *Br J Ophthalmol.* 1994; 78 (6): 449-53.

Harris, A. Measuring ocular blood flow: A technical overview. *Ocular Surgery News.* 1997; Suppl Dec: 4-6.

Harris, A., Anderson, D.R., Pillunat, L., Joos, K., Knighton, R.W., Kagemann, L., Martin, B.J. Laser doppler flowmetry measurement of changes in human optic nerve head blood flow in response to blood gas perturbations. *J Glaucoma.* 1996; 5 (4): 258-65.

Harris, A., Arend, O., Wolfe, S., Cantor, L.B., Martin, B.J. CO_2 dependance of retinal arterial and capillary blood velocity. *Acta Ophthalmol Scand.* 1995; 73: 421-4.

Hayreh, S.S. Blood supply and vascular disorders of the optic nerve. In: Cant, J.S., ed. *The optic nerve.* Saint-Louis: The C.V. Mosby Company, 1972: 59-67.

Hayreh, S.S. Blood supply of the optic nerve head in health and disease. In: Lambrou, G.N., Greve, E.L, ed. *Ocular blood flow in glaucoma: Means , methods and measurements.* Berkeley: Kugler & Ghedini Publications, 1989: 3-48.

Hayreh, S.S., Bill, A., Sperber, G.O. Effects of high intraocular pressure on the glucose metabolism in the retina and optic nerve in old atherosclerotic monkeys. *Graefes Arch Clin Experim Ophthalmol.* 1994; 232 (12): 745-52.

Henkind, P., Hansen, R.I., Szalay, J. Ocular circulation. In: Duane, T.D., Jaeger, E.A., ed. *Biomedical foundation of ophthalmology.* Vol 2. Philadelphia: Lippincott Company, 1988; 5: 1-53.

Hill, D.W., Young, S. Regional retinal blood flow in the cat. In: Cant, J.S, ed. *Vision and circulation .* London: The C.V. Mosby Company, 1974: 60-65.

Hollo, G., van den Berg, T.J., Greve, E.L. Scanning laser Doppler flowmetry in glaucoma. *International Ophthalmol.* 1996-97; 20 (1-3): 63-70.

Jonas, J.B., Naumann, G.O.H. The optic nerve: Its embryology, histology, and morphology. In: Varma, R., Spaeth, G.L., Parker, K.W.,ed. *The optic nerve in glaucoma.* J. Philadelphia: J. B. Lippincott Company, 1993; 1: 3-26.

Kendell, K.R., Quigley, H.A., Kerrigan, L.A. Primary open-angle glaucoma is not associated with photoreceptor loss. *Invest Ophthalmol Vis Sc.* 1995; 36 (1): 200-5.

Kiel, J.W., van Heuvan, W.A.J. Ocular perfusion pressure and choroidal blood flow in the rabbit. *Invest Ophthalmol Vis Sc.* 1995; 36 (3): 579-85.

Klopfer, J., Paikowsky, S.J. Epidemiology and clinical impact of the glaucomas. In: Lewis, T.L., Fingeret, M., ed. *Primary care of the glaucomas.* Norwalk: Appleton & Lange,1993; 2: 7-16.

Kuwabara, T. Blood vessels in the normal retina. In: Straatsma, B.R., Hall, M.O., Allen, R.A. and Crescitelli, F., ed. *The retina: Morphology, function and clinical characteristics.* UCLA Forum Med. Sci. No.8, Los Angeles: University of California Press, 1969; 163-76.

Langham, M.E. Ocular blood flow and vision in healthy and glaucomatous eyes. *Survey Ophthalmol.* 1994; 38 Suppl: S161-8.

Leske, M.C., Connell, A.M., Schachat, A.P., Hyman, L. The Barbados Eye Study. Prevalence of open- angle glaucoma. *Arch Ophthalmol.* 1994; 112 (6): 821-9.

Lewis, T.L. Definition and classification of glaucomas. In: Lewis, T.L., Fingeret, M., ed. *Primary care of the glaucomas.* Norwalk: Appleton & Lange,1993; 1: 3-5.

Lewis, T.L., Chronister, C.L. Etiology and pathophysiology of primary open-angle glaucoma. In: Lewis, T.L., Fingeret, M., ed. *Primary care of the glaucomas.* Norwalk: Appleton & Lange,1993; 5: 65-77.

Lewis, T.L., Wing, J.T. Anatomy and physiology of the optic nerve. In: Lewis, T.L., Fingeret, M., ed. *Primary care of the glaucomas.* Norwalk: Appleton & Lange,1993; 4: 47-62.

Lovasik, J.V. Evidence for autoregulation of blood flow in the human choroidal vasculature. *Opto Vis Sc.* 1996; 73 (12): 76

Manni, G., Lambiase, A., Centofanti, M., Mattei, E., De Gregorio, A., Aloe, L., de Feo, G. Histopathological evaluation of retinal damage during intraocular hypertension in rabbit: involvement of ganglion cells and nerve fiber layer. *Graefes Arch Clin Exp Ophthalmol.* 1996; 234 Suppl 1: S209-13.

Mendel, M., Riva, C.E., Petrig, B.L. Regulation of optic nerve blood flow: effect of diffuse luminance flicker. In: Fourth International Symposium on ocular circulation and neovascularization. Budapest: 1995: May 22-26.

Meyer, P., Haefliger, I.O., Flammer, J., Luscher, T.F. Endothelium-dependent regulation in ocular vessels. In: Kaisers, H.J., Flammer, J., Hendrickson, Ph., ed. *Ocular blood flow. New insights into the pathogenesis of ocular diseases.* Switzerland: Karger, 1996: 64-73.

Michelson, G., Groh, M.J., Groh, M.E., Grundler, A. Advanced primary open-angle glaucoma is associated with decreased ophthalmic artery blood-flow velocity. *German J Ophthalmol.* 1995; 4 (1): 21-4.

Michelson, G., Langhans, M.J., Groh, M.J. Perfusion of the juxtapapillary retina and the neuroretinal rim area in primary open angle glaucoma. *J Glaucoma.* 1996; 5 (2): 91-8.

Michelson, G., Langhans, M.J., Groh, M.J.M. Clinical investigation of the combination of a scanning laser ophthalmoscope and laser Doppler flowmeter. *German J Ophthalmol.* 1995; 4: 342-9.

Mikelberg, F.S., Drance, S.M., Schulzer, M., Yidegiligne, H.M., Weis, M.M. Axon count and axon diameter distribution. *Ophthalmology.* 1989; 96 (9):1325-8.

Minckler, D.S. Neuronal damage in glaucoma. In: Varma, R., Spaeth, G.L., Parker, K.W.,ed. *The optic nerve in glaucoma*, Philadelphia: J. B. Lippincott Company, 1993; 4: 51-8.

Müller, H. Anatomische Beitrage zur ophthalmologie: Ueber Nervean-Verandeungen ander Eintrittsstelle des Scherven. *Arch Ophthalmol.* 1958; 4:1.

Nasemann, J.E., Carl, T., Pamer, S., Scheider, A. Perfusion time of the central retinal artery in normal pressure glaucoma. Initial results. *Ophthalmologe.* 1994; 91 (5): 595-601.

Nesterov, A.P, Egorov, E.A. Pathological physiology of primary open-angle glaucoma: the optic nerve changes. In: Cairns, J.E., ed. *Glaucoma.* Vol 1. London: Grune & Stratton, 1986; 18: 369-90.

Nickells, R.W. Retinal ganglion cell death in glaucoma: the how, the why, and the maybe. *J Glaucoma.* 1996; 5 (5): 345-56.

Niessen, A.G., van den Berg, T.J., Langerhorst, C.T., Greve, E.L. Retinal nerve fiber layer assessment by scanning laser polarimetry and standardized photography. *Am J Ophthalmol.* 1996; 121: 484-93.

Orgül, S., Cioffi, G.A. The vasomotor effect of arterial oxygen on the optic nerve microvasculature. In: Kaisers, H.J., Flammer, J., Hendrickson, Ph., ed. *Ocular blood flow. New insights into the pathogenesis of ocular diseases.* Switzerland: Karger, 1996: 87-92.

Ouertani, A., Zhioua, R., Trabelsi, A., Jrad, J. Prévalence du glaucome chronique à angle ouvert dans une commune de Tunis. *J Français Ophtalmol.* 1995; 18 (3): 178-82.

Petrig, B.L., Riva, C.E. Optic nerve head laser Doppler flowmetry: Principles and computer analysis. In: Kaisers, H.J., Flammer, J., Hendrickson, Ph., ed. *Ocular blood flow. New insights into the pathogenesis of ocular diseases.* Switzerland: Karger, 1996: pp 120-7.

Pillunat, L.E., Anderson, D.R., Knighton, R.W., Joos, K.M., Feuer, W.J. Effects of increased intraocular pressure on optic nerve head blood flow. In: Kaisers, H.J., Flammer, J., Hendrickson, Ph., ed. *Ocular blood flow. New insights into the pathogenesis of ocular diseases.* Switzerland: Karger, 1996: 138-44.

Pournaras, C.J. Autoregulation of ocular blood flow. In: Kaisers, H.J., Flammer, J., Hendrickson, Ph., ed. *Ocular blood flow. New insights into the pathogenesis of ocular diseases.* Switzerland: Karger, 1996: 40-50.

Quaranta, L., Manni, G., Donato, F., Bucci, M.G. The effect of increased intraocular pressure on pulsatile ocular blood flow in low tension glaucoma. *Survey Ophthalmol.* 1994; 38 Suppl: S177-81; Discussion S182.

Quigley, H.A., Enger, C., Katz, J., Sommer, A., Scott, R., Gilbert, D. Risk factors for the development of glaucomatous visual field loss in ocular hypertension. *Arch Ophthalmol.* 1994; 112 (5): 644-9.

Quigley, H.A., Flower, R.W., Addicks, E.M., Mc Leod, D.S. The mechanism of optic nerve damage in experimental acute intraocular pressure elevation. *Invest Ophthalmol Vis Sc.* 1980; 19: 505.

Quigley, H.A., Vitale, S. Models of open-angle glaucoma prevalence and incidence in the United States. *Invest Ophthalmol Vis Sc.* 1997; 38 (1): 83-91.

Ravalico, G., Pastori, G., Toffoli, G., Croce, M. Visual and blood flow responses in low-tension glaucoma. *Survey Ophthalmol.* 1994; 38 Suppl: S173-6.

Riva, C.E., Cranstoun, J.E., Petrig, B.L. Choroidal blood flow in the foveal region of the human ocular fundus. *Invest Ophthalmol Vis Sc.* 1994; 35 (13): 4273-81.

Riva, C.E., Shonat, R.D., Petrig, B.L., Pournaras, C.J., Barnes, J.B. Noninvasive measurement of the optic nerve head circulation. In: Lambrou, G.N., Greve, E.L, ed. *Ocular blood flow in glaucoma: Means , methods and measurements.* Berkeley: Kugler & Ghedini Publications, 1989: 129-34.

Salmon, J.F., Mermoud, A., Ivey, A., Swanevelder, S.A., Hoffman, M. The prevalence of primary angle closure glaucoma and open-angle glaucoma

in Marne, western Cape, South Africa. *Arch Ophthalmol.* 1993; 111 (9): 1263-9.

Schulte, K., Wolf, S., Arend, O., Harris, A., Henle, C., Reim, M. Retinal hemodynamics during increased intraocular pressure. *German J Ophthalmol.* 1996; 5 (1): 1-5.

Schuman, J.S., Hee, M.R., Puliafito, C.A., Wong, C., Pedut-Kloizman, T., Lin, C.P., Hertzmark, E., Izatt, J.A., Swanson, E.A., Fujimoto, J.G. Quantification of nerve fiber layer thickness in normal and glaucomatous eyes using optical coherence tomography. *Arch Ophthalmol.* 1995; 113 (5): 586-96.

Schuman, J.S., Pedut-Kloizman, T., Hertzmark, E., Hee, M.R., Wilkins, J.R., Coker, J.G., Puliafito, C.A., Fujimoto, J.G., Gloor, B. Value of scanning laser ophthalmoscopy and polarimetry compared with perimetry in evaluating glaucomatous changes in the optic papilla and nerve fiber layer. *Ophthalmologe.* 1996; 93 (5): 520-6.

Shapley, R. Retinal ganglion cell function. In: Varma, R., Spaeth, G.L., Parker, K.W.,ed. *The optic nerve in glaucoma*, Philadelphia: J. B. Lippincott Company, 1993; 2: 27-34.

Shields, M.B. *A study guide for glaucoma.* Baltimore: Williams & Wilkins, 1982.

Spaeth, G.L. *The pathogenesis of nerve damage in glaucoma: Contribution of fluorescein angiography.* New York: Grune & Stratton, 1977.

Spalton, D.J., Hitchings, R.A., Hunter P.A. *Atlas of clinical ophthalmology.* 2nd ed. London: Mosby- Year Book Europe (Wolfe), 1994.

Sperber, G.O., Bill A. The 2-deoxyglucose method and ocular blood flow. In: Lambrou, G.N., Greve, E.L, ed. *Ocular blood flow in glaucoma: Means , methods and measurements.* Berkeley: Kugler & Ghedini Publications, 1989: 73-80.

Sponsel, W.E., De Paul, K.L., Zetlan, S.R. Retinal hemodynamic effects of carbon dioxide, hyperoxia, and mild hypoxia. *Invest Ophthalmol Vis Sc.* 1992; 33: 1864-9.

Thomas, J.V. General considerations. In: Thomas, J.V., ed. *Glaucoma surgery.* St-Louis: Mosby Year Book, 1992; 1: 1-2.

Thomas, J.V. Primary open-angle glaucoma. In: Moses, R.A., Hart, W.M., ed. *Adler's physiology of the eye: Clinical application.* 9th ed. Saint-Louis: Mosby Year Book, 1992; 117: 1342-62.

Tielsch, J.M., Katz, J., Sommer, A., Quigley, H.A., Javitt, J.C. Hypertension, perfusion pressure, and primary open-angle glaucoma. A population-based assessment. *Arch Ophthalmol.* 1995; 113 (2): 216-21.

Tjon-Fo-Sang, M.J., Lemij, H.G. The sensitivity and specificity of nerve fiber layer measurements in glaucoma as determined with scanning laser polarimetry. *Am J Ophthalmol.* 1996; 123: 62-9.

Tuulonen, A., Lehtola, J., Airaksinen, P.J. Nerve fiber layer defects with normal visual fields. Do normal optic disc and normal visual field indicate absence of glaucomatous abnormality? *Ophthalmol.* 1993; 100 (5): 587-97; discussion 597-8.

Uchida, H., Tomita, G., Onda, E., Sugiyama, K., Kitazawa, Y. Relationship of nerve fiber layer defects and parafoveal visual field defects in glaucomatous eyes. *Japanese J Ophthalmol.* 1996; 40 (4): 548-53.

Van Buskirk, E.M. Is glaucoma a pressure disease? In: Ball, S.F., Franklin, R.M., ed. *Glaucoma: Diagnosis and therapy.* New Orleans: New Orleans Academy of Ophthalmology, 1993: 51-7.

Varma, R., Skaf, M., Barron, E. Retinal nerve fiber layer thickness in normal human eyes. *Ophthalmology.* 1996; 103 (12): 2114-9.

von Jaeger, E. Ueber Glaucom und sein Heilung durch iridectomie. *Z Ges der Aerztezuwren.* 1858; 14: 465-84.

Wang, F., Quigley, H.A., Tielsch, J.M. Screening for glaucoma in a medical clinic with photographs of the nerve fiber layer. *Arch Ophthalmol.* 1994; 112 (6): 796-800.

Wang, J.J., Mitchell, P., Smith, W. Is there an association between migraine headache and open-angle glaucoma? Findings from the Blue Mountains Eye Study. *Ophthalmology.* 1997; 104 (10): 1714-9

Weinreb, R.N., Dreher, A.W., Coleman, A., Quigley, H., Shaw, B., Reiter, K. Histological validation of Fourier-ellipsometry measurements of retinal nerve fiber layer thickness. *Arch Ophthalmol.* 1990; 108: 557-60.

Weinreb, R.N., Shakiba, S., Sample, P., Shahrokni, S., van Horn, S., Garden, V.S., Asawaphureekorn, S., Zangwill, L. Association between quantitative nerve fiber layer measurement and visual field loss in glaucoma. *Am J Ophthalmol.* 1995; 120: 732-8.

Weinreb, R.N., Shakiba, S., Zangwill, L. Scanning laser polarimetry to measure the nerve fiber layer of normal and glaucomatous eyes. *Am J Ophthalmol.* 1994; 119: 627-36.

Wilson, M.R. Glaucoma: epidemiology and risk factors. In: Higginbotham, E.J., Lee, D.A., ed. *Management of difficult glaucoma: A clinician's guide.* Boston: Blackwell Scientific Publications, 1994; 1: 3-7.

Wise, G. N., Dollery, C.T., Hendkind, P., *The retinal circulation.* 1st ed. New York: Harper & Row, 1971.

Wolf, S., Arend, O., Haase, A., Schulte, K., Remky, A., Reim, M. Retinal hemodynamics in patients with chronic open-angle glaucoma. *German J Ophthalmol.* 1995; 4 (5): 279-82.

Wygnanski, T., Desatnik, H., Quigley, H.A., Glovinsky, Y. Comparison of ganglion cell loss and cone loss in experimental glaucoma. *Am J Ophthalmol.* 1995; 120 (2): 184-9.